Analysis of the effect of suppression of expression of Syntrophin class of PDZ proteins and their effect on ABCA1 dependent cholesterol efflux in cell culture and in-vivo mouse experiments

by

Hawwa Ozotu OSHAFU

A final project report

In fulfillment of the requirements for the

Marshall Plan Scholarship

of the Austrian Marshall Plan Foundation

Degree Program: Master Medical and Pharmaceutical Biotechnology, IMC FH Krems

Area of emphasis: Immunology

Academic advisor: Prof. (FH) Mag. Dana Mezricky

External advisor: Michael Fitzgerald, Ph.D.

Submitted on: 28.02.2014

STATUARY DECLARATION

I declare in a lieu of an oath that I have written this master thesis myself and that I have not used any sources or resources other than stated for its preparation. I further declare that I have clearly indicated all direct and indirect quotations. This master thesis has not been submitted elsewhere for examination purposes.

February 28, 2014

Hawwa Ozotu Oshafu

List of Contents

Analysis of the effect of suppression of syntrophin class of PDZ proteins and their effect on ABCA1 dependent cholesterol efflux in cell culture

2014

List of Figures

List of Tables

Abbreviations

ABCA1	Adenosine triphosphate - binding cassette transporter A1
DNA	Deoxyribonucleic acid
dsRNA	double-stranded RNA
m7G cap	7-methylguanylate cap
miRNA	micro RNA
mRNA	messenger RNA
Poly-A-tail	Polyadenine tail
PTGS	Post transcriptional gene silencing
RNA	Ribonucleic acid
RNAi	RNA interference
siRNA	short interfering RNA/ small interfering RNA
SNTA1	Syntrophin, alpha 1
SNTB1	Syntrophin, beta 1
SNTB2	Syntrophin, beta 2
ChS	Chalcone Synthase
ssRNA	single stranded RNA
S pombe	*Sacchoromyces pombe*
A Thaliana	*Aradopsis Thaliana*
C elegans	*Caenorhabditis elegans*
Drosophila	*Drosophila melanogaster*
RNase	Ribonuclease
kD	kilo Dalton
PAZ	Piwi Argonaute Zwille domain
DUF283	Domain of unknown function 283
RNaseIIIa/ IIIb	Ribonuclease IIIa or IIIb domain
dsRBD	double-stranded RNA binding domain
OB fold	oligonucleotide/ oligosaccharide binding
Dcr1/ Dcr2	Dicer1/ Dicer2
TRBP	TAR RNA binding protein

Giardia	*Giardia intestinalis*
Ago	Argonaute
ATP	Adenosine triphosphate
UTR	Untranslated region
VSR	Viral suppressors of RNAi
TLR	Toll-like receptors
PAMP	Pathogen-Associated Molecular Patterns
TRIF	TIR domain containing adaptor inducing interferon β
Myd88	Myeloid differentiation factor 88
NF-kB	Nuclear factor kappa-light-chain-enhancer of activated B cells
miRBase	miRNA database
PCR	Polymerase chain reaction
RT-PCR	Reverse Transcriptase - Polymerase chain reaction
cDNA	complementary DNA
Gag	Group specific antigen
VSV-G	Vesicular Stomatitis Virus-G protein
Tet	Tetracycline gene
PDZ domain/ motif	PSD-95/Discs-large/ZO-1 domain
HDL	High density lipoprotein
LDL	Low density lipoprotein
VLDL	Very Low density lipoprotein
Ox-LDL	Oxidized-low density lipoprotein
Apo	Apolipoprotein
MCP-1	Monocyte chemoattractant protein-1

Abstract

Cholesterol homeostasis is essential for life to avoid inflammatory and life threatening conditions. The evolutionarily conserved Adenosine triphosphate - binding cassette subfamily A member 1 transporter, ABCA1, is a key regulator of cholesterol efflux out of the cell to maintain normal conditions as most cells do not have the machinery to metabolize cholesterol.

ABCA1's roles in human physiology and pathophysiology have been well established by multiple publications. However there are only few publications on the molecular mechanism how ABCA1 achieves its cholesterol efflux function. Recently PDZ class proteins named Syntrophins have been demonstrated to stabilize ABCA1 expression.

This Master thesis will focus on the discussion of the ABCA1 and Syntrophin protein-protein interaction and the use of experimental RNA interference to analyze the effect of suppression of Syntrophins on ABCA1 dependent cholesterol efflux in cell culture and in-vivo mouse models.

Analysis of the effect of suppression of syntrophin class of PDZ proteins and their effect on ABCA1 dependent cholesterol efflux in cell culture

2014

1 Introduction

1.1 Cholesterol

Cholesterol is a lipid of immense value to the cell with various cellular functions.

Cholesterol content in the cell membrane can aid in maintaining membrane fluidity to enable membrane processes such as transport or signal transduction to occur (Berg, Tymoczko, and Stryer; 2002).

Additionally, Cholesterol serves as a building block to bile acids, Vitamin D and steroid hormones (Berg, Tymoczko, and Stryer; 2002).

The main source of Cholesterol for the body is food. Particularly animal-derived food has a high Cholesterol percentage (Tracy Fulton, University of California San Francisco UCSF, online lecture).

High cholesterol levels are a risk factor for developing cardiovascular disease CVD (Peter Lechner, IMC University of Applied Sciences IMC UAS Krems, lecture)

In the body, cholesterol can be broken down, with the help of bile acids, Liver and Intestine, to smaller lipophilic molecules. These cholesterol breakdown products can act as ligands to a cell membrane bound receptor leading to downstream induction of a certain nuclear hormone receptor, Liver X receptor LXR to induce ABCA1 mRNA transcription (Venkateswaran et al, 2000).

1.1.1 Nuclear hormone receptors and ABCA1-mediated cholesterol efflux function

LXR are members of the large nuclear hormone receptor family. Structurally, the nuclear hormone receptors are characterized by a central DNA binding domain that allows them to bind response elements within the promoters of target genes (Fitzgerald, Moore and Freeman; 2002).

LXR acts as a heterodimer with Farnesoid X receptor FXR, to initiate ABCA1 mRNA transcription (figure 1). Liver X receptor and Farnesoid X receptors ligands are Hydroxycholesterol and Bile acids respectively (Janowski et al; 1999. Fitzgerald, Moore and Freeman; 2002).

When an oxysterol ligand i.e. oxidized-low density lipoprotein Ox-LDL, binds an extracellular transmembrane receptor on the cell membrane, receptor-mediated endocytosis occurs. Endocytic vesicles in the cytoplasm can progressively mature into membrane enclosed organelles named Lysosomes that have an acidic interior environment of pH 5 (Dominiska and Dykxhoorn; 2010. Cooper; 2002).

In the lysosome, receptor bound Ox-LDL is degraded to cholesterol. Cholesterol can be oxidized in the cell forming Oxysterol (Venkateswaran et al, 2000) (figure 1).

Oxysterol is the ligand for the nuclear located heterodimer LXR/ RXR which in concert induce the transcription of ABCA1 mRNA via their DNA binding amino-terminal A/B domains (Fitzgerald, Moore and Freeman; 2002).

The ABCA1 transmembrane protein functions in cholesterol and/ or Phospholipid efflux from the cell to extracellular acceptors e.g. Apolipoprotein-AI ApoAI (figure 1).

Figure 1 Model for the regulation of ABCA1 expression and cellular cholesterol efflux by LXR in response to lipid loading
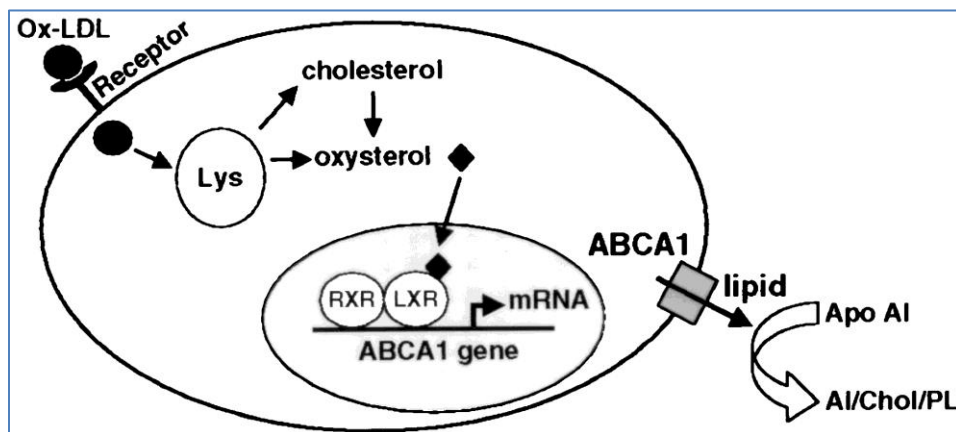
Fig. 1 shows the model for the regulation of ABCA1 expression and cellular cholesterol efflux by LXR in response to lipid loading. Oxysterol, here seen as Ox-LDL, can bind to a membrane bound receptor leading to internalization of the receptor and its lysosomal degradation allowing release of cholesterol and oxysterol into the cytoplasm. Oxysterol is the ligand of nuclear LXR/ RXR resulting in ABCA1 transcription and ABCA1-mediated cholesterol efflux. Venkateswaran et al; 2000.

1.2 ABCA1

ABCA1 belongs to a large group of ATP-dependent transporters evolutionarily conserved in eukaryotes and prokaryotes, all functioning as cellular pumps to export specific molecules (Dean; 2002).

ATP-dependent transporters share in common that they are transmembrane proteins that require the cellular energy "currency" Adenosine triphosphate ATP for export of molecules (figure 2). ATP-dependent transporters can bind ATP intracellularly via their ATP binding domain initiating ATP reduction to Adenosine diphosphate ADP and release of a phosphate (figure 2).

Furthermore, several publications state mutations in ATP-dependent transporter genes that cause severe genetic disorders (Dean; 2002). For example specific ABCA1 gene mutations can result in Tangier disease or familial HDL deficiency (Delude; 2009. Genetics home reference [GHR] 2012).

Figure 2: The molecular structure of ABCA1
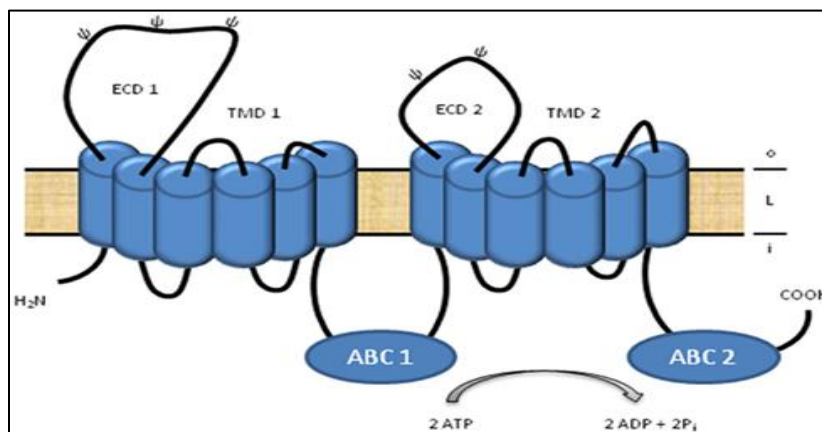
Figure 2 shows the molecular structure of ABCA1 including membrane spanning segments, extracellular domain ECD, transmembrane domain TMD, and ATP-binding cassette ABC. ATP can be bound by ABC1 and ABC2 leading to indicated reaction when a lipid molecule is exported from the cell. Source of figure: Piehler, Özcürümez and Kaminski, 2012

The ABCA1 transmembrane protein stretches over a length of 2261 amino acids, divided into 12 membrane-spanning α-helices (UniProt; 2014. Piehler, Özcürümez and Kaminski, 2012). ABCA1 is found in every human tissue, but macrophages have a distinct higher ABCA1 expression level than other tissue (UniProt; 2014).

ABCA1 plays a rate rate-limiting role in the transport of cholesterol from inside the cell onto extracellular acceptors named Apolipoproteins Apo (Fitzgerald et al; 2002). It is important to note that Cholesterol cannot be metabolized by the cell therefore it needs to be excreted to maintain cholesterol homeostasis. If too much cholesterol is present in a cell cytotoxic conditions can arise as seen in the case of Tangier patients (Tangier disease and its link to high density lipoprotein HDL topic will be discussed in further sections of this Master thesis).

Even though a lot is known about ABCA1-mediated cholesterol efflux and cholesterol's subsequent effect on cell physiology, little is known about the underlying molecular mechanism of ABCA1 function and interaction with extracellular acceptors ApoAI and ApoE. In the next paragraph the current advances in ABCA1 research will be listed.

ABCA1 activity is regulated both at the transcriptional level and at the post-translational level (Tamehiro et al; 2008). Similar to receptors, ABCA1 activity can be down regulated by the cell through endocytosis (Santamarina-Fojo et al, 2001). ABCA1 and amphipathic apolipoproteins form high-affinity molecular complexes required for cholesterol efflux via their membrane spanning α-helices (Fitzgerald et al; 2004).

Utilizing immunoprecipitation approaches and purification of ABCA1 the Freeman/ Fitzgerald Lab could identify a series of candidate interactions that the transporter could engage in. Amid these promising candidates were Serine palmitoyltransferase enzyme SPTLC1 and Syntrophins.

SPTLC1 was shown to co-purify with ABCA1 and negatively regulates its function (Tamehiro et al; 2008).

ABCA1-Syntrophin interaction was discovered during the investigation of a natural Tangier mutation that deleted the last 42 amino acids of the transporter. This work identified a novel ABCA1 VFVNFA motif and a PSD-95/Discs-large/ZO-1 PDZ motif which is bound by class 1 PDZ domains found in Syntrophins (Okuhira et al; 2005). There are three Syntrophin isoforms bound to ABCA1: Syntrophin α1 SNTA1, Syntrophin β1 SNTB1 and Syntrophin β2 SNTB2.

The three Syntrophin genes are differently expressed i.e. SNTA1 is found in a wide variety of tissues, SNTB1 is highly expressed in Liver and macrophages while SNTB2 is highly expressed in striated muscle (Ahn et al; 1996).

1.2.1 Syntrophins class of PDZ proteins

Syntrophins, by virtue of their PDZ domains and other protein-protein interaction modules, are a family of scaffolding proteins that can tether kinases, channels, and transporters to the cytoskeleton.

Syntrophins were discovered as part of a Dystrophin-associated protein complex (Tinsley et al; 1994). Dystrophin, the protein product of the Duchenne muscular Dystrophy locus, is a protein of the membrane cytoskeleton that associates with a complex of integral and membrane-associated proteins (Ahn and Kunkel; 1995).

Similar to Syntrophin-ABCA1 interaction, Syntrophins can link to Dystrophin and cellular phospholipid Phosphoinositides through their PDZ domains (Wawrzyniak, Kashyap and Zimmermann; 2013). It is believed that Syntrophins have a role in mediating cell signaling.

This belief might be true in regards to Syntrophin and ABCA1 protein-protein interactions. Okuhira et al; 2005 demonstrated that Syntrophin stabilizes the expression of ABCA1 (figure 3). The major points of this paper were:

a) ABCA1 and Syntrophin interact in human embryonic kidney HEK293 cells over expressing ABCA1. Syntrophins co-purified with ABCA1.

b) ABCA1 and Syntrophin interaction was confirmed in human THP-1 macrophages and mouse liver. It is important to note that Liver and Macrophages are vital to maintaining cholesterol homeostasis in the body (the importance of liver and macrophages in lipid metabolism will be discussed in further sections of this Master thesis).

c) Small interfering RNA siRNA inhibition of SNTB1 expression reduced cholesterol efflux from primary skin fibroblasts by 50% while decreasing efflux 30% in bone marrow-derived macrophages.

d) Inhibition of SNTB1 decreased ABCA1 protein levels, whereas over expression of SNTB1 increased ABCA1 cell-surface expression and stimulated efflux to apoA-I.

Figure 3: Stabilization of ABCA1 by Syntrophins
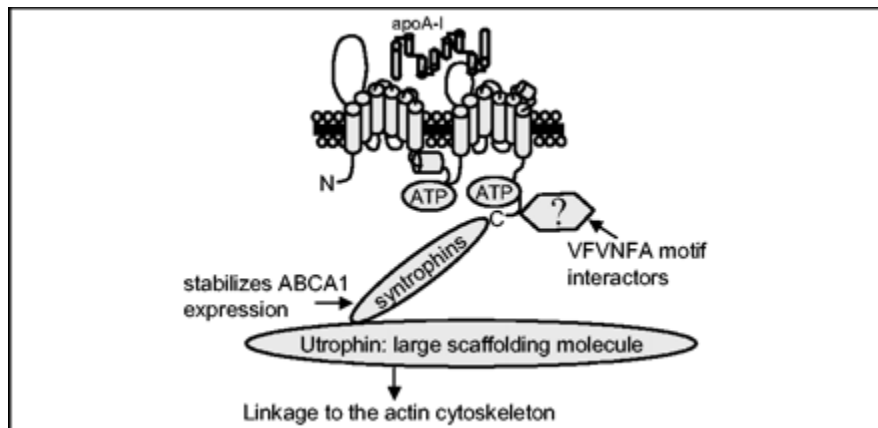
Fig. 3 shows the stabilization of ABCA1 expression by Syntrophins. Syntrophins interact with ABCA1 over ABCA1's VFVNFA motif. ApoA-I cholesterol efflux acceptor is indicated. Source of figure: Okuhira et al; 2005

ABCA1 interacts with ApoA1 which is an apolipoprotein found in high density lipoprotein HDL (figure 3).

1.3 Liproprotein

Lipoproteins are responsible for the transport of Cholesterol to the site of need in the body (Lund-Katz and Philips; 2010). There are four Lipoprotein subclasses: Chylomicrons, very low density lipoprotein VLDL, low density lipoprotein LDL and HDL (Alves and Lima; 2008) (table 1).

Lipoproteins derive their name according to their separation characteristics after centrifugation of a lipid mixture. All lipoproteins have in common a non-polar lipid core and a polar lipid coat. The non-polar lipid core carries Cholesterol esters and triglycerides whereas polar lipid coat consists of apoprotein, unesterified cholesterol and polar phospholipid (Tracy Fulton, UCSF, online lecture).

Lipoproteins differ in their composition and origin (Table 1).

The lipoproteins of significance for cellular cholesterol homeostasis are LDL and HDL which are often referred to as "good" cholesterol and "bad" cholesterol respectively. The function of LDL is to supply total cholesterol to cells (Alves and Lima; 2008) (table 1 and figure 4).

HDL function counteracts the transport of total cholesterol to cells, by taking up excess cholesterol from cells back to the liver for excretion (Alves and Lima; 2008) (table 1 and figure 4). Hence movement of cholesterol laden macrophages back to the organ of origin is referred to as reverse Cholesterol transport RCT.

Table 1: Subclasses of Lipoproteins

Properties	Chylomicrons	VLDL	LDL	HDL
Composition (%)				
Cholesterol	3	22	50	20
Triglycerides	90	55	5	5
Phospholipids	6	15	25	25
Proteins	1	8	20	50
Origin	Intestine	Liver, intestine	Product of VLDL metabolism	Liver, intestine
Function	Transports triglycerides from diet	Transports hepatic triglycerides	Supplies TC to cells	Performs TC reverse transport

VLDL: very low-density lipoprotein; LDL: low-density lipoprotein; HDL: high-density lipoprotein; and TC: total cholesterol.

Table 1 lists the properties of the subclasses of Lipoproteins; Chylomicrons, VLDL, LDL and HDL. Source of figure: Alves and Lima; 2008.

LDL is the product of VLDL metabolism in the liver and intestine. The liver is the site for HDL biogenesis in the body (Alberts et al; 2007. figure 4).

Figure 4: Subclass of Lipoprotein origin
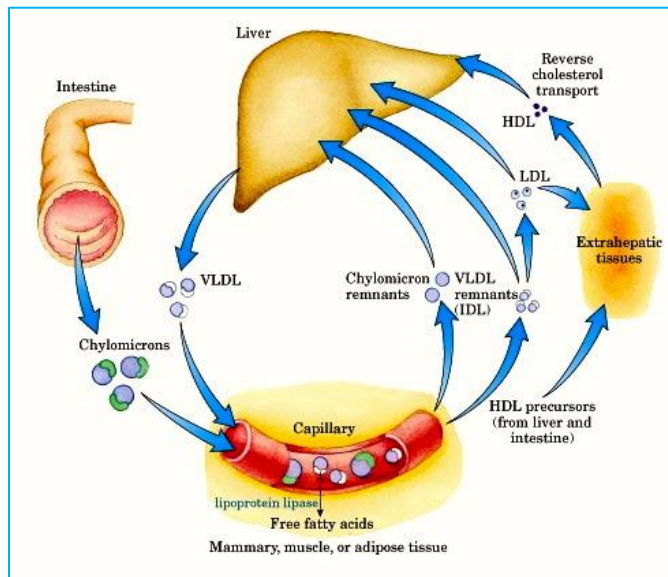
Fig. 4 shows the origin of Chylomicrons, VLDL, LDL and HDL in the body. LDL can transport cholesterol to extrahepatic tissue and Liver whereas HDL undergoes reverse cholesterol transport. Source: Cassie Turano; Pathophysiology flashcards.

1.3.1 LDL and Atherosclerosis

LDL can deliver total cholesterol to endothelial cells from the liver by moving into the sub endothelium (figure 5). LDL in contrast to other lipoproteins has a cellular half life of ~2 days (Tracy Fulton, UCSF, online lecture). This long half life makes LDL molecules more susceptible to undergo alterations due to actions of Oxygen free radicals, glucose, toxins, smooth muscle cells or macrophages in the body (Tracy Fulton, UCSF, online lecture. Michael Brainin, IMC UAS Krems, Stroke lecture).

Specifically oxidized LDL poses a major threat to health. Oxidized LDL is an abnormal or foreign molecule which can be recognized and bound by Scavenger receptor class A SR-A on Macrophages triggering immune responses (Peiser and Gordon; 2001. Kim, Ordija and Freeman; 2004).

Oxysterol ligands can induce the Phosphoinositide-3-kinase pathway in Macrophages which in turn through downstream protein-protein interactions turns on transcription factor nuclear factor NF-kappa-B p105 subunit NF-kB (Kim, Ordija and Freeman; 2004. UniProt; 2013). NF-kB's task is to induce the transcription of cytokine specific genes

Analysis of the effect of suppression of syntrophin class of PDZ proteins and their effect on ABCA1 dependent cholesterol efflux in cell culture

2014

initiating increased transcription and secretion of cytokines by macrophages (Murphy; 2012). The release of key cytokines such as Monocyte chemoattractant protein-1 MCP-1 and Interleukin 1 IL1, signals the attraction and recruitment of Monocytes to the site of inflammation in the subendothelium (Murphy; 2012. Michael Brainin, IMC UAS Krems, Stroke lecture). Monocytes are guided to the endothelium by intercellular adhesion molecules on the membranes of inflamed endothelial cells (Lim et al; 2003. Murphy; 2012). Once at the site of inflammation monocytes can extravasate from blood crossing the endothelial barrier to underlying cells (figure 5).

Monocytes are the myeloid precursors of macrophages, which when in the subendothelium differentiate into Macrophages (Murphy; 2012. Figures 5 and 6). Differentiated Macrophages can again bind and internalize oxidized sterol found in sites of inflammation leading to an increased outpour of cytokines.

While cytokines are released, growth factors to stimulate smooth muscle proliferation are released (Michael Brainin, IMC UAS Krems, Stroke lecture).

Additionally foam cells appear in the sub endothelium which is basically cholesterol engorged Macrophages impaired in cholesterol efflux due to excess Cholesterol amounts (Michael Brainin, IMC UAS Krems, Stroke lecture.Figure 5).

This repetitive cycle of cytokine secretion and additional monocyte recruitement to inflammation sites ultimately results in atherosclerotic plaque formation (figure 5).

Under the action of collagenases and elastases the fibrous cap of atheroclerotic plaques is degraded giving rise to plaque rupture and subsequent thrombus formation (figure 5). A Thrombus can be potentially deadly depending on body site to which it is transported to by the blood. A Thrombus can lead to Angina, Myocardial infarction or Stroke (Tracy Fulton, UCSF, online lecture).

Figure 5: LDL and atherosclerotic plaque formation
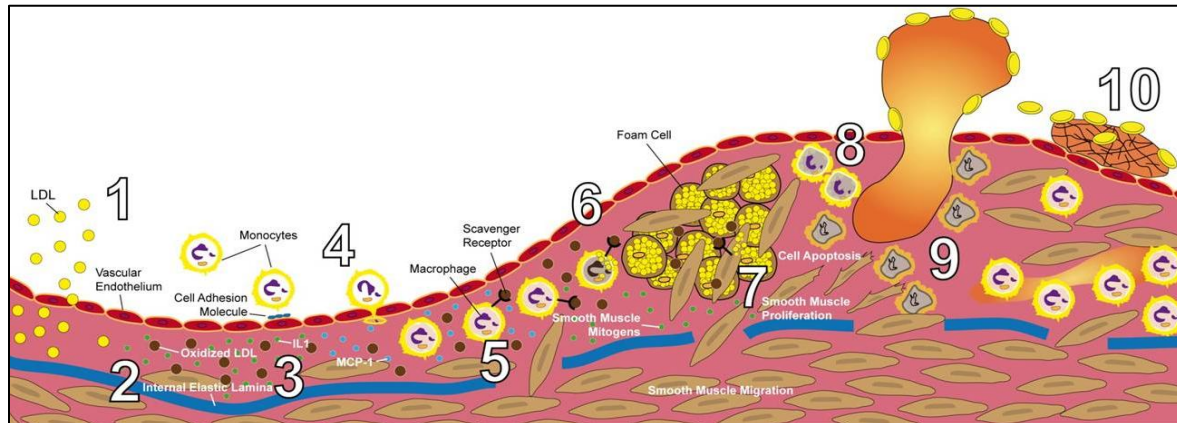
Figure 5 shows the effect of LDL on atherosclerotic plaque formation. 1. LDL diffuses into the subendothelium. 2. LDL is oxidized by macrophages or smooth muscle cells. 3. Secretion of cytokines IL1, MCP-1 by inflamed cells 4. The extravasation of chemokine-attracted monocytes into sub endothelium 5. Oxidized LDL binds cavenger receptor A expressed on differentiated macrophages and accumulation of foam cells. 7. Growth factor triggered smooth muscle proliferation. 8. Atherosclerotic plaque formation. 9. Degradative action of colleganases on fibrous cap of atherosclerotic plaque. 10. Thrombus ruptures into the blood stream.

Figure 6: Monocyte differentiation into Macrophage
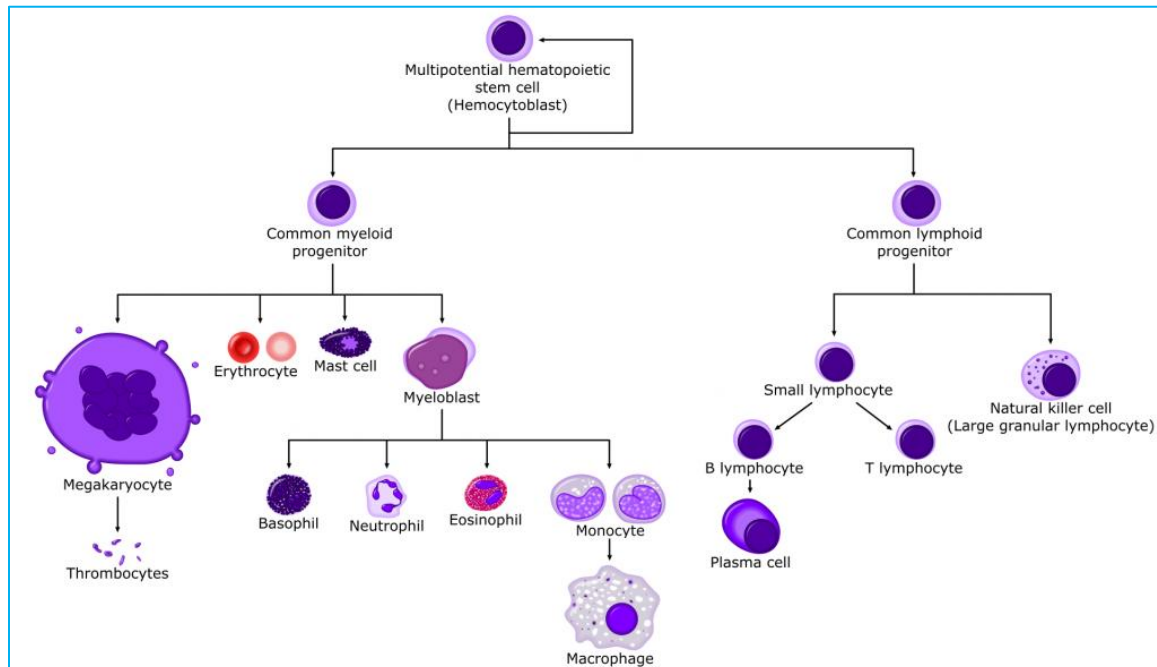
Figure 6 illustrates how monocytes differentiate into Macrophages during Hematopoiesis. Source of figure:Tisha Rowland.

1.3.2 The atheroprotective role of ABCA1 and HDL seen in the example of Tangier disease

Reverse cholesterol transport per HDL is actually an anti-inflammatory means to eliminate excess Cholesterol in cells (Fitzgerald, Mujawar and Tamehiro; 2010).. Furthermore, HDL possesses potent anti-oxidative activity to prevent the formation of oxidized LDL this preventing formation of plaques in the arterial subendothelium and so preventing subsequent myocardial infarction or stroke (Kontush and Chapman; 2006).

Low HDL is a risk factor for CVD (Peter Lechner, IMC University of Applied Sciences IMC UAS Krems, lecture). Therefore the primary aim of the available medications for CVD e.g. Statins, is to reduce LDL levels and increase HDL levels (Freeman; 2006).

It is clear that ABCA1 has a critical role in HDL metabolism through the example of Tangier disease. Tangier disease is a rare inherited disorder caused by mutation in the ABCA1 gene leading to impaired function of the transporter (Fitzgerald, Mujawar and Tamehiro; 2010). As a consequence of this defect cholesterol accumulates in macrophages leading to, among other pathologies, yellow enlarged tonsils in affected individuals and significantly reduced levels of HDL in the blood (figure 7).

Figure 7: Tangier disease
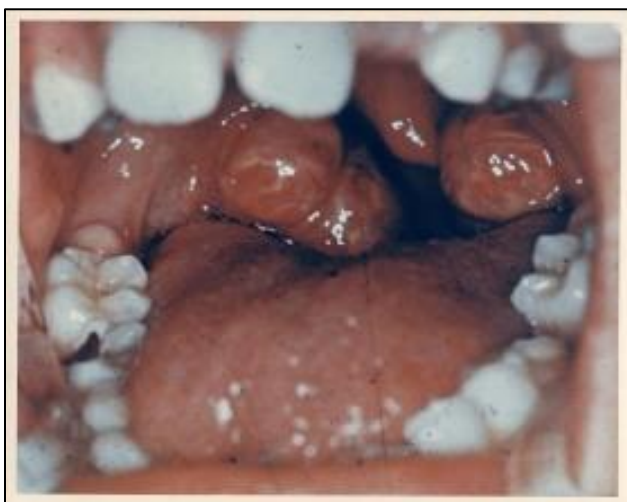
Figure 7 illustrates the characteristic yellowish enlarged cholesterol stuffed tonsils of a Tangier disease patient. Source of figure: Nursing-resource, 2010.

In contrast to normal HDL, an abnormal HDL variant was shown to induce endothelial dysfunction promoting hypertension and atherosclerosis, through the activation of Toll-like receptor-2 TLR 2 on macrophages (Speer et al; 2013).

1.4   RNA interference as a research tool

The central dogma of molecular biology involves DNA and RNA molecules to produce proteins in the cell e.g. ABCA1 gene is transcribed to "ABCA1" mRNA and then translated to functional ABCA1 protein (figure 8).

Transcription is the first step of gene expression occurring in the nucleus, followed by translation in the cytoplasm. During transcription, the genetic information DNA of a gene is copied to mRNA. After addition of a Poly-A-tail and a 7-methylguanylate m7G cap to increase stability against nucleases, the mature mRNA can be exported to the cytoplasm (Alberts et al; 2007).

At this point in the cytoplasm, the interfering action of RNA interference RNAi, on mRNA translation to protein takes place. RNAi is mediated by small RNA fragments which in a homology- and sequence-dependent manner hybridize to target mRNA leading to translational repression (Carthew and Sontheimer; 2009). The total effect of RNAi is seen as a down regulation or knockdown of target mRNA encoded protein synthesis.

Figure 8: Point of RNAi during protein synthesis
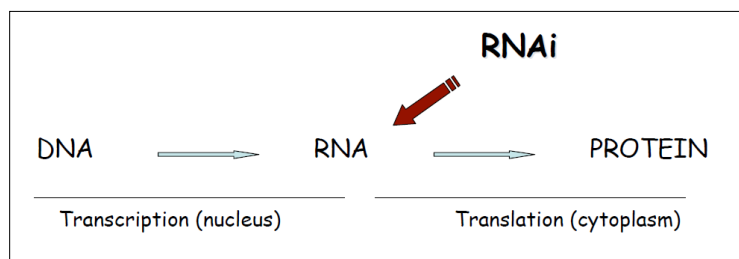
Fig. 8 highlights the interfering point of RNAi (red arrow) during protein synthesis in a cell. In order for protein synthesis to occur DNA is transcribed into RNA, RNA is then translated into protein. Transcription occurs in the nucleus while translation occurs in the cytoplasm. Source: RNA as a drug.pdf, Alexander Mankin Lab.

The term RNA interference, or "RNAi," was initially coined by Fire and coworkers to describe the observation that double-stranded RNA dsRNA can block gene expression when it is introduced into nematode worms (Fire et al., 1998).

With the finding that dsRNA was the causative agent for RNAi, the link between posttranscriptional gene silencing mechanisms, RNAi, quelling and post transcriptional gene silencing PTGS, could be established.

RNAi, quelling and PTGS can be summarized under the term RNA silencing.

The following sections will firstly discuss the evolution and biological function of RNAi; followed by the signature components of RNAi; detailed description of the small interfering RNA siRNA pathway and micro RNA miRNA pathway; their functions and experimental realizations.

1.4.1 Evolution of RNA interference

The first hint towards the discovery of RNAi was in 1990 by the observation of PTGS in plants. In an effort to change the pigmentation of Petunia flowers to a darker shade of purple, additional copies of the Chalcone Synthase ChS gene were introduced into Petunia flowers (Sidahmed and Wilkie; 2010). ChS is a plant enzyme necessary for the biosynthesis of anthocyanin pigments in plants (Ferrer et al, 1999).

The rationale for the introduction of additional ChS genes was that if there are more copies of the gene present in a cell, over expression of anthocyanin pigment will occur leading to more intense shades of purple. Surprisingly the transgenic petunia offspring had a fully or partially white coloration.

In search for the cause of this phenomenon, numerous assays were performed, with the conclusion that the cause of gene silencing was not due to reduced transcription of the ChS gene but due to an increased mRNA degradation rate. Although it was proven that the interfering point was after transcription of the ChS gene, the causative agent for this phenomenon could not be identified at that time (figure 9).

In the same decade as the discovery of PTGS in plants another process, quelling in the fungus *Neurospora crassa*, involving posttranscriptional, homology dependent RNA

silencing was identified (Sidahmed and Wilkie; 2010. figure 9). Again no causative agent for quelling could be distinguished.

By 1998, a major milestone towards understanding the mechanism of PTGS and quelling was accomplished; RNAi and its cause dsRNA were unraveled in _Caenorhabditis. elegans_ C elegans (Fire et al; 1998. Figure 9).

C. elegans is a eukaryotic nematode worm with at least 83% homology to humans (Lai et al, 2000), used as a model system to understand gene function.

Fire and coworkers predicted, on the basis of publications on hybridization and experimental introduction of RNA into diverse organisms e.g. plants, that dsRNA might be the cause for RNA silencing. In order to prove this prediction, single stranded RNA ssRNA, purified sense strand and antisense strand of a dsRNA duplex, or double stranded RNA were injected into the body cavity or gonads of adult _C. elegans_ (Fire et al, 1998). As a control _C. elegans_ were additionally fed with dsRNA-expressing _Escherichia Coli_ bacteria.

All delivered RNA's targeted the 742 nucleotide segment of the unc-22 gene which encodes an abundant but nonessential myofilament protein in _C elegans_ (Fire et al, 1998. Sidahmed and Wilkie; 2010).

Down regulation of unc-22 expression was achieved systematically in all worms seen by a characteristic twitching phenotype. This twitching phenotype was still seen in further generations of _C elegans_ to an even higher intensity than in parents (Fire et al, 1998). This shows that RNAi capabilities could be epigenetically inherited onto next worm generation by parents.

In 2002 RNAi was named 'Technology of the year' by the high impact Science magazine (American association for the advancement of Science [AAAS]; 2002) (figure 9).

In 2006 Andrew Fire and Craig Mello, were awarded the Nobel Prize in Medicine or Physiology for their discovery of "RNA interference – gene silencing by double-stranded RNA (Nobel Committee for Physiology and Medicine; 2006) (see figure 9).

Figure 9 Evolution of RNAi
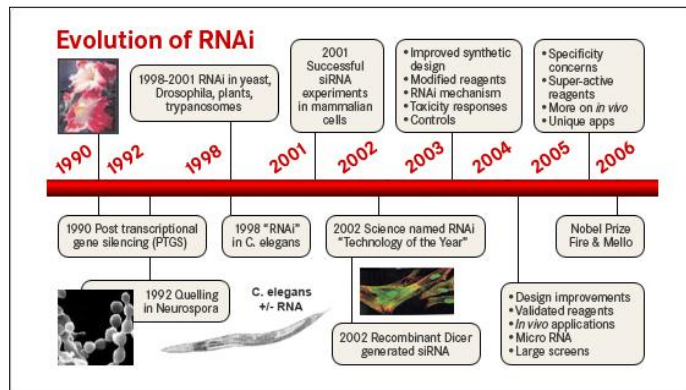
Fig. 9 shows the evolution of RNAi indicating major discoveries and milestones of recent years. Source of figure: Lifetechnologies.com

The revolutionary finding of Andrew Fire and Craig Mello opened the doors to a completely new field. The application of RNAi in mammals has the potential to allow the systematic analysis of gene expression and holds the possibility of therapeutic gene silencing (Dyxhoorn, Novina, Sharp; 2003).

Additionally RNAi provides a valuable insight into evolution, as RNAi is evolutionary conserved in prokaryotes and eukaryotes, and serves as a defense mechanisms of organisms to fight off foreign molecules i.e. viruses and transposons to maintain genome integrity.

Furthermore RNAi has several advantages over traditional complete gene knockout approaches. RNAi's advantages are that it is an easier, less time and money consuming alternative to gene knockout (RNA interference guide, Ambion, Inc 2006) .

1.4.2 Signature components of RNA silencing

Over the years after the discovery of RNAi in C. elegans, a considerable progress in understanding RNAi mechanism has been made.

Research in model systems such as fission yeast *Sacchoromyces pombe*; plant *Aradopsis Thaliana;* fruit fly *Drosophila melanogaster*; nematode worm *Caenorhabditis elegans* and mammals, which all observe RNA silencing, paved the way in finding integral parts of RNAi (Meister and Tuschl; 2004).

RNAi is a stepwise process which requires signature components: **short non-coding RNA, Dicer and Argonaute.**

1. **Short non-coding RNA:**

DsRNA is the trigger of RNAi (Fire et al; 1998). Although at the time of this discovery, the underlying molecular mechanism for the dsRNA-dependent RNAi phenomenon was unclear, further research by other laboratories aided in explains.

In 2000 and 2001, two publications showed that RNAi is mediated by products of dsRNA cleavage named siRNA (Zamore et al; 2000. Elbashir et al; 2001a).

SiRNA are small noncoding RNA with molecular hallmarks of 21-24 nucleotide length, a 19 nucleotide duplex region, 5' phosphorylated ends and 3' unphosphorylated dinucleotide 2nt overhangs (Dykxhorn et al; 2003. see figure 11).

Figure 10: Molecular hallmarks of siRNA

Fig. 10 highlights the molecular hallmarks of siRNA. siRNA have a characteristic 21-23 nucleotide length. Molecular hallmarks of siRNA comprise of 5' phosphorylated ends, a 19nt duplexed region and 3'-dinucleotide unpaired and unphosporylated ends. The sense strand or passenger strand is shown in purple, the anti-sense or guide strand in black. Abbreviations 5' or 3' are reference to the 5' and 3' ends of siRNA strands, p = phosphate group, OH = hydroxyl group. Picture modified from Dykxhoorn and Sharp; 2003.

The discovery of siRNA was accomplished with Drosophila embryo lysates which recapitulate RNAi in vitro; providing a tool for biochemical analysis of the mechanism of RNAi (Zamore et al 2000 and Elbashir et al; 2001a). Using drosophila in vitro system, Zamore et al 2000 and Elbashir et al; 2001a, in summary, demonstrated that

- long dsRNA ≥ 150bp, is needed for efficient siRNA generation in Drosphila
- double-stranded RNA directs the ATP-dependent cleavage of mRNA at 21 to 23 nucleotide intervals

In accordance to Drosophila in vitro RNAi, it was shown that siRNA mediate RNAi in cultured mammalian cells (Elbashir et al 2001b. Figure 9).

This finding is of critical importance as it shows that RNAi can be induced in vitro in human cells enabling the research of human gene functions.

So far it is well established that Dicer is the enzyme necessary for dsRNA cleavage into 21-23nt siRNA and that siRNA needs to be unwound into two strands to elicit RNAi effect (Bernstein et al; 2004. Carthew and Sontheimer; 2009).

The siRNA duplex consists of a guide strand aka anti-sense strand and a passenger strand aka sense strand (Matranga et al; 2005. Schwarz et al; 2005).

The single-stranded antisense strand of siRNA is mostly used to guide the multinuclease RNAi effector complex; RNA induced silencing complex RISC to target mRNA (Martinez et al, 2002). A guide strand is antisense meaning in RNAi context that the guide strand has a sequence exactly opposite to a target mRNA molecule, enabling binding to mRNA to prevent proteins from being made (Genetics home reference [GHR]). Once bound to complementary mRNA, the Argonaute protein in RISC takes action on target mRNA to induce the RNAi end effect, translational repression or mRNA cleavage.

Interestingly even before the unraveling of siRNA in *Drosophila* in the year 2000, another small non-coding RNA fragment, known as miRNA, was revealed in *C elegans* as of 1993. Just in recent years the relation between siRNA and miRNA could be figured out i.e. both are small non-coding RNA involved in posttranscriptional gene silencing processes, have a short nucleotide length (~22 nt) with similar end structure, 3'-dinucleotide overhangs needed for RNAi machinery recognition, use inherent antisense sequence to bring about translational repression effect and require processing by Dicer.

The identification of the first miRNA, the product of the lin-4, was accomplished in the Ambros Laboratory at the University of Massachusetts.

The heterochronic gene Lin-4 is essential for the normal temporal control of diverse postembryonic developmental events in C. elegans (Lee, Feinbaum and Ambros; 1993). Lin-4 acts by negatively regulating the level of Lin-14 protein creating a temporal decrease in Lin-14 proteins starting in the first larval stage (Lee, Feinbaum and Ambros; 1993). The downregulatory effect of Lin-4 on Lin-14 proteins is achieved through the

antisense complimentarity of products of Lin-4 to repeated sequence elements in the 3' untranslated region UTR of Lin-14 mRNA.

Even though a third category of small non-coding RNA exists, piwi-interacting RNA (piRNA), this thesis will only discuss the siRNA and miRNA.

The listed siRNA and miRNA findings provided the basis for the discovery of subsequent signature components of RNAi; Dicer and Argonaute.

2. **Dicer**

The products of dsRNA or pre-miRNA transcript processing, siRNA and miRNA share molecular hallmarks of 5' phosphorylated ends and 3'-dinucleotide unpaired, unphosphorylated overhangs.

RNA molecules with these properties are standard cleavage products of RNase H nucleases (Song, Smith, Hannon and Joshua-Tor; 2004). In particular, the bidentate dsRNA-specific RNase-III-type endonuclease Dicer has been implicated for cleaving exogenous dsRNA and endogenous dsRNA into siRNA and miRNA (Bernstein, Caudy, Hammond and Hannon; 2001. Fukanaga et al; 2012).

Dicer mRNA is expressed at all developmental stage (Bernstein, Caudy, Hammond and Hannon; 2001). Dicer is an evolutionarily conserved protein long believed to localize only in the cytoplasm. A recent publication contradicts this belief stating that human Dicer can also localize in the nucleus by a nuclear localization signal found in one of its domains (Doyle et al; 2013).

Dicer consists of multiple domains with a total size of ~ 150-220kD (Welker et al; 2010. Lau et al 2012). Depending on species, variations of Dicer domains can exist which reflect in the overall size of Dicer i.e. large and complex higher eukaryotes have more Dicer domains than lower eukaryotes.

Human Dicer has five domains, Helicase, DUF283, PAZ, RNaseIIIa/ IIIb and dsRBD domain, while protozoan parasite *Giardia intestinalis* Dicer has two domains, PAZ and RNaseIIIa/ IIIb (figure 12).

Despite *Giardia* Dicer lacking three domains, in contrast to its human variant, it still remains active (McRae et al; 2006). *Giardia* Dicer structure provided the fundamentals for the resolution of human Dicer structure (figure 12).

Human dicer domains are arranged in following primary sequence from amino-N-terminus to carboxyl-C-terminus:

1. **Helicase domain:**

   The Helicase domain forms a clamp-like structure adjacent to the Dicer RNaseIII active site, facilitating recognition of pre-miRNA loops or translocation on long dsRNAs (Lau et al 2012)

2. **Domain of unknown function 283, DUF283:**

   The function of DUF283 is unknown. What is known is that DUF283 is an evolutionary conserved domain spanning approximately 100 amino acids (McRae et al 2006)

3. **Piwi-Argonaute-Zwille, PAZ, domain:**

   The PAZ domain is evolutionary conserved in PIWI, Argonaute and Zwille proteins (Carthew and Sontheimer 2009). The domain derives its name from these proteins. PAZ domain harbors a vital oligonucleotide/ oligosaccharide binding OB fold, needed for recognizing dsRNA ends having a 3' dinucleotide overhang (McRae et al 2006).

4. **Ribonuclease RNaseIIIa and RNaseIIIb domain:**

   RNaseIIIa and RNaseIIIb domains are aligned after each other in Dicer (see figure 4). Both domains contain active sites crucial for Dicer catalytic activity due to divalent metal ion binding site for Dicer cofactors.

   The main cofactor for Giardia Dicer dsRNA cleavage is Magnesium Mg^{2+}, alternatives could be divalent cations like Manganese Mn^{2+}, Nickel Ni^{2+}, or Cobalt Co^{2+} (McRae et al; 2006).

   Once a cofactor is bound to Dicer active site, the amino acids Glutamine and asparagines in the active site allow dsRNA cleavage (McRae et al; 2006).

5. **Double stranded RNA binding domain dsRBD:**

   DsRBD is needed for Dicer binding to dsRNA substrates and contains a nuclear localization signal for transport of Dicer from the cytoplasm to the nucleus (Doyle et al; 2013).

The interplay of these domains allows Dicer to act as a 'molecular ruler' to precisely dice long exogenous or endogenous dsRNA into smaller 21-23nt RNA fragments.

Dicer gene number and protein interaction partners can vary from species to species. Those species with more than one Dicer gene, commonly display functional specificity for a non-coding RNA e.g. two Dicers exist in *D.* melanogaster, Dcr1 and Dcr2. Dcr1 is specific for miRNA while Dcr2 is specific for siRNA.

In regards to different Dicer interaction partners, Drosophila Dcr1 interacts with Loquacious whereas Dcr2 interacts with R2D2 (Sidahmed and Wilkie; 2010).

The interaction partner of Human Dicer is TAR RNA binding protein TRBP.

Loquacious, R2D2 and TRBP share in common an encoded dsRNA binding domain and function to transfer siRNA and miRNA to RISC.

To analyze the function of a gene, common scientific approaches are loss-of-function studies by complete gene knockout from the genome.

Dicer loss-of-function studies resulted in embryonic lethality of knockout mice indicating that Dicer is essential for development (Devasthanam and Tomasi; 2013). As a way to avoid premature mouse death, the Dicer gene was deleted in adult stage by Cre-Lox recombination (for further details on Cre-LoxP recombination, see Pharmacodynamics and Pharmacokinetics lecture notes on mouse models).

As expected, mouse embryonic stem cells with Dicer floxed allele, Dicer$^{flx/flx}$, experience accumulation of siRNA after viral infection (Maillard et al; 2013).

Adult mice with Dicer$^{flx/flx}$ show impaired differentiation of cells in the myeloid lineage leading to early death; and impaired immune response upon antigen introduction into system (Devasthanam and Tomasi; 2013).

Furthermore, *S. pombe* Dicer$^{-/-}$cells (as well as Argonaute$^{-/-}$ and RNA-dependent RNA polymerase RdRP$^{-/-}$) encounter misregulation of heterochromatic silencing and Histone H3 Lysine methylation (Volpe et al; 2002).

Figure 11: Human Dicer versus Giardia Dicer
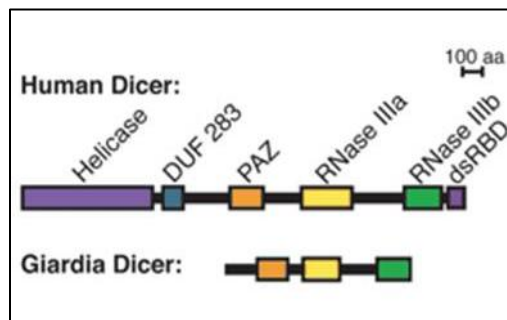
Fig. 12 shows the structure of Human Dicer in opposition to *Giardia* Dicer. Respective domains are highlighted in different colors for easy differentiation. Source of figure is McRae et al 2006.

3. **Argonaute**

Argonaute, Ago, are another example of an evolutionarily conserved nuclease found in RNA silencing. Ago are the functional elements of RISC needed for the interaction with siRNA, miRNA and respective complementary target mRNA (Target identification and validation; chapter 4).

RISC has a size of ~ 360kD (Nykaenen, Hailey and Zamore: 2001).

Co-immunoprecipitation analyses present RISC carrying Ago to be tightly linked to polyribosomes or the ribosomal small subunit in cytoplasm (Rao, Vorhies, Senzer and Nomanaitis; 2009).

Argonaute has two roles in RNAi. The first Ago role is Adenosine triphosphate ATP-dependent cleavage of the passenger strand in siRNA/ miRNA duplex, leading to its ejection from RISC and degradation (Nykaenen, Hailey and Zamore; 2001. Rand et al 2005. Meister and Tuschl; 2004).

Some publications believe that siRNA and miRNA duplex have to undergo ATP-dependent unwinding by an Ago helicase to release the passenger strand (Pfeffer, Meister, Landthaler and Tuschl; 2005. Sidahmed and Wilkie; 2010).

Anyway, passenger strand ejection is necessary for the full activation of RISC to enable processing of the single stranded guide strand.

Based on the thermodynamic stabilities of 5' base pair siRNA or miRNA ends either the antisense or sense strand can be incorporated into RISC (Schwarz et al; 2003). Although if the sense strand is used for target mRNA recognition, RNAi off specific effect increase.

Argonaute's second role is to cleave target mRNA by the guide of an antisense guide strand (Hutvagner and Simard; 2008).

Guide strand binding to complementary mRNA occur at translation when mRNA is being translated to protein on the ribosome (Pfeffer, Meister, Landthaler and Tuschl; 2005). A guide strand 5' end seed region, ranging from nucleotides 2-8, is necessary for Watson Crick base pairing to 3' mRNA UTR.

Ago cleaves target mRNA in the middle of the complementary region, ten nucleotides upstream of the nucleotide paired with the 5' end of the guide strand (Meister and Tuschl; 2004). Depending on the degree of sequence complementarity, complete or partial complementarity, either target mRNA degradation or translational repression are evoked (Ouellet and Provost; 2010).

Ago can in addition to cytoplasm also localize in the nucleus.

Variation in Ago gene number can occur in species. Eight Argonaute genes exist in humans, five in *Drosophila*, ten in *A thaliana*, one in *S pombe* and 26 in *C.elegans*. (Hutvagner and Simard, 2008).

4 of the 8 human Argonaute genes encode Argonautes needed for siRNA or miRNA cleavage (Sidahmed and Wilkie; 2010). These are Ago1, Ago 2, Ago3 and Ago4.

Among human Ago1-4, only Ago 2 possesses the ability to cleave siRNA due to an intrinsic active site (Gavrilov and Saltzman; 2012. Sidahmed and Wilkie; 2010). Ago2 loses its siRNA specificity when a missense mutation is even introduced near to the Ago2 gene leading to conversion to Ago1 (Song, Smith, Hannon and Joshua-Tor; 2004).

Ago1, Ago3 and Ago4 specifically use miRNA (Sidahmed and Wilkie; 2010).

Ago1 has additionally been shown to act in co-transcriptional gene silencing CTGS in *S. pombe a mechanism* used for maintaining heterochromatin state (Castel and Martienssen; 2013)

But how does Ago molecular architecture look like?

An answer to this question was provided by the crystal structure of prokaryotic *Pyrococcus furiosus* Ago. The primary sequence of Ago *Pyrococcus furiosus* is divide into an N-terminal, PAZ, Mid and PIWI domain (Song, Smith, Hannon and Joshua-Tor; 2004. Gavrilov and Saltzman; 2012. See figure 11).

Human Ago has the same domains as Ago *Pyrococcus furiosus* (Schirle and McRae; 2012). Once translated into protein, human Ago assumes a bi-lobed conformation, identical to its bacterial form (figure 13).

The most important domains for Ago 'slicer' activity are the evolutionary conserved PAZ and PIWI domain.

A PAZ domain is as well present in Dicer. PAZ is needed for siRNA, miRNA and mRNA binding (McRae et al 2006).

PIWI domains are unique to Ago nuclease (Rand et al; 20005). PIWI domain carry the Ago active site needed for small RNA cleavage (Gavrilov and Saltzman; 2012).

The remaining Ago domains, N-terminal and mid domain, are suggested as base of Ago to properly position guide strand for cleavage by the PIWI domain (see figure 13).

The PIWI domain of the fly Ago1 directly interacts with GW182, a protein that is characteristic of cytoplasmic processing bodies, P-bodies (Hutvagner and Simard; 2008). Of recent Ago2, Ago3 and Ago4 have also been implicated with GW182 interaction (Kulkarni, Ozgur and Stoecklin; 2010).

Figure 12: Argonaute primary sequence and model for siRNA guide strand tethering by Ago2 and target mRNA recognition and slicing
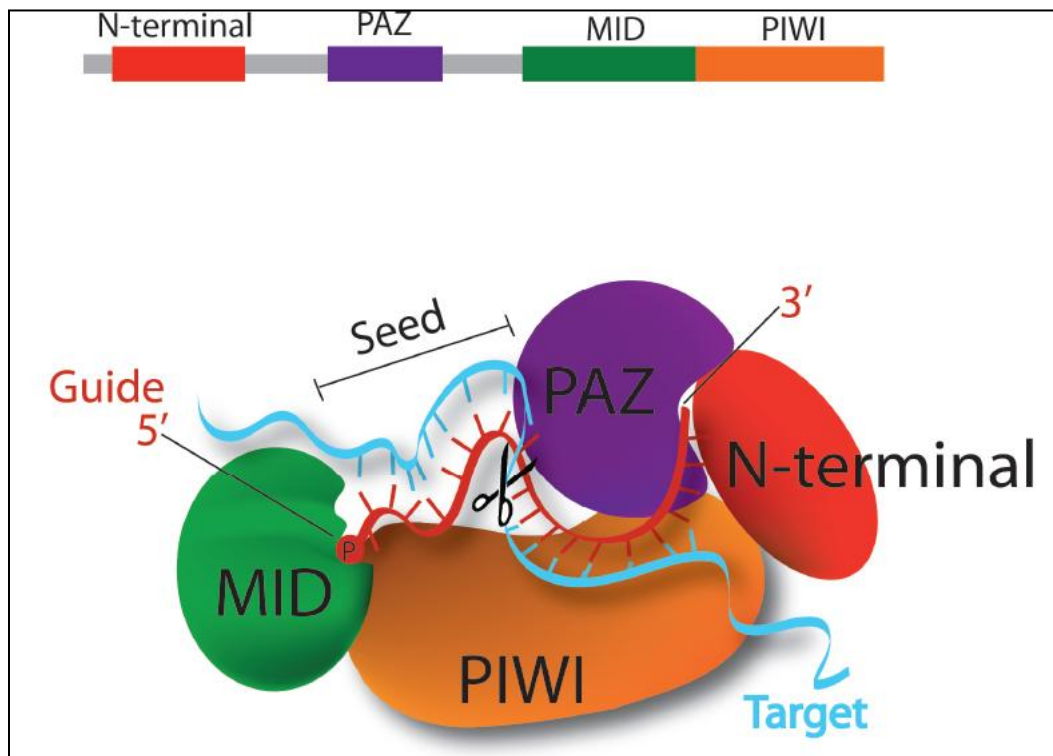
Fig. 13 shows in the upper part the Argonaute primary sequence and in the lower part the model for siRNA guide strand tethering by Ago2 and target mRNA recognition and slicing. Ago primary sequence is divided into an N-terminal domain, PAZ domain, MID domain and PIWI domain (differentiated with colors). In the model the guide strand 5' end and 3' end are bound by MID domain and PAZ domain respectively enabling seed region dependent Ago2 slicing. Source of figure is Gavrilov and Saltzman; 2012.

The duty of GW182 is to recruit Ago2, along with associated RISC, guide strand and mRNA, to P bodies (Kulkarni, Ozgur and Stoecklin; 2010. figure 12c).

In P bodies mRNA degradation or mRNA translational repression, the two end effects of RNAi, are carried out by P-body associated translation repression and mRNA decay machinery (Parker and Sheth; 2009).

P body enzymes engage in deadenylation-decapping 5'-3' pathway of mRNA degradation. P bodies function in contrast to endosomes another cytoplasmic site of mRNA degradation which specializes in deadenylation-decapping in a 3'-5' manner.

P-bodies are cytoplasmic foci visible by light microscopy in somatic cells of vertebrate and invertebrate origin as well as in yeast, plants and trypanosomes (Kulkarni, Ozgur and Stoecklin; 2010. Figure 14a). Markers of P bodies are enhancer of decapping Hedls and exoribonuclease Xrn1 (Kulkarni, Ozgur and Stoecklin; 2010. Figure 14a).

P-bodies accumulate short half lived mRNA. It is believed that P bodies help in storing translationally repressed or degraded mRNA to maintain a feedback loop between mRNA translation and degradation to ensure that only a certain ration of mRNAs are translated at a certain time (Beckham and Parker, 2006). Examples can be seen, depending on cellular need, when once translationally repressed mRNA can be recycled to return to translation or decapped and degraded by 5'-3' exonuclease Xrn1 (Beckham and Parker, 2006).

Figure 13: P bodies and their cytoplasmic localization
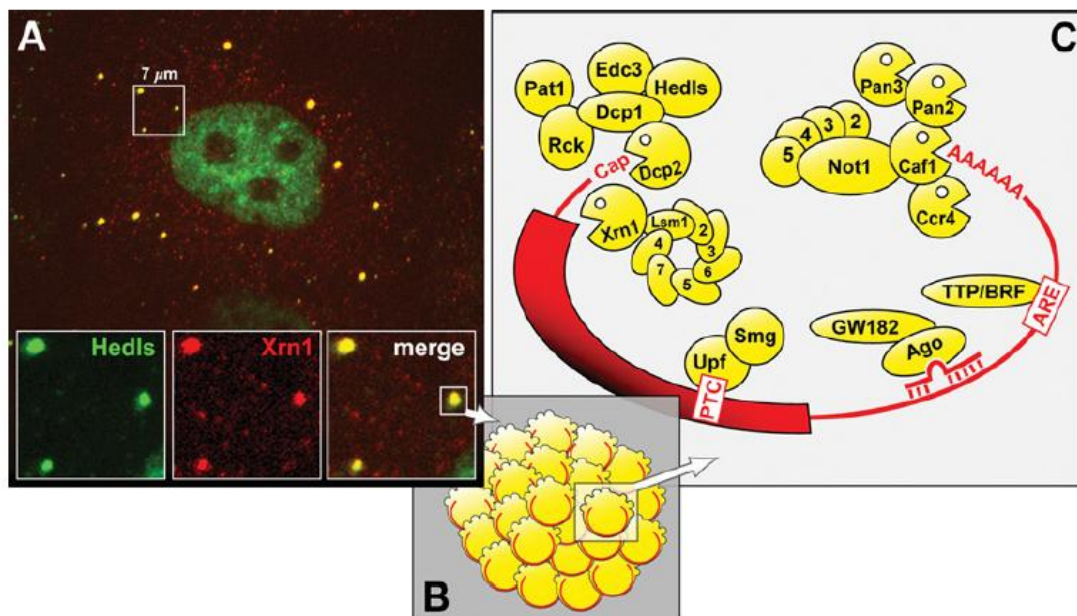
Fig. **14A** shows P-bodies (yellow) in the cytoplasm. Hedls and Xrn1, P- body markers, were respectively stained with green and red fluorescent dyes and merged resulting in yellowish color of P bodies. Figure **14B** shows an accumulation of P-bodies with highlight of one P body shown in figure **14C**. Figure **14C** shows an example of P body contents. This includes proteins of mRNA translation repression and mRNA degradation machinery acting on an mRNA with characteristic cap and poly-A-tail. Abbreviations: PTC = premature termination codon, ARE = AU-rich element. Source of figure is Kulkarni, Ozgur and Stoecklin; 2010.

1.5   SiRNA pathway versus miRNA pathway

siRNA and miRNA bear a lot of similarities in a multitude of points. But essentially the ultimate fates of siRNA and miRNA are different.

In prior sections of this Master thesis, the similarities of the siRNA and miRNA pathway were discussed; in the following sections the differences will be listed.

1.5.1   siRNA pathway

The siRNA pathway can start in two ways to generate long dsRNA in the cytoplasm (Pfeffer, Meister, Landthaler and Tuschl, 2005. Figure 7)

1. Injection of viral RNA's
2. Transfection of exogenous RNA

Long dsRNA is known to be the substrate of Dicer.

At first, Dicer binds dsRNA via its associated dsRNA binding partner, the protein varies depending on species and Dicer gene. Then Dicer cleaves bound long dsRNA into characteristic 21-23nt siRNA with 5' phosphorylated ends and 3' dinucleotide overhangs.

5' phosphorylated ends are a prerequisite for siRNA function (Nykaenen, Hailey and Zamore; 2001). With the help of Dicer interaction partner's, siRNA is transferred to small interfering RNA induced silencing complex siRISC.

Ago2 nuclease in siRISC is specific for siRNA duplex cleavage. Ago2 siRNA specificity can be severely influenced by even slight variation in its genomic environment. For example when a missense mutation is introduced just near to the Ago2 catalytic PIWI domain catalytic activity is so severely impaired that siRNA can no longer be used for mRNA degradation (Song, Smith, Hannon and Joshua-Tor; 2004).

Ago2 at first cleaves the passenger strand leading to its removal from siRISC. Once the passenger strand is discarded siRISC becomes fully activated.

With the guidance of a single stranded guide strand, siRISC is guided to target mRNA undergoing translation on the Ribosome. The antisense guide strand needs its seed region to recognize and bind fully complementary mRNA regions.

P body protein GW182 interacts with Ago2 and recruits RISC along with linked mRNA and guide strand to P-bodies.

In P bodies Ago2 cleaves target mRNA for mRNA degradation.

In the case of C. elegans RNAi can be amplified and affect both somatic and germ cells leading to epigenetic inheritance of RNAi from C. elegans parent to offspring (Fire et al 1998). Epigenetic inheritance is made possible by RNA-dependent RNA polymerase RdRP, an enzyme that can use generated primary siRNA as a primer to synthesize new long dsRNA (Yu, DeRuiter and Turner; 2002). New dsRNA can undergo another cycle of siRNA pathway with the production of secondary siRNAs.

RdRP is not encoded in the human genome thus no RNAi amplification in human exists (National Center for Biotechnology Information [NCBI]).

The biologic function of siRNA pathway is to act as an antiviral defense mechanism. By means of RNAi cells acquire the ability to protect themselves against viral infection. RNAi machinery can recognize and destroy foreign viral mRNA undergoing translation. This means RNAi enables the cell to potently inhibit viral replication to prevent assembly of new viral particles able to infect other cells.

However as an RNAi counter defense mechanism, members of different viruses encode proteins known as viral suppressors of RNAi VSR (Maillard et al; 2013).

The purposes of VSR's are to suppress the activity of specific components of RNAi to allow unlimited viral replication e.g. VSR B2 protein encoded by Nodamura Virus inhibits Dicer activity (Li et al; 2013. Maillard et al; 2013).

Antiviral RNAi has been proven in lower eukaryotes i.e. plants, Drosophila, C elegans. In mammals, there are a few controversial publications on antiviral RNAi in mammalian cells (Maillard et al; 2013. Li et al 2013). Two studies using baby hamster kidney cells and mouse embryonic stem cells showed accumulation of viral derived siRNA after Nodamura Virus infection. (Maillard et al; 2013. Li et al 2013). The sparked controversy

was due to the cells used in stated publications which are in a developmental stage where cells do not possess immune response activity against viruses. This raises the question if baby hamster kidney cells and mouse embryonic stem cells are the optimal cell models for analyzing RNAi's role in antiviral immunity of mammalian cells.

It is believed that RNAi assists the mammalian immune system in antiviral defense

1.5.2 Immune system stimulation by viral DNA

The mammalian immune system is in constant surveillance of body compartments to detect foreign molecules (Murphy; 2012). Whenever a foreign molecule is encountered the task of the immune system is to destroy it through diverse immune responses.

Evolutionary ancient Toll-like receptors TLRs play a critical role in innate immune response cellular resistance against viral, bacterial and fungal infection (Murphy; 2012). 11 TLRs exist in humans and 13 in mice that can be found either extracellular on cell membranes or intracellular in endosomal membranes (AbD serotec MorphoSys UK Ltd. figure 14). TLRs are expressed on immune cells such as natural killer cells, plasmacytoid dendritic cells, bone marrow B cells, eosinophils and basophils (Murphy; 2012).

All TLR share in common that they are one-pass transmembrane protein divided into two parts by transversed membrane, can sense pathogen-associated molecular patterns PAMP, form dimers after activation (hetero- or homodimers) and can induce cytokine production (Murphy; 2012).

Intracellular trafficking of a virus can start by three ways: phagocytosis, receptor-mediated endocytosis or macropinocytosis (Murphy; 2012). All intracellular trafficking ways ultimately result in cytoplasmic membrane enclosed vesicles known as endosomes (Dominska and Dykxhorn; 2010)

In the endosome intracellular TLR-3 responds to viral dsRNA, TLR-7 and TLR8 react to viral ssRNA (Murphy; 2012).

TLR-3, TLR-7 and TLR-8 intracellular part contains Leucine rich repeats LRR predicted to aid in target recognition while the TLR's endosomal part carries a Toll interleukin 1 receptor TIR domain (Murphy; 2012).

TLR ligand binding results in receptor activation and a conformational change allowing the Toll-interleukin1 receptor TIR domain in TLR cytoplasmic tail to interact with other downstream TIR domain containing proteins i.e. myeloid differentiation factor 88 Myd88 (AbD serotec MorphoSys UK Ltd. Figure 14).

Through protein-protein interactions ultimately the release of transcription factor NF-kB is triggered, leading to NF-kB translocation to the nucleus to induce cytokine production (Murphy; 2012).

Cytokine can mediate Apoptosis of viral infected cells, confer cell mediated immunity or lead to bacterial death (in case of a bacterial infection) (AbD serotec MorphoSys UK Ltd. Figure 14).

Figure 14: Toll-like receptors and mediated cytokine immune response
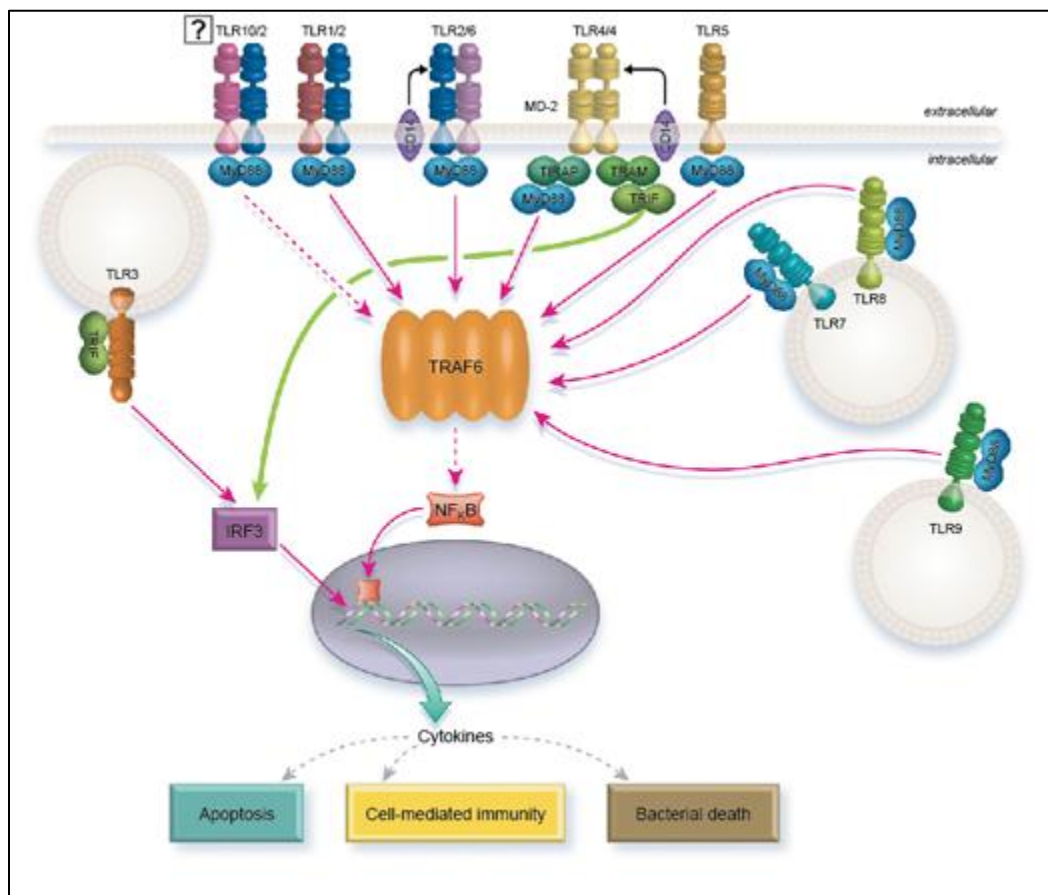
Figure 14 shows the Toll-like receptors and mediated cytokine immune response. The cellular locations of TLR1-10 are indicated in this figure in addition to the respective adaptor proteins/ transcription factors needed for inducing Cytokine production. Source of figure: AbD serotec MorphoSys UK Ltd.

1.5.3 miRNA pathway

miRNAs have been implicated in cellular roles as diverse as developmental timing in worms, cell death and fat metabolism in flies/ mice, haematopoiesis in mammals, and leaf development and floral patterning in plants (Griffiths-Jones et al; 2005. Ramirez et al; 2013). There is increasing evidence that miRNAs might also function in human cancer (Ouellet and Provost; 2010. Griffiths-Jones et al; 2005).

There are currently 24521 miRNA entries in miRBase, a searchable database of published miRNA sequences and annotations [miRNA database [miRBase]; 2013].

The miRNA pathway starts with the transcription of primary miRNA transcript in the nucleus (Pfeffer, Meister, Tuschl and Landthaler; 2005. figure 15). In the initial step of miRNA biogenesis, primary miRNA transcript is processed into pre-miRNA by RNaseIII Drosha and its associated DGCR8 (Pfeffer, Meister, Tuschl and Landthaler; 2005. figure 15).

DGCR8 function as a molecular anchor necessary for the recognition of pri-miRNA at dsRNA-ssRNA junction and directs Drosha to cleave 11 base pair away from the junction to release hairpin-shaped pre-miRNAs that are subsequently cut by cytoplasmic Dicer to generate mature miRNAs (UniProt; 2013).

The Dicer generated miRNA-miRNA* duplex is unwound by an ATP-dependent Helicase to release the passenger strand for degradation (figure 15) (Pfeffer, Meister, Tuschl and Landthaler; 2005. Figure 15). The remaining single stranded guide strand of miRNA-miRNA* duplex is used by RISC to induce, depending on complementarity, translational repression or mRNA degradation.

Usually miRNAs have an incomplete complementarity to their target mRNA sequence this results in translational repression of mRNA encoded sequence (Ouellet and Provost; 2010. Figure 15).

At times when miRNA has complete complementarity, mRNA cleavage by Ago and subsequent mRNA degradation can occur (Pfeffer, Meister, Tuschl and Landthaler; 2005. Figure 15).

Figure 15: The siRNA and miRNA pathways
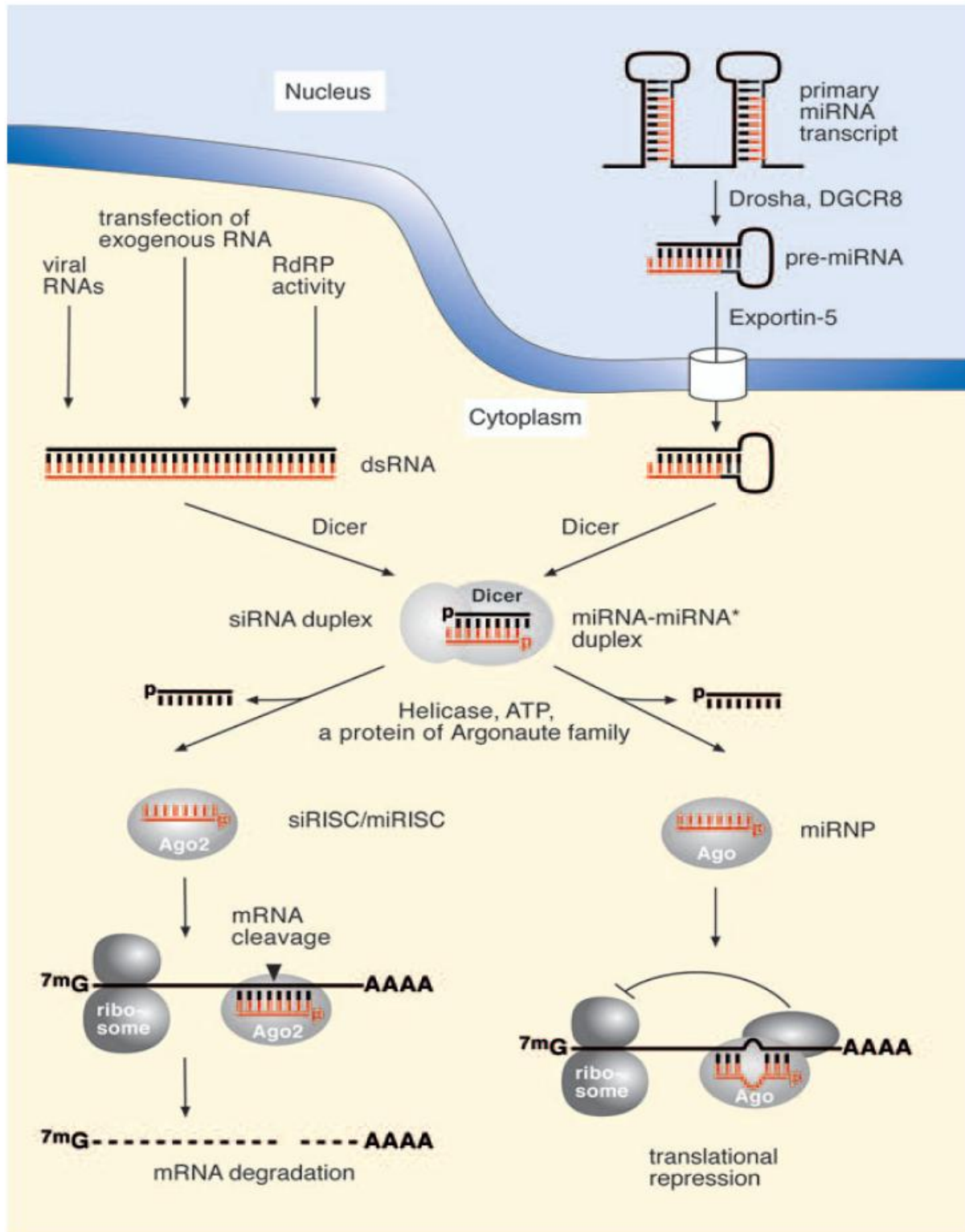
Fig. 15 shows the siRNA and miRNA pathways in the cell indicating points of RNA processing and RNAi effects. Source of figure: Pfeffer, Meister, Tuschl and Landthaler; 2005.

1.6 Experimental realization of RNAi

The groundbreaking discovery that synthetic siRNAs can be used in mammalian cells without triggering immune response (Elbashir et al; 2001a and 2001b), supported the major advance in experimental RNAi applications over the last decade.

To date there are five ways to experimentally realize RNAi in order to analyze gene function (Ambion; 2006). These include (figure 16):

1) Plasmids and viral vectors expressing shRNAs
2) In vitro transcription
3) siRNA prepared by endoribonuclease
4) PCR derived siRNA cassette
5) Synthetic siRNA

Figure 16: Ways of experimental RNAi
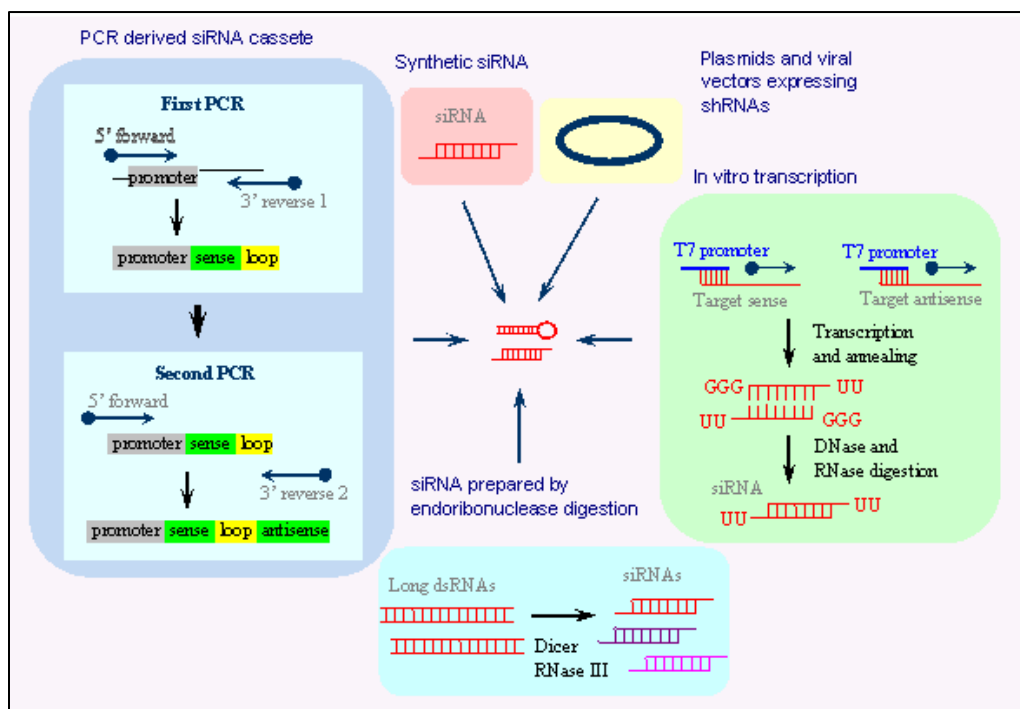
Fig.16 shows the five ways of experimental RNAi leading to the generation of shRNA or siRNA. Source of figure: Ambion, Inc.

1.6.1 Viral vectors expressing shRNAs

Using viral vectors is advantageous to using synthetic duplexes synthetic duplexes for inducible knockdown, long-term knockdown and for transfecting difficult or hard-to-transfect cells (Success with lentiviral based RNAi online seminar, Invitrogen™)

Viral vectors are based on Adenovirus, Retrovirus and Lentivirus Success with lentiviral based RNAi online seminar, Invitrogen™). The Lentivirus is the only virus capable to integrate into the genome of both dividing and non-dividing cells i.e. neural cells.

In order to insert target gene sequence into a vector following steps have to be followed:

1) **Transfect packaging cells:** Three vectors have to be cotransfected into packaging cells when lentivirus-based constructs are used. Two vectors carry elements needed for lentiviral replication and packaging in transfected cells i.e. VSV-G, Gag, Pol, Rev and Tat, while one vector solely carries cDNA or shRNA of interest (Labome 2013; figure 17).

   In packaging cells cDNA/ shRNA is packaged into newly generated virions.

   For Retrovirus one vector containing cDNA/ shRNA is needed (Labome 2013; figure 17).

2) Collect virus particle: 48 hours after transfection virus particles can be collected in infected media of packaging cells (Broad Institute; USA. Stewart et al; 2003).

3) Transduce target cells: cDNA/ shRNA be delivered into target cells upon infection with viral particle carrying cDNA/ shRNA sequence (Labome 2013; figure 17).

Figure 17: Viral vectors to express shRNAs for RNAi
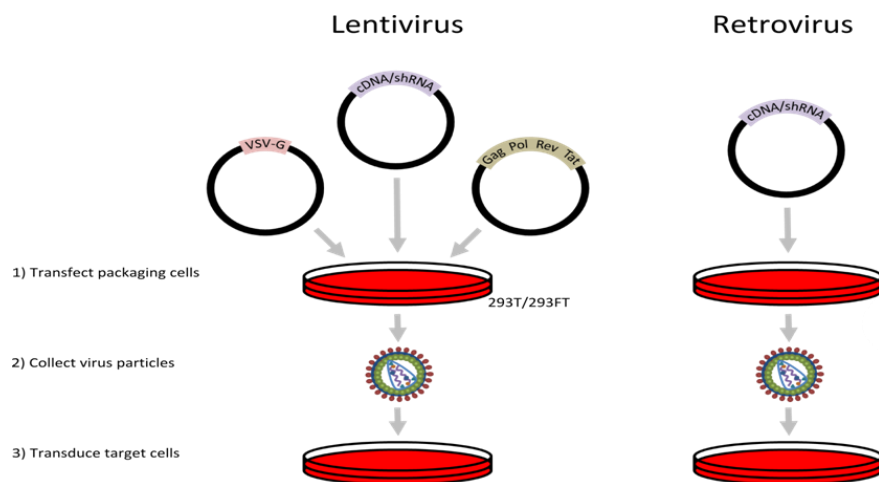
Fig. 17 shows lentiviral and retroviral based vectors to express cDNAs/ shRNA. Experimental steps to acquire virus particles and transduce target cells are listed. Source: Labome, 2013.

1.6.2 Synthetic siRNA

Synthetic siRNA have the advantage over viral vectors expressing shRNAs, that they can immediately be used by cellular RNAi machinery and cannot trigger adverse immune responses in mammalian cells (Aigner; 2007. Behlke; 2006).

There are vendors available that can produce siRNA for research based on target gene and an algorithm to avoid immune stimulatory sequences.

Synthetic siRNA do not require Dicer processing since siRNA can directly be integrated into RISC to achieve mRNA degradation. Synthetic siRNA is a negatively charged molecule which renders siRNAs incapable of diffusing through the, also negatively charged, cell membrane to its site of action in the cytoplasm (Nguyen and Szoka; 2012). siRNAs are therefore dependent on different delivery strategies to deliver siRNA into the cell.Amongst these strategies are conjugating siRNA to molecules that are known to bind to the cell membrane or by enveloping siRNA with certain materials or reagents. siRNA can be linked to cholesterol, a dynamic polyconjugate, aptamers, antibody or ligand (Dominiska and Dykxhoorn; 2010. Figure 18).

An example of antibody-conjugated siRNA cell delivery can be seen in figure 18. The siRNA-conjugated antibody is specific against a receptor on the cell membrane enabling receptor recognition and binding by antibody. Through receptor-mediated endocytosis, receptor and bound antibody-conjugated siRNA can be ingested into the cell (figure 18). The endocytic vesicle in which receptor and bound antibody-conjugated siRNA is situated can become progressively more acidic with development into early endosome, late endosome/ multivesicular body MVB and lysosome (Dominiska and Dykxhoorn; 2010. Figure 18).

It is important that siRNA escapes endocytic vesicle before progression to Lysosomes otherwise siRNA will be degraded (Nguyen et al; 2012. figure 10).

If endosomal escape is successful siRNA can be loaded onto RISC-loading complex RLC, transferred to RISC to ultimately achieve mRNA degradation.

Endosomal escape is the rate limiting step for RNAi.

Figure 18: Examples of siRNA-conjugates and rate limiting endosomal escape
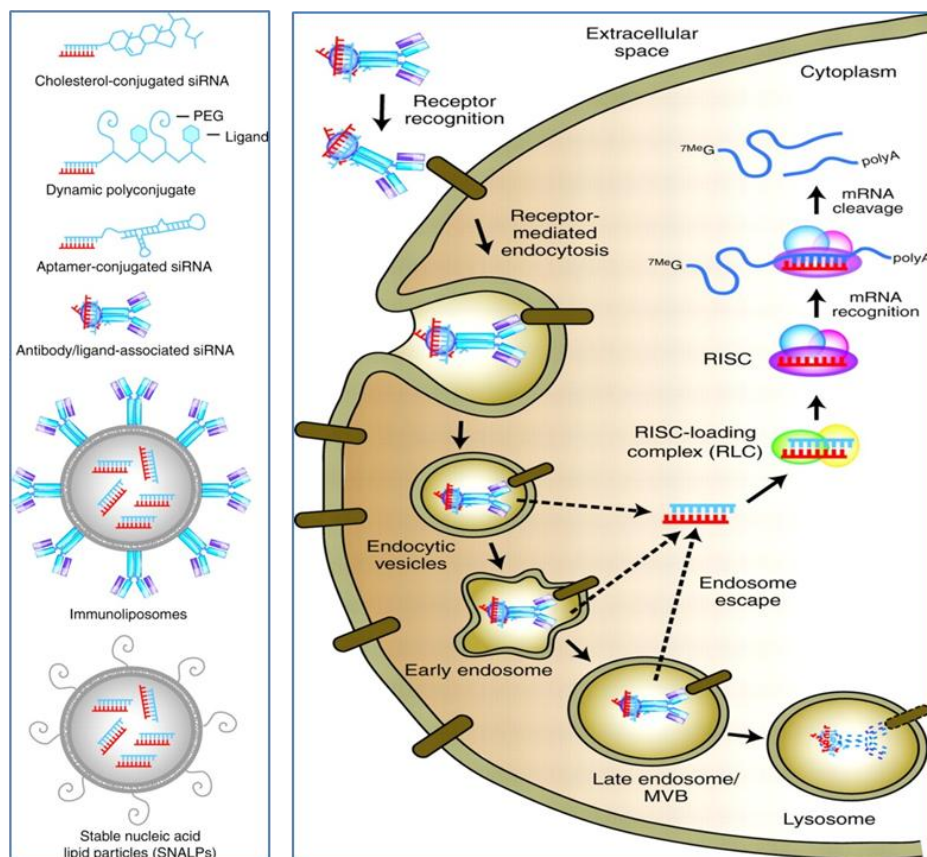
Fig. 18 illustrates examples of siRNA-conjugates used to achieve siRNA uptake by cells. The rate limiting step of RNAi is endosomal escape. Endosome progerseeion to lysosome is indicated along with RNAi machinery needed to achieve mRNA cleavage. Source of figure is Dominiska and Dykxhoorn; 2010.

In addition cationic lipid-mediated transfection can be used to deliver siRNA to cell.

Cationic lipids have a positive charge enabling interaction with negatively-charged siRNA and negatively-charged cell membrane (Mechanism of cationic lipid-mediated transfection, Invitrogen™) (figure 19). It is believed that cationic lipid-siRNA is taken up by the cell per endocytosis.

Electroporation which involves increasing membrane permeability by application of an electric field to deliver siRNA is another option of experimental realization of RNA (RNA interference guide, Ambion, Inc 2006)

The main disadvantage is that many cells die during the process due to high voltage (RNA interference guide, Ambion, Inc 2006).

Figure 19: Cationic lipid mediated transfection
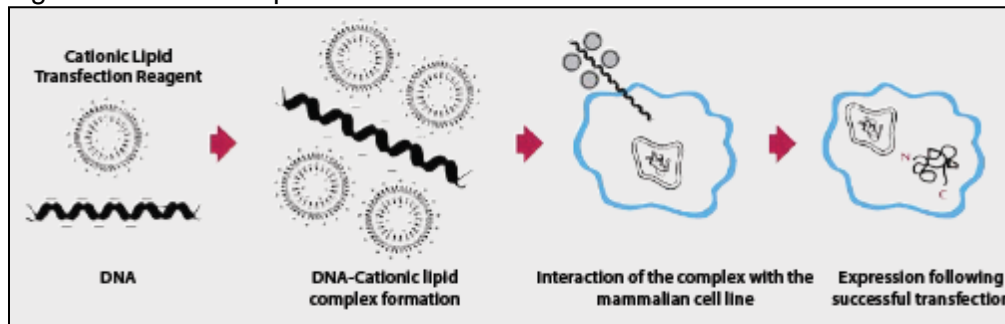
Fig. 19 shows the general lipid design and proposed mechanism of DNA entry into cells through cationic lipid mediated DNA or siRNA transfection. Source of figure: Mechanism of cationic lipid-mediated transfection, Invitrogen™.

Cationic lipid-mediated siRNA transfection can additionally be applied to in-vivo mouse models to induce RNAi. A prerequisite for in vivo models is that siRNA and transfection reagent does not trigger immune responses (RNA interference guide, Ambion, Inc 2006).

With regard to systemic RNAi application, several studies rely on the hydrodynamic transfection of siRNAs, i.e., the rapid (~20s) high-pressure injection of large volumes (up to 2 ml) of siRNA-containing solution (Aigner; 2007). There are multiple strategies to hydrodynamically inject siRNA into mice (RNA interference guide, Ambion, Inc 2006. Figure 19).

Hydrodynamic injection has been successful in reaching efficient induction of RNAi in liver as well as in kidney, lung, pancreas, and spleen and is probably due to the transient enhancement of membrane-permeability (Aigner, 2007. Behlke; 2006).

Nevertheless incidences of side effects were observed in animals hydrodynamically injected with siRNA (Aigner, 2007).

Figure 20: Strategies for the delivery of siRNA molecules in vivo
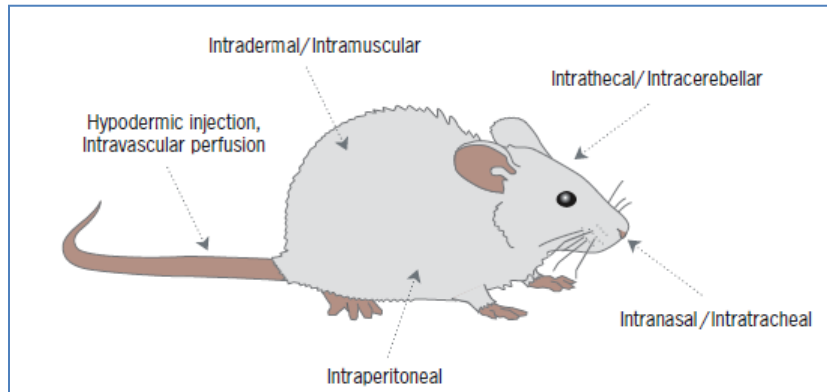
Fig. 20 highlights the strategies for the delivery of siRNA molecules in vivo using a mouse. Source of figure: RNA interference guide, Ambion, Inc 2006

2 Materials & Methods

2.1 Cell culture

Cell culture reagents: Dulbecco's modified eagle medium, DMEM (Gibco®, Ref. # 11995-065) supplemented with 10% fetal bovine serum, FBS, (Cat # 10437-028) and 1% Penicillin/ Streptomycin (10,000 U/mL, Gibco, Cat # 15140-122). Dulbecco's phosphate buffered saline (DPBS) (Gibco, Cat # 14190-144). 0.05% Trypsin (sterile filtered solution; provided by Massachusetts general Hospital). OptiMEM (reduced Serum media. Gibco®, Cat. # 11058-021).

Cultured immortalized cell lines:

1. Macrophage Syntrophin $^{\alpha 1-/-\beta 2-/-}$ Syn$^{\alpha 1-/-\beta 2-/-}$
2. Macrophage C57BL/6J (wildtype)
3. Macrophage ABCA1$^{+/+}$
4. Macrophage ABCA1$^{-/-}$
5. Human embryonic kidney HEK 293ETN cells

2.1.1 Mouse lines

2.1.1.1 HEK293ETN cells

Cell line description:

Biological source: Kidney, embryo from human

Growth mode: adherent

Karyotype: 2n 46, hypotriploid, modal no. 64

Morphology: epithelial

HEK 293 ETN cells were kind gifts from Resma Niedra; Massachusetts General Hospital MGH

2.1.1.2 Macrophage Syn $^{\alpha1-/-\beta2-/-}$ and ABCA1$^{-/-}$

Mice that were heterozygous for a null allele at the ABCA1 locus on a DBA/1 X C57BL/6J hybrid background were obtained from Jackson laboratories and were intercrossed to produce homozygous ᴍɪᴄᴇ and littermate wild type controls for these studies. Syn $^{\alpha1-/-\beta2-/-}$ mice carrying null mutations at both the SNTA1 and SNTB2 loci have been back bred 10 generations into the C57BL/6J background.

All animal procedures were approved by the MGH Subcommittee on Research Animal Care and were conducted in accordance with the U.S. Department of Agriculture USDA Animal Welfare Act and the U.S. Public Health Service PHS Policy for the Humane Care and Use of Laboratory Animals.

All mentioned steps were carried out by Norimasa Tamehiro, MGH.

2.1.1.2.1 Immortalization of bone marrow derived macrophages Syn $^{\alpha1-/-\beta2-/-}$ and ABCA1$^{-/-}$

Immortalized macrophage cell lines were derived by transducing bone marrow derived myeloid precursors from a C57BL/6J mouse with a J2 recombinant retrovirus carrying the v-myc and v-raf oncogenes.

The rationale for using viral vectors encoding oncoproteins is the transformation of a cell in an immortalized state by silencing the cell cycle checkpoint and cell cycle regulators (Maqsood et al 2013)**.** This has the consequence of evasion of cellular senescence enabling infinite life span of cells. In addition, the combination of two viral oncogenes, v-myc and v-raf, induces the selective proliferation of monocytic cells from fresh murine bone marrow in the absence of a specific growth factor supplement (Blasi et al, 1985).

In brief, primary bone marrow cultures were incubated in L929 mouse fibroblast-conditioned media for 3-4 days to first induce the macrophage differentiation pathway. Subsequently, cells were infected with concentrated J2 virus and selected for growth in the absence of L929 conditioned media. Clonal lines were established by limiting dilution from the initial mixed cultures and their macrophage phenotype was verified by

flow cytometry detection of CD11b and F4/80 antigen cell surface expression levels. A control line was established from the respective littermate wild type animals.

All mentioned steps were carried out by Norimasa Tamehiro, MGH

2.1.2 Experimental procedure

2.1.2.1 Western blot

The Western blot method requires primary antibodies specific against a protein antigen and secondary antibodies specific against the species in which the respective primary antibody was produced.

The secondary antibodies used in this Master study were labeled with an infrared dye which when excited by laser light of the Infrared imager (Odyssey, LiCor Biosciences) emit infrared light of a characteristic wavelengths.

Table 2: Western blot primary antibodies

Antigen; type of antibody	Size kD	Host	WB dilution	Supplier	Cat #
SNTB1; monoclonal	58kD	rabbit	1:1000	Stefan Froenher, University of Washington; USA	-
Anti-Syntrophin aka Pan-Syntrophin; monoclonal	58kD	rabbit	1:1000	Affinity Bio Reagents (ABR)	MA1-745
β-actin; polyclonal	42kD	rabbit	1:1000	Sigma-Aldrich	A2066
c-myc; monoclonal	49kD	mouse	1:1000	Covance	MMS-150P
GAPDH	36kD	mouse	1 μg/ ml	Ambion	AM4300
Mouse ABCA1; monoclonal	220kD	rat	1: 500	Affinity Bio Reagents (ABR)	MA1-16937
Apolipoprotein E (ApoE)	34kD	rabbit	1:500	Meridian	K23100R

Table 2 lists the primary antibodies used for Western blot experiments including respective type of antibody, antigen it can bind, size of antigen in kD, the host in which primary antibody was produced, Western blot WB dilution, supplier and catalog # cat# (if applies).

Table 3: Western blot infrared dye-labeled secondary Antibodies

Name	Host	Against species	Supplier	Cat #
IRDye® 800CW donkey anti-rabbit IgG (H+L)	Donkey	Anti-rabbit	LI-COR Biosciences; USA	926-32213
IRDye® 800CW goat anti-mouse IgG (H+L)	Goat	Anti-mouse	LI-COR Biosciences; USA	926-32210

Table 3 lists the name, host, species specificity, Suppliers and Cat # of Western blot infrared labeled secondary antibody.

2.1.2.1.1 Preparing cell lysates

After thawing, cell lysates samples were kept on ice throughout all following procedures. One mini complete protease inhibitor cocktail tablet (Roche, Cat # 11626400) was added to 10ml of Radio-Immunoprecipitation assay RIPA buffer (composition: 50 mM Tris-HCl, pH 8.0, with 150mM sodium chloride, 1.0% Igepal CA-630 (NP-40), 0.5% sodium deoxycholate, and 0.1% sodium dodecyl sulfate. Sigma-Aldrich, Cat. # R0278) and vortexed until the tablet dissolved. RIPA + pill solution was kept on ice. 1000µL of RIPA + pill solution were added to the Eppendorf tube containing cells. Tubes were vortexed thoroughly and left on ice for 10 minutes. After incubation, samples were spun down at 4°C, 5000rpm for 10 minutes (Fisher Scientific, Model: Marathon 3000R). Supernatant was transferred to fresh Eppendorf tubes and stored at –20°C. Tubes containing cell debris were discarded. Quantification of total protein in the supernatants was done with Bicinchoninic acid BCA protein assay kit (Thermo Scientific Pierce, Cat. # 23227) and pre-diluted protein assay standards: Bovine Serum Albumin BSA Set, 7 × 3.5ml (Cat # 23208).

2.1.2.1.2 Sodium dodecyl sulfate- Polyacrylamide gel electrophoresis SDS-PAGE

Equal concentration of cell lysates had to be pipetted into respective well of SDS-PAGE gel (10% Polyacrylamide Mini-PROTEAN® TGX pre-cast gels, 10 well, 30µl. Bio-Rad Laboratories Inc., Cat. # 456-1033). 5x SDS loading buffer (composition: 12 % Glycerol by volume; 60 mM Na$_2$EDTA pH 8; 0.6% by weight SDS; 0.003% by weight Bromophenol blue. ABM, Cat. # G031) was mixed with respective sample volume, to dilute to 1x loading buffer. Cell lysates were incubated for 5 minutes at 95-100°C on a heating block. Samples were left to cool down to room temperature.

SDS-PAGE apparatus (Mini-PROTEAN tetra cell. Bio-Rad Laboratories Inc., Cat. # 165-800) was assembled and filled with SDS running buffer (Composition: 1g SDS, 3g Tris base, 14.4g Glycine and dH$_2$0 to 1L. Self-made). Samples and protein standards (Precision plus protein dual Xtra color standard. Mixture of 12 recombinant proteins (2–250 kD), 9 blue-stained bands, and 3 pink reference bands (2, 25, 75 kD) (fig 1). Bio-

Rad Laboratories Inc., Cat. # 161-0377) (Precision plus protein Kaleidoscope standard. Mixture of 10 multicolor recombinant proteins (10–250 kD). Bio-Rad Laboratories Inc., Cat. # 161-0375) were loaded onto SDS-PAGE gel. SDS-PAGE gel was run at 150mV until SDS loading buffer front reached gel bottom.

Figure 21: Western blot standards
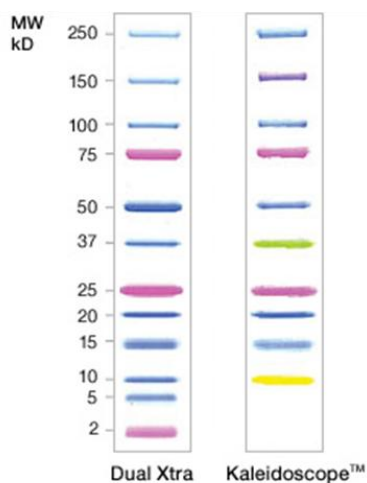
Fig. 1A shows the standards used for Western blot, Precision plus Protein™ dual Xtra color standard and Precision plus protein™ Kaleidoscope™ standard. The molecular weight MW in kD of recombinant proteins in standard are indicated. Figure modified from: Bio-Rad Laboratories, Inc.

2.1.2.1.3 Transferring the SDS-PAGE gel to a PDVF membrane

Western blot apparatus (BIO-RAD mini trans-Blot electrophoretic transfer cell. Bio-Rad Laboratories Inc., Cat. # 170-3930), except for PVDF membrane, were assembled (according to instruction manual) and soaked in a glass container filled with transfer buffer (composition: 3g Tris Base, 14.4g Glycine, 200ml Methanol and dH_2O filled to 1L) PVDF membrane (Immun-blot PVDF. Bio-Rad Laboratories Inc., Cat. # 162-0177) was activated with Methanol (EMD Millipore. Cat. # MX-0475-1) for 5 minutes. A small stir bar was added to the transfer tank. Apparatus was set up in order described in instruction manual. After set up of complete Western blot apparatus, transfer tank was filled up with transfer buffer. Transfer tank was placed in an ice bucket to ensure cool conditions during transfer. Transfer of proteins from SDS-PAGE gel to PVDF membrane at 170mA for 1.5 hours.

2.1.2.2 Probing the membrane for a specific protein

Western blot was blocked overnight in Blotto (composition: 5% dry milk, 1% bovine serum albumin (BSA) in 100ml solvent solution, 1xPBS, 0.1% Tween-20. Self-made) at 4°C. Blocked membrane was incubated in Blotto with the primary antibody for 2 hours at RT under shaking. Membrane was washed 2x quickly, 1x for 10 minutes in 1xPBS, 0.1% Tween-20 under shaking. Washed membrane was incubated in Blotto with the appropriate secondary antibody for 1-2 hours at RT under shaking. Membrane was washed same way as mentioned before, except that an additional 5 minute wash was added after the 10 minute wash. Secondary antibody infrared signal was detected with Odyssey infrared imager (Li-Cor. Serial # ODY-0960).

2.1.2.3 Coomassie staining

Coomassie staining solutions:

- Coomassie stain solution: 0.1% Coomassie R250, 10% acetic acid, 40% methanol, filled up with distilled water (self made solution). Solution was filtered to remove particulates and stored at room temperature.
- Coomassie destain solution: 20% Methanol, 10% Acetic acid, filled with distilled water to final volume of 1L (self made solution). Destain solution was stored at room temperature.

2.1.2.3.1 Protocol Coomassie staining

Samples were run on an SDS-PAGE gel. When loading buffer front reached bottom of gel, gel was rinsed once with distilled water and transferred to a plastic container with lid. Gel was covered with Coomassie stain solution. After blue bands were visible in gel, Coomassie stain solution was discarded. Coomassie destain solution was added to cover gel. Overnight destaining at room temperature. Gel was developed with scanner (Epson perfection V700 photo).

2.2 Lipid-mediated transfection

2.2.1 Lipofectamine® 2000 DNA transfection

Reagents: Lipofectamine® 2000 (Invitrogen™, Cat # 11668-027).

Equipment: Poly-D-lysine-coated 24-well tissue culture plates

Expression constructs/ vectors for Lipofectamine 2000 transfection**:**

Table 4: Expression constructs for Lipofectamine 2000 transfection

Plasmid DNA	Concentration µg/ml	Cat #
1. pcDNA3.1	2.62 µg/ml	V790-20
2. pSKO -253	0.93 µg/ml	-

Table 4 lists the expression constructs and concentration for Lipofectamine 2000 transfection.

- SNTB1 expression constructs pSKO253:

PSKO253 has 10 amino acids of c-myc cloned before SNTB1 gene. This leads to the synthesis of myc-tagged SNTB1 recombinant protein by transfected cells.

Steps for myc-tagged SNTB1 cloning were carried out by Kei Okuhira; MGH. Banked by Nori Tamehiro; MGH.

Figure 22: Expression vector pcDNA3.1 plasmid card

Comments for pcDNA3.1 (+)
  5428 nucleotides

CMV promoter: bases 232-819
T7 promoter/priming site: bases 863-882
Multiple cloning site: bases 895-1010
pcDNA3.1/BGH reverse priming site: bases 1022-1039
BGH polyadenylation sequence: bases 1028-1252
f1 origin: bases 1298-1726
SV40 early promoter and origin: bases 1731-2074
Neomycin resistance gene (ORF): bases 2136-2930
SV40 early polyadenylation signal: bases 3104-3234
pUC origin: bases 3617-4287 (complementary strand)
Ampicillin resistance gene (*bla*): bases 4432-5428 (complementary strand)
  ORF: bases 4432-5292 (complementary strand)
  Ribosome binding site: bases 5300-5304 (complementary strand)
  bla promoter (P3): bases 5327-5333 (complementary strand)

Figure 22 shows the plasmid card for pcDNA3.1. Source of figure: pcDNA™3.1(+) pcDNA™3.1(−) User manual; Invitrogen™.

Figure 23: Lipofectamine® 2000 DNA transfection reagent protocol

Figure 23 shows the Lipofectamine® 2000 DNA transfection reagent protocol. 24 well plate formats were used for transfections of this Master study (highlighted in red).Source of figure: Invitrogen™.

Experimental procedure Lipofectamine 2000 transfection:

Lipofectamine 2000 DNA transfection protocol in figure 2 was followed for experimental procedures. 24 hours after transfection cells were visualized in the case of positive control transfection or immediately lysed for Western blot. For cell lysis procedure see section on Western blot.

2.2.2 Lipofectamine RNAiMAX transfection

Material:

1) HEK293 ETN cells
2) Poly-D-lysine coated 24 well plate
3) Opti-MEM
4) Lipofectamine RNAiMAX (Invitrogen; Cat # 13778030)
5) Plasmid DNA

Figure 24: Plasmid DNA for Lipofectamine RNAiMAX transfection

Plasmid DNA	Concentration (µg/ml)
1. pcDNA3.1	2.62 ug/ul
2. pSKO253	0.93 ug/ul

Figure 24 lists the plasmid DNA used for Lipofectamine RNAiMAX transfections

6) Synthetic siRNA

Table 5: Synthetic siRNAs for Lipofectamine RNAiMAX transfection

Non-fluorescent synthetic siRNAs	Initial concentration	Supplier; Cat#
1. SNTB1 custom siRNA (SNTB1cus), in vivo ready	1 µmole	Ambion; 4457309
2. Silencer® SNTB1 pre-designed siRNA (SNTB1), in vivo ready	1 µmole	Ambion; 44577310
3. Silencer® select negative control #1 siRNA, in vivo ready	250 nmole	Ambion 4457299
Fluorescent synthetic siRNA positive control	**Initial concentration**	**Supplier; Cat#**
4. BLOCK-iT™ Alexa Fluor® Red fluorescent control	20 molar	Invitrogen; 14750-100
5. Silencer® FAM-labeled GAPDH siRNA	5 nmole	Ambion; AM4650

Table 5 lists all the information regarding the synthetic siRNAs used for Lipofectamine RNAiMAX transfection

7) Ultrapure RNase &DNase free distilled water for preparation of stocks

Experimental procedure Lipofectamine RNAiMAX transfection:

Lipofectamine RNAiMAX DNA transfection protocol in figure 24 was followed for experimental procedures. Except that 5 minutes before transfection of siRNA and plasmid DNA lipoplexes HEK293ETN cells had a fresh media change of 400ul Opti-MEM. After transfection cells were left to incubate for 1 hour at 37°C, 5% Carbondioxide CO_2. After this period 1ml of DMEM supplemented with 10% FBS and 1% Pen/Strep were added into wells of transfected cells.

In addition, in the case of HEK293ETN transfected with fluorescent fluorophores the DMEM media was replaced with 1ml PBS/ well before visualization to enhance visibility of fluorophores. After visualizing depending on experiment cells were either lysed or PS was aspirated and replaced with DMEM media.

24 hours after transfection cells were visualized in the case of positive control transfection or immediately lysed for Western blot. For Cell lysis procedure see section on Western blot.

Figure 25: Lipofectamine RNAiMAX transfection protocol

Timeline		Steps	Procedure Details			
			Component	96-well	24-well	6-well
Day 0	1	Seed cells to be 60-80% confluent at transfection	Adherent cells	$1–4 \times 10^4$	$0.5–2 \times 10^5$	$0.25–1 \times 10^6$
Day 1	2	Dilute Lipofectamine® RNAiMAX Reagent in Opti-MEM® Medium	Opti-MEM® Medium	25 µL	50 µL	150 µL
			Lipofectamine® RNAiMAX Reagent	1.5 µL	3 µL	9 µL
	3	Dilute siRNA in Opti-MEM® Medium	Opti-MEM® Medium	25 µL	50 µL	150 µL
			siRNA (10 µM)	0.5 µL (5 pmol)	1 µL (10 pmol)	3 µL (30 pmol)
	4	Add diluted siRNA to diluted Lipofectamine® RNAiMAX Reagent (1:1 ratio)	Diluted siRNA	25 µL	50 µL	150 µL
			Diluted Lipofectamine® RNAiMAX Reagent	25 µL	50 µL	150 µL
	5	Incubate	Incubate for 5 minutes at room temperature.			
	6	Add siRNA-lipid complex to cells	Component	96-well	24-well	6-well
			siRNA-lipid complex per well	10 µL	50 µL	250 µL
			Final siRNA used per well	1 pmol	5 pmol	25 pmol
			Final Lipofectamine® RNAiMAX used per well	0.3 µL	1.5 µL	7.5 µL
Day 2–4	7	Visualize/analyze transfected cells	Incubate cells for 1–3 days at 37°C. Then, analyze transfected cells.			

Figure 25 shows the Lipofectamine® RNAiMAX transfection reagent protocol. 24 well plate formats were used for transfections of this Master study (highlighted in red).Source of figure: Invitrogen™.

3   Results

The aim of this Master thesis was to test if suppression of SNTB1 in the context of $Syn^{\alpha1-/-\beta2-/-}$ macrophages has a more dramatic impact on macrophage cholesterol efflux function mediated by ABCA1. For this purpose immortalized macrophage cell lines $Syn^{\alpha1-/-\beta2-/-}$, deficient of SNTA1 and SNTB2 isoforms, and $ABCA1^{-/-}$ were analyzed using various methods.

Immortalized C57BL/6J and $ABCA1^{+/+}$ macrophages were included in analysis as respective littermate wild type controls to $Syn^{\alpha1-/-\beta2-/-}$ and $ABCA1^{-/-}$ cells.

3.1   Is there a compensatory response of SNTB1 in $Syn^{\alpha1-/-\beta2-/-}$ cells?

The ABCA1/ Syntrophin protein complex is increased in an LXR dependent manner and can bind apoA-I in $ABCA1^{+/+}$ wild type macrophages (unpublished data). It is believed that SNTA1, SNTB1 and SNTB2 protein-protein interactions stabilize macrophage ABCA1 cholesterol efflux function (Okuhira et al, 2006).

Based on the fact that SNTB1 is the last Syntrophin isoform present in $Syn^{\alpha1-/-\beta2-/-}$ cells, it seems plausible to predict SNTB1 up regulation as a compensatory response to maintain ABCA1 cholesterol efflux function after SNTA1 and SNTB2 knockout. In agreement to this prediction, unpublished data using the same immortalized $Syn^{\alpha1-/-\beta2-/-}$ cells showed SNTB1 mRNA and SNTB1 protein up regulation.

The first objective of this Master thesis was confirming prior unpublished SNTB1 compensatory results in $Syn^{\alpha1-/-\beta2-/-}$ cells and to thereby validate $Syn^{\alpha1-/-\beta2-/-}$ cell phenotype.

To check for $Syn^{\alpha1-/-\beta2-/-}$ cell phenotype and SNTB1 up regulation a Western blot of $Syn^{\alpha1-/-\beta2-/-}$ cells of different passages had to be prepared and probed for SNTB1. The reason for including cell lines of different passages is that cell lines at high passage numbers experience alterations in morphology, response to stimuli, growth rates, protein expression and transfection efficiency, compared to lower passage cells (Tech

bulletin No. 7; ATCC). Therefore adding $Syn^{\alpha1-/-\beta2-/-}$ and C57BL/6J control cells of higher passage number to Western blot confirmed cell integrity after multiple cell passages. $Syn^{\alpha1-/-\beta2-/-}$ cells passages 17, 24, 26, and C57BL/6J cells passages 22, 30, 32, were lysed and separated by SDS-PAGE.

For validation of even protein loading before Western blot, a Coomassie staining of the $Syn^{\alpha1-/-\beta2-/-}$ and C57BL/6J cells SDS-PAGE gel was done. Coomassie staining is based on the principle that the bound number of Coomassie dye molecules is proportional to the amount of protein present per band (Carl Roth GmbH). The SDS-PAGE gel of $Syn^{\alpha1-/-\beta2-/-}$, C57BL/6J cells was coomassie dye stained and destained (see materials and methods section for Coomassie staining procedure). The blue protein bands of destained SDS-PAGE gel could be visualized using a scanner. Comparable blue bands, which represent an estimate of protein concentration, affirmed even protein loading in most SDS-PAGE gel lane (figure 26).

After check of protein loading, $Syn^{\alpha1-/-\beta2-/-}$ and C57BL/6J cell protein of SDS-PAGE gel were transferred onto a PVDF membrane for Western blot. The Western blot was probed for SNTB1 and β-Actin (as protein loading control). Infrared signal of SNTB1 and β-actin secondary antibodies was imaged with an infrared imager.

Surprisingly no characteristic SNTB1 58kD band was detected in all $Syn^{\alpha1-/-\beta2-/-}$ and C57BL/6J cells on developed Western blot after SNTB1 probe. Instead an unspecific 15kD band was detected (figure 27).

In the β-Actin loading control all $Syn^{\alpha1-/-/\beta2-/-}$ and C57BL/6J cells expressed β-Actin 42kD at equal levels (see figure 27).

Figure 26: Coomassie staining SDS-PAGE gel of Syn$^{\alpha1-/-\beta2-/-}$ and C57BL/6J cells
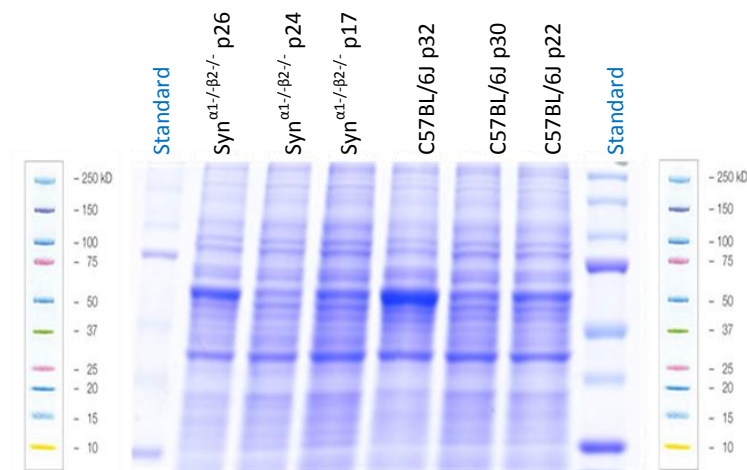
Fig. 26 shows the results of Coomassie staining SDS-PAGE gel of Syn$^{\alpha1-/-\beta2-/-}$ cells passages 17, 24, 26, and C57BL/6J cells passages 22, 30, 32. The intensity of detected blue bands is related to protein concentration. Two standards were included in the first and last lane of the gel, to be used as size marker for evaluating protein size.

Figure 27: Western blot of Syn$^{\alpha1-/-\beta2-/-}$ and C57BL/6J cells. Probe for SNTB1
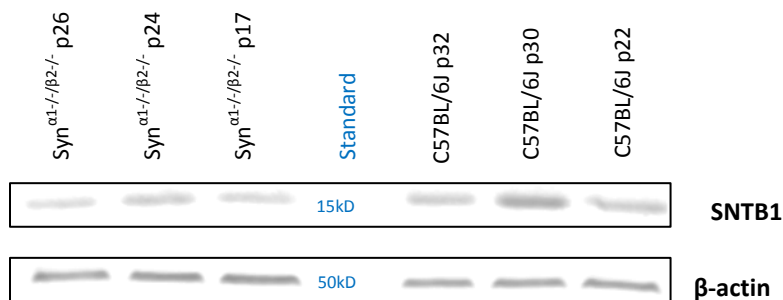
Fig. 27 shows the Western blot of Syn$^{\alpha1-/-\beta2-/-}$ cells passages 17, 24, 26 and C57BL/6J cells passages 22, 30, 32 probed for SNTB1 and β-actin. Unspecific 15kD bands were detected in SNTB1 probed Western blot. β-Actin loading controls are evenly expressed at 42kD by all cells.

Taken together Western blot analysis of SNTB1 Syn$^{\alpha1-/-\beta2-/-}$ and C57BL/6J cells showed no SNTB1 expression due to a non-specific SNTB1 antibody. Syn$^{\alpha1-/-\beta2-/-}$ cell phenotype and unpublished data on their SNTB1 compensatory response could not be confirmed.

3.2 Confirmation of Syn$^{\alpha1-/-\beta2-/-}$ cell phenotype

Considering that the used SNTB1 antibody was unspecific, another Syntrophin antibody had to be added to Western blot analysis to confirm Syn$^{\alpha1-/-\beta2-/-}$ phenotype. The alternative antibody was anti-Syntrophin (aka Pan-Syn), an antibody specific against all Syntrophin isoforms, SNTA1, SNTB1 and SNTB2, when in native state.

In contrast when Syntrophin proteins are in denatured state i.e. during SDS-PAGE and subsequent Western blot, the anti-Syntrophin "pan-Syn" antibody property is lost and only SNTA1and SNTB2 can be bound (technical information from Michael Fitzgerald; MGH).

The same Western blot of Syn$^{\alpha1-/-\beta2-/-}$and C57BL/6J cells in figure 2 was stripped of bound antibodies and probed for SNTA1and SNTB2 by anti-Syntrophin antibody.

As expected immunoblotting results showed that Syn$^{\alpha1-/-\beta2-/-}$ cells did not express SNTA1 and SNTB2 while C57BL/6J cell controls did express SNTA1 and SNTB2 (see figure 28).

All β-Actin loading controls were expressed uniformly at 42kD in Syn$^{\alpha1-/-\beta2-/-}$ and C57BL/6J macrophages (see figure 28).

Figure 28: Western blot of Syn$^{\alpha1-/-\beta2-/-}$ and C57BL/6J macrophages. Probe for SNTA1 and SNTB2
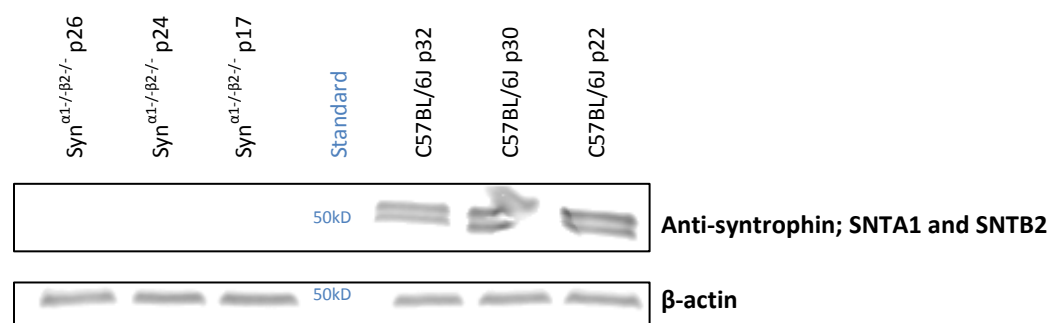
Fig. 28 displays the Western blot of Syn$^{\alpha1-/-\beta2-/-}$ cells passages 17, 24, 26 and C57BL/6J cells passages 22, 30, 32 probed for SNTA1 and SNTB2 with anti-Syntrophin antibody. Only C57BL/6J cells express SNTA1 and SNTB2. β-actin bands are detected and evenly expressed at 42kD in Syn$^{\alpha1-/-\beta2-/-}$ and C57BL/6J cells.

Figure 27 and figure 28 indicate that although SNTB1 expression could not be verified in $Syn^{\alpha 1-/-\beta 2-/-}$ cells, the $Syn^{\alpha 1-/-\beta 2-/-}$ cell phenotype could be partially confirmed by absence of SNTA1 and SNTB2 bands after anti-Syntrophin probe of Western blot.

3.3 ABCA1 and ApoE expression in $Syn^{\alpha 1-/-\beta 2-/-}$ and $ABCA1^{-/-}$ macrophages

Further interests for Western blot analysis, were ABCA1 and ApoE expression in $Syn^{\alpha 1-/-\beta 2-/-}$ and $ABCA1^{-/-}$ macrophages. The main questions were:

- Do ABCA1 expression levels in immortalized knockout cell lines vary?
- Is ApoE still expressed in $Syn^{\alpha 1-/-\beta 2-/-}$ macrophages?

Based on the importance of ApoE in inflammatory diseases i.e. Alzheimer's disease (Piehler et al; 2012), a reviewer of an unpublished Freeman/ Fitzgerald laboratory paper on ABCA1 Syntrophin interaction, was interested if ApoE still acts as a cholesterol efflux acceptor in $Syn^{\alpha 1-/-\beta 2-/-}$ macrophages.

By immunoblotting ABCA1 and ApoE expression of $Syn^{\alpha 1-/-\beta 2-/-}$ and $ABCA1^{-/-}$ macrophages could be analyzed.

ABCA1 expression in $Syn^{\alpha 1-/-\beta 2-/-}$ cells

For immunoblotting, $Syn^{\alpha 1-/-\beta 2-/-}$ macrophages passages 17, 24, 26 and C57BL/ 6J wild type macrophages passages 22, 30, 32 were lysed, ran on an SDS-PAGE gel and transferred to a PVDF membrane. Cells of different passage number were included in Immunoblot for the same aforementioned reasons. The Western blot was probed for ABCA1 and β-actin, as loading control. The infrared signal of ABCA1 secondary antibody was developed through an infrared imager.

Figure 29 shows that ABCA1 220kD is expressed to varying degrees in $Syn^{\alpha 1-/-\beta 2-/-}$ and C57BL/6J macrophages. Variation in ABCA1 protein levels was also seen in unpublished publication.

Actin loading control showed even protein loading onto SDS-PAGE gel (figure 29).

Figure 29: Western blot of Syn$^{\alpha1-/-\beta2-/-}$ and C57BL/ 6J macrophages. Probe for ABCA1
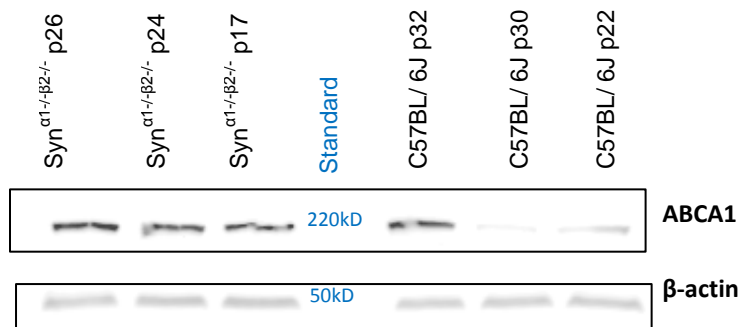
Fig. 29 shows the Western blot of Syn$^{\alpha1-/-\beta2-/-}$ and C57BL/ 6J macrophages, probed for ABCA1 and β-actin. ABCA1 is expressed at 220kD in Syn$^{\alpha1-/-\beta2-/-}$ and C57BL/ 6J cells. Actin loading control bands 42kD are present in all cells of Western blot.

In summary the data demonstrates that ABCA1 is expressed in Syn$^{\alpha1-/-\beta2-/-}$ macrophages.

3.4 ApoE expression in Syn$^{\alpha1-/-\beta2-/-}$ cells

For the Western blot to evaluate ApoE expression, mouse sera was added to Syn$^{\alpha1-/-\beta2-/-}$ and C57BL/6J cells. The rationale for this was that C57BL/6J macrophages are controls for intracellular ApoE expression while C57BL/6J mouse sera are controls for extracellular ApoE levels in the blood.

Mouse serum was either "neat" undiluted, 1:10 or 1:100 diluted. A Mouse serum is a highly concentrated protein reservoir therefore it had to be diluted to reduce concentration. Reducing mouse sera concentration can improve intensity of detected bands on Western blot.

Cell lysates of Syn$^{\alpha1-/-\beta2-/-}$ cells passages 17, 24, 26 and C57BL/6J wildtype cells passages 22, 30, 32 were prepared. Syn$^{\alpha1-/-\beta2-/-}$ and C57BL/6J macrophages were loaded with neat, 1:10 and 1:100 diluted mouse sera onto a SDS-PAGE gel, transferred to a PVDF membrane and probed for ApoE. Additionally Western blot was probed for β-

actin. The infrared signals of ApoE and β-actin secondary antibodies were developed through an infrared imager.

Interestingly no ApoE expression was detected in Syn$^{\alpha1-/-\beta2-/-}$ macrophages (figure 30). Controls, C57BL/6J macrophages and neat, 1:10 diluted mouse sera expressed ApoE (figure 30). In 1:100 diluted mouse sera no characteristic 34kD ApoE band was detected (figure 30). Probably the ApoE protein concentration in 1:100 diluted mouse sera was so low, that ApoE could no longer be detected by infrared imaging.

The β-actin probe validates even protein loading of Syn$^{\alpha1-/-\beta2-/-}$ and C57BL/6J macrophages (figure 30).

Figure 30: Western blot of Synα1-/-β2-/-, C57BL/6J macrophages and mouse sera. Probe for ApoE

Figure 30 shows the Western blot of Syn$^{\alpha1-/-\beta2-/-}$ cells passages 17, 24, 26, C57BL/6J cells passages 22, 30, 32 and neat, 1:10 or 1:100 diluted mouse sera; probed for ApoE and β-actin. ApoE is expressed in C57BL/6J cells and neat, 1:10 diluted mouse sera. Actin bands at 42kD confirm even protein loading. Abbreviation MS = mouse sera.

In summary figure 30 highlights that ApoE is absent in Syn$^{\alpha1-/-\beta2-/-}$ macrophages.

3.4.1 ABCA1 and ApoE expression in Syn$^{\alpha1-/-\beta2-/-}$ versus ABCA1$^{-/-}$ macrophages

To compare ABCA1 or ApoE expression in Syn$^{\alpha1-/-\beta2-/-}$ and ABCA1$^{-/-}$ macrophages, another Western blot had to be prepared. The aim of this comparison was to evaluate if there is a difference in ABCA1 and ApoE protein levels of Syn$^{\alpha1-/-\beta2-/-}$ versus ABCA1$^{-/-}$ macrophages.

$Syn^{\alpha1-/-\beta2-/-}$, $ABCA1^{-/-}$ macrophages along with respective controls C57BL/6J and $ABCA^{+/+}$ were lysed, ran on an SDS-PAGE gel and transferred to a PVDF membrane. The Immunoblot was probed for ABCA1, ApoE and β-actin. The infrared signals of ABCA1, ApoE and β-actin secondary antibodies were developed through an infrared imager.

After ABCA1 probe, a non-specific ABCA1 ~150kD band was detected in $Syn^{\alpha1-/-\beta2-/-}$, $ABCA1^{-/-}$, C57BL/6J and $ABCA^{+/+}$ macrophages (figure 31). An ABCA1 band should have run at 220kD and be present in $Syn^{\alpha1-/-\beta2-/-}$, C57BL/6J and $ABCA^{+/+}$ cells.

Surprisingly, an ApoE band was only seen in C57BL/6J macrophages on ApoE probed Western blot (figure 31). It was expected that $ABCA^{+/+}$ macrophages expressed ApoE too. No ApoE expression in $ABCA^{+/+}$ cells make one doubt cell phenotype and integrity. In confirmation to figure 5, figure 6 illustrates that no ApoE is present in $Syn^{\alpha1-/-\beta2-/-}$ cells. The β-actin probe confirmed even protein loading of $Syn^{\alpha1-/-\beta2-/-}$, $ABCA1^{-/-}$, C57BL/6J and $ABCA^{+/+}$ macrophages (figure 31).

Figure 31: Western blots of 4 cell lines. Probe for ABCA1, ApoE and Actin
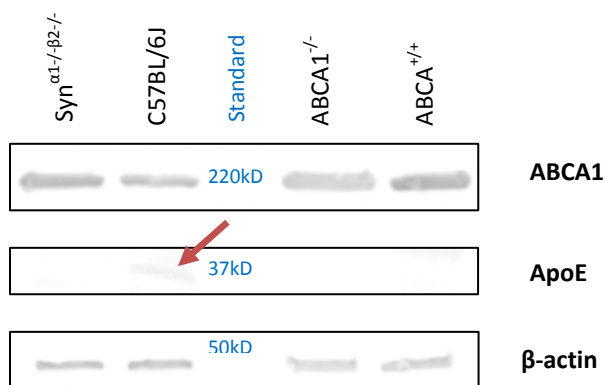
Figure 31 shows the Western blot of 4 cell lines, $Syn^{\alpha1-/-\beta2-/-}$, $ABCA1^{-/-}$, C57BL/6J and $ABCA^{+/+}$ macrophages; probed for ABCA1, ApoE and Actin. Non-specific bands are seen in all cells after ABCA1 probe. ApoE is expressed only in C57BL/6J cells (highlighted with a red arrow). β-actin 42kd bands confirm equal protein loading.

In conclusion, ApoE is expressed in $Syn^{\alpha1-/-\beta2-/-}$ macrophages. Integrity of $ABCA^{+/+}$ wildtype macrophages has to be checked due to absence of ApoE expression in cells.

3.5   Synthetic RNAi experiments

The objective of synthetic RNAi experiments was to assess if SNTB1 suppression in $Syn^{\alpha 1-/-\beta 2-/-}$ macrophages had an impact on ABCA1 cholesterol efflux function in cell culture and in-vivo mouse experiments.

RNAi was the method of choice to knockdown SNTB1 expression in cultured immortalized $Syn^{\alpha 1-/-\beta 2-/-}$ macrophages and in murine liver cells. Utilizing lipid mediated delivery, synthetic SNTB1 siRNAs could be delivered into $Syn^{\alpha 1-/-\beta 2-/-}$ cells and $Syn^{\alpha 1-/-\beta 2-/-}$ mice. The experimental RNAi work plan was to start with cell culture experiments to at first distinguish the most favourable siRNA transfection conditions and achieve SNTB1 knockdown in $Syn^{\alpha 1-/-\beta 2-/-}$ cells before advancing to RNAi experiments within $Syn^{\alpha 1-/-\beta 2-/-}$ mice

RNAi is a research tool which requires optimization of experimental steps to achieve high knockdown efficiencies (Petri and Meister; 2010). The threshold set for this study to interpret a siRNA as highly knockdown efficient is 50%. For example if a SNTB2 specific siRNA can trigger 50% or more SNTB2 knockdown, the siRNA is described to be high knockdown efficient.

Macrophages are known to be hard to transfect cells (Simoes et al; 1999). Therefore easy-to-transfect HEK293ETN (Thomas and Smart; 2004), were picked as a cell model for optimizing synthetic siRNA transfection before actual RNAi experiments in $Syn^{\alpha 1-/-\beta 2-/-}$ macrophages.

Another reason for picking HEK293ETN cells is that they are polarized cells like Liver cells which are the targets for in vivo SNTB1 RNAi. HEK293ETN cell siRNA transfection data will provide the insight needed for designing subsequent SNTB1 RNAi experiments in $Syn^{\alpha 1-/-\beta 2-/-}$ cells and $Syn^{\alpha 1-/-\beta 2-/-}$ mice.

Important transfection points that demand fine tuning in HEK293ETN cells are the number of seeded cells before transfection, cell confluency, transfected siRNA concentration, ratio of plasmid DNA:siRNA in lipoplexes, cytotoxic concentrations of siRNA etc (RNA interference guide, Ambion, Inc; 2006)

.

An experimental challenge was normally low SNTB1 expression levels in HEK293ETN cells. But in order to properly evaluate knockdown efficiency on Western blot of transfected HEK293ETN cells a good starting point is high SNTB1 protein levels.

To circumvent this challenge a myc-tagged SNTB1 expression construct named pSKO253 was used to over express SNTB1 in HEK293ETN cells.

3.5.1   Validation of myc-tagged SNTB1 expression constructs pSKO253

The functionality of pSKO253 had to be validated in order to progress on to subsequent SNTB1 RNAi experiments. PSKO253 DNA was transfected into cells with lipid based Lipofectamine 2000 reagent.

A day before pSKO253 transfection, HEK293ETN cells were seeded into wells of a poly-D-lysine coated 24 well plate. The next day pSKO253 DNA was transfected into HEK293ETN cells. As controls to pSKO253 transfected cells, another set of HEK293ETN were transfected with "empty" vector, pcDNA3.1. Expression vector pcDNA3.1 had no additional protein sequences cloned into its multiple cloning sites whereas pSKO253 had 10 c-myc amino acids cloned before the SNTB1 gene. Except myc-tagged SNTB1 in pSKO253, pSKO253 and pcDNA3.1 have the same fundamental vector structure.

PSKO253 and pcDNA3.1 transfected HEK293ETN were lysed 24 hours after plasmid DNA transfections, triplicates of transfected cells were ran on an SDS-PAGE gel, transferred onto a PVDF membrane and probed for c-myc. The c-myc antibody can bind its c-myc antigen in myc-tagged SNTB1 recombinant protein. This means with c-myc detection the total size of myc-tagged SNTB1 can be evaluated on Western blot. Myc-tagged SNTB1 size should be 59.1kD as a result of 1.1kD c-myc and 58kD SNTB1.

Accordingly myc-tagged SNTB1 bands at ~59kD were seen in pSKO253 transfected HEK293ETN cells after probe with c-myc (figure 32). C-myc bands at 49kD were detected in pSKO253 and pcDNA3.1 transfected HEK293ETN cells (figure 32).

The Western blot of pSKO253 and pcDNA3.1 transfected HEK293ETN cells was additionally probed for SNTB1. The same nonspecific SNTB1 antibody as used for the

Western blot of Syn$^{\alpha1-/-\beta2-/-}$and C57BL/6J cells was chosen to confirm prior non-detected SNTB1 band results. This time as alternative to former SNTB1 probed Western blot, a higher dilution of SNTB1 antibody and a longer incubation period of immunoblot in SNTB1 antibody were chosen.

Again no SNTB1 bands were seen on developed SNTB1 probed Immunoblot confirming prior results of non-specific binding of SNTB1 antibody (figure 32).

Figure 32: Western blot of pSKO253 and pcDNA3.1 transfected HEK293ETN cells. Probe for c-myc and SNTB1
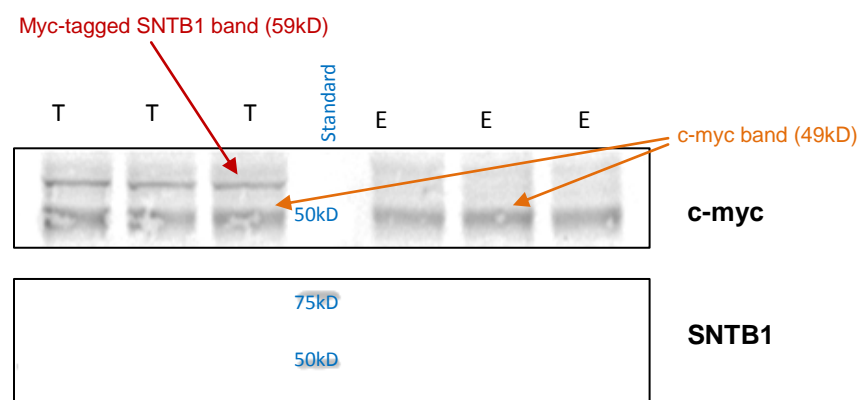
Fig. 32 shows the Western blot of pSKO253 and pcDNA3.1 transfected HEK293ETN cells probed for c-myc and SNTB1. T means cells transfected with pSKO253 vector. E means samples transfected with pcDNA3.1 "empty" vector. Myc-tagged SNTB1 bands measured 59kD and can be found only in T cells (highlighted byarrow). C-myc 49kD bands are present in T and E (indicated by arrows). SNTB1 58kD was not detected in T and E vector. E and T were loaded in triplicates.

In short pSKO253 mediated SNTB1 over expression was successful as seen in figure 32. PSKO253 expression constructs work as intended.

Positive SNTB1 over expression results allow one to move forward to RNAi experiments with the goal to knockdown over expressed SNTB1 by synthetic siRNAS.

3.5.2   Validation of fluorescent positive controls for SNTB1 RNAi

RNAi experiments require positive and negative controls for evaluation of target knockdown efficiencies (Behlke, 2006. Petri and Meister; 2013).

The experimental plan for SNTB1 RNAi was to transfect pSKO253 and siRNA into the same well of HEK293ETN cells. At the same time when SNTB1 is over expressed in HEK293ETN cells by pSKO253, SNTB1 specific synthetic siRNAs can induce SNTB1 knockdown.

But how can SNTB1 siRNA cellular intake and off-target effects be checked?   The answer is with fluorescent siRNA positive controls to monitor siRNA cellular intake and non-fluorescent negative controls which can be included in transfections to determine if off-target effects were triggered in cells.

However, also the pSKO253 transfected wells require "empty' vector controls to reference SNTB1 overexpression results.

Tables 6, 7 and 8 provide an overview of the positive and negative controls for synthetic siRNAs and expression vectors included in SNTB1 RNAi experiments.

Table 6: Florescent siRNA positive controls

Name	Fluorophore label	Function
Block iT™ Alexa fluor	Alexa fluor, emits red light	Its sequence is not homologous to any known gene, ensuring against induction of non-specific cellular events caused by introduction of siRNA duplex into cells (Invitrogen).
Silencer® FAM-labeled GAPDH siRNA	FAM™, emits green light	It has a Fluorescein derivative FAM label on the sense strand 5' end of siRNA duplex (Ambion Inc). Is designed for monitoring delivery in transfection experiments using Silencer siRNAs and human, mouse or rat cells (Ambion Inc). FAM-labeled GAPDH sequence is specific for Glyceraldehyde-3-phosphate dehydrogenase GAPDH (Ambion Inc).

Table 6 lists the fluorescent siRNA positive controls included in SNTB1 RNAi experiments, along with respective fluorophore labels and function

Table 7: Non-fluorescent siRNA negative controls

Name	Function
Silencer® select negative control #1 siRNA, in vivo ready	Used as a negative control siRNA for experiments involving Ambion in vivo siRNA delivery to animal (Ambion, Inc). This control affects no gene in the mouse genome and for this reason controls non-specific effects of RNAi (Ambion, Inc).

Table 7 lists the non-fluorescent siRNA negative control included in SNTB1 RNAi experiments and its function

Table 8: SNTB1 expression construct control

Name	Function
pSKO253	Functions as control for pSKO253+negative control siRNA #1 transfected wells for comparing SNTB1 knockdown, before and after RNAi
pcDNA 3.1 ("empty" vector)	Functions as control to pSKO253 transfected wells for comparing SNTB1 knockdown, before and after RNAi

Table 8 lists the SNTB1 expression construct control added to SNTB1 RNAi experiments and their function

In advance of SNTB1 RNAi in SNTB1 over expressing HEK293ETN cells, knockdown efficiency of positive siRNA controls Alexa Fluor and FAM-labeled GAPDH had to be validated in regards to siRNA cellular intake and protein knockdown efficiency.

The target protein for positive control RNAi was glyceraldehyde-3-phosphate dehydrogenase GAPDH. GAPDH is a ubiquitously expressed gene found and required in every cell. The product of this gene catalyzes an important energy-yielding step in carbohydrate metabolism, the reversible oxidative phosphorylation of glyceraldehyde-3-phosphate in the presence of inorganic phosphate and nicotinamide adenine dinucleotide NAD (National Center for Biotechnology Information [NCBI] 2013).

Alexa Fluor was added to RNAi experiment to serve as control, in order to reference knockdown efficiency of GAPDH by FAM-labeled GAPDH siRNA. The Alexa Fluor oligonucleotide sequence is not homologous to any known mammalian gene, ensuring against induction of non-specific cellular events caused by introduction of RNA duplex into cells (Block iT Alexa fluor protocol. Invitrogen™).

3.5.2.1 Visualization of Alexa fluor and FAM-labeled GAPDH cellular intake

One day pre-transfection of positive siRNA controls, 100000 HEK293ETN cells were seeded into each well of a poly-D-lysine coated 24-well plate.

24 hours after seeding, Alexa Fluor and FAM-labeled GAPDH concentrations of 75, 100, 125, 150, 175 and 200 nanomolar respectively, were transfected onto seeded HEK293ETN cells in wells of the 24 well plate. A broad concentration range of Alexa Fluor and FAM-labeled GAPDH were introduced into cells to discern the siRNA concentration for best GAPDH knockdown efficiency.

24 hours after transfection, direct observation of cellular uptake, distribution, and localization of fluorescent siRNAs could be visualized using fluourescence microscopy. Visualizotion of cellular siRNA intake was made possible through fluorophore labels on Alexa Fluor and FAM-labeled GAPDH sense strand 5' end. These fluorescent moieties can be excited by specific wavelengths of a laser to re-emit light. Alexa fluor emits red light upon excitation while FAM-labeled GAPDH emits green light upon excitation.

After siRNA transfection there is a concern for cytotoxic effects on cells when too high siRNA concentrations are used (Tech notes, Life technologies™. Fedorov et al; 2006).

This was not the case in either of the concentrations used for siRNA transfection. No cytotoxicity or abnormal morphology of transfected HEK293ETN cells was observed (figure 33 and 34). Interestingly Alexa fluor 75, 100, 125, 150, 175 and 200 nanomolar concentrations achieved higher siRNA uptake than respective FAM-GAPDH 75, 100, 125, 150, 175 and 200 nanomolar. Alexa fluor and FAM-labeled GAPDH concentrations indicated that even higher amounts of transfected siRNA could not achieve higher cellular uptake of siRNA. This means that no dose response of HEK293ETN cells could be achieved with increasing Alexa fluor or FAM-labeled GAPDH concentrations.

Since no dose response was seen, images of only the first three Alexa fluor or FAM-labeled GAPDH concentrations were taken (figure 33 and 34).

Figure 33: Dose response experiment HEK293ETN cells one day after Alexa Fluor 75nm, 100nm and 125nm
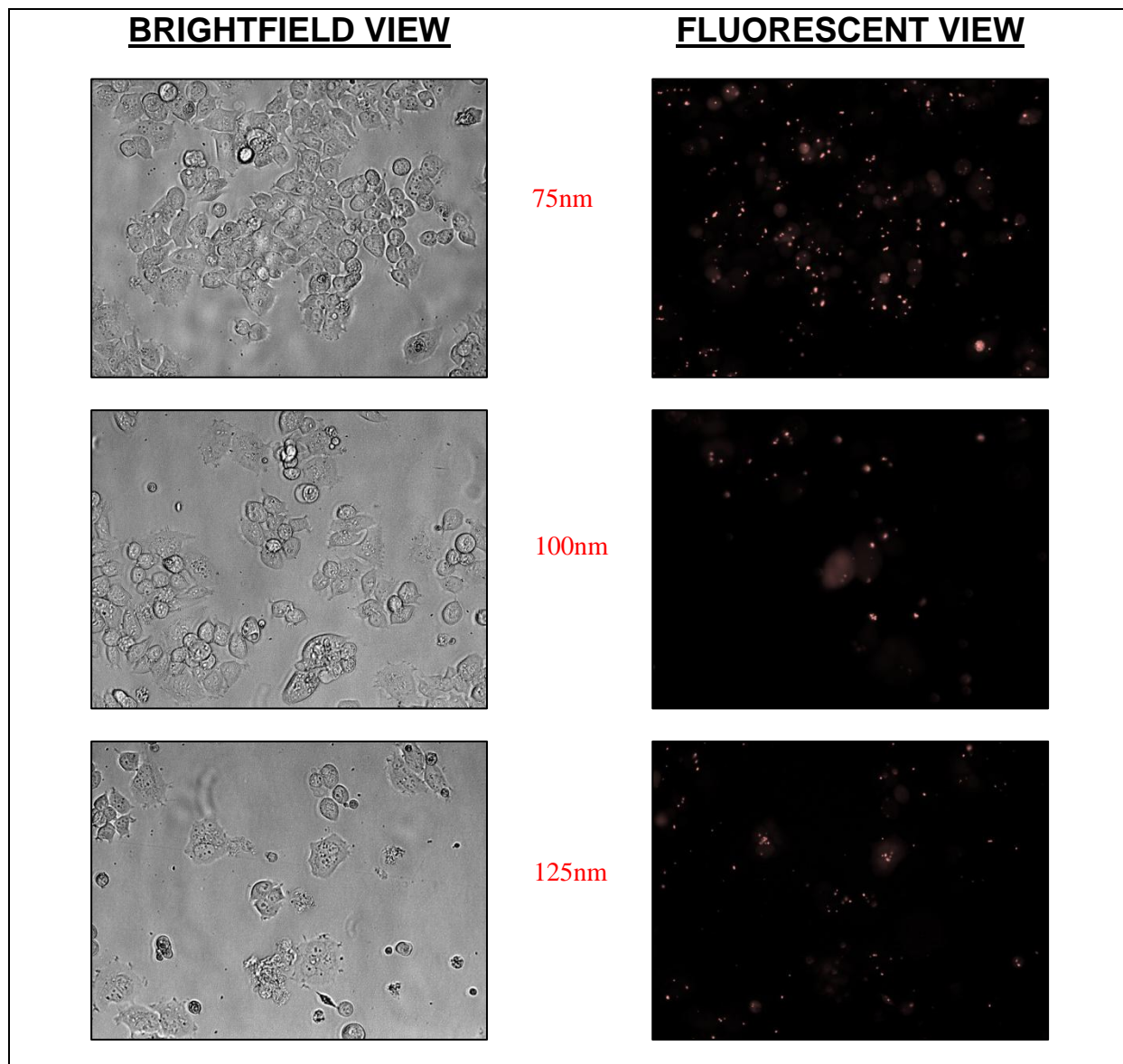
Fig. 33 shows images taken 24 hours after HEK293ETN cells were transfected with 75, 100 and 125 nanomolar Alexa fluor red positive control. There is no dose response of HEK 293ETN cells. Cells are shown in bright field versus fluorescent view.

Figure 34: Dose response experiment HEK293ETN cells one day after FAM-labeled GAPDH 75nm, 100nm and 125nm transfection
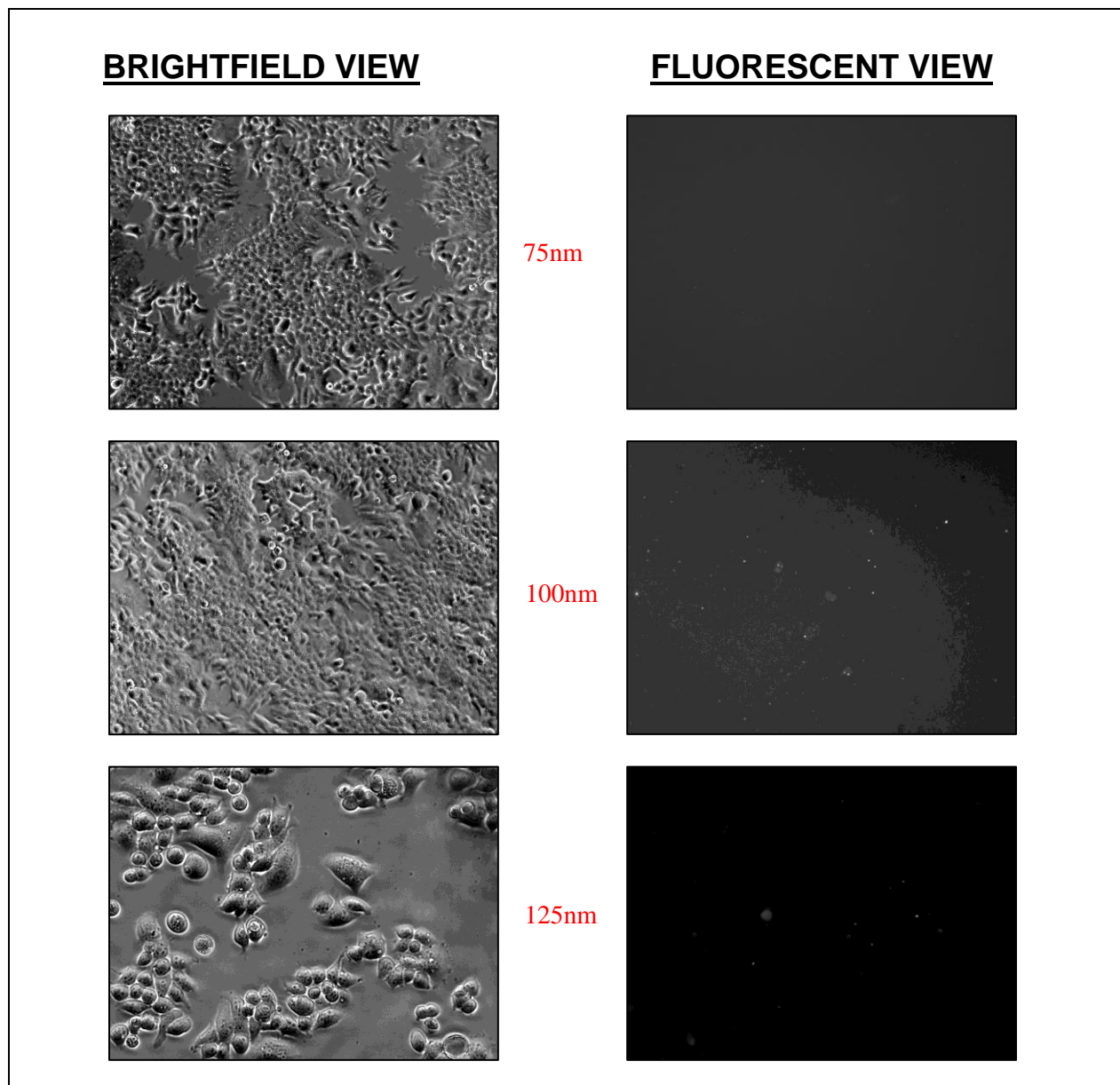
Fig. 34 shows images, taken 24 hours after HEK293ETN cells were transfected with 75, 100 and 125 nanomolar FAM-labeled GAPDH green positive siRNA control. There is no dose response of HEK 293ETN cells. Cells are shown in bright field versus fluorescent view. For clear view of FAM-labeled GAPDH uptake fluorescent view was not shown in green color.

Synthetic RNAi is transient lasting in average from 4-7 days. To evaluate if there is an increase in siRNA cellular uptake a repeat of lipid mediated transfection with Alexa fluor and FAM-labeled GAPDH 75, 100, 125, 150, 175 and 200 nanomolar concentrations was done. Images of cells were taken once every day in a time frame of 3 days. Alexa

fluor transfected cells had more fluorescence in comparison to FAM-labeled GAPDH transfected ones (figure 35). No increase in cellular uptake of Alexa fluor and FAM-labeled GAPDH were observed over three days (figure 35). Rather the opposite, a decrease or loss of fluorescent signal was seen. As no dose response was seen one image per day and positive control were taken (figure 35).

Figure 35: Day1-3 Alexa fluor and FAM-labeled GAPDH transfected HEK 293ETN cells

	ALEXA FLUOR	FAM-labeled GAPDH
Day 1		
Day 2		
Day 3		
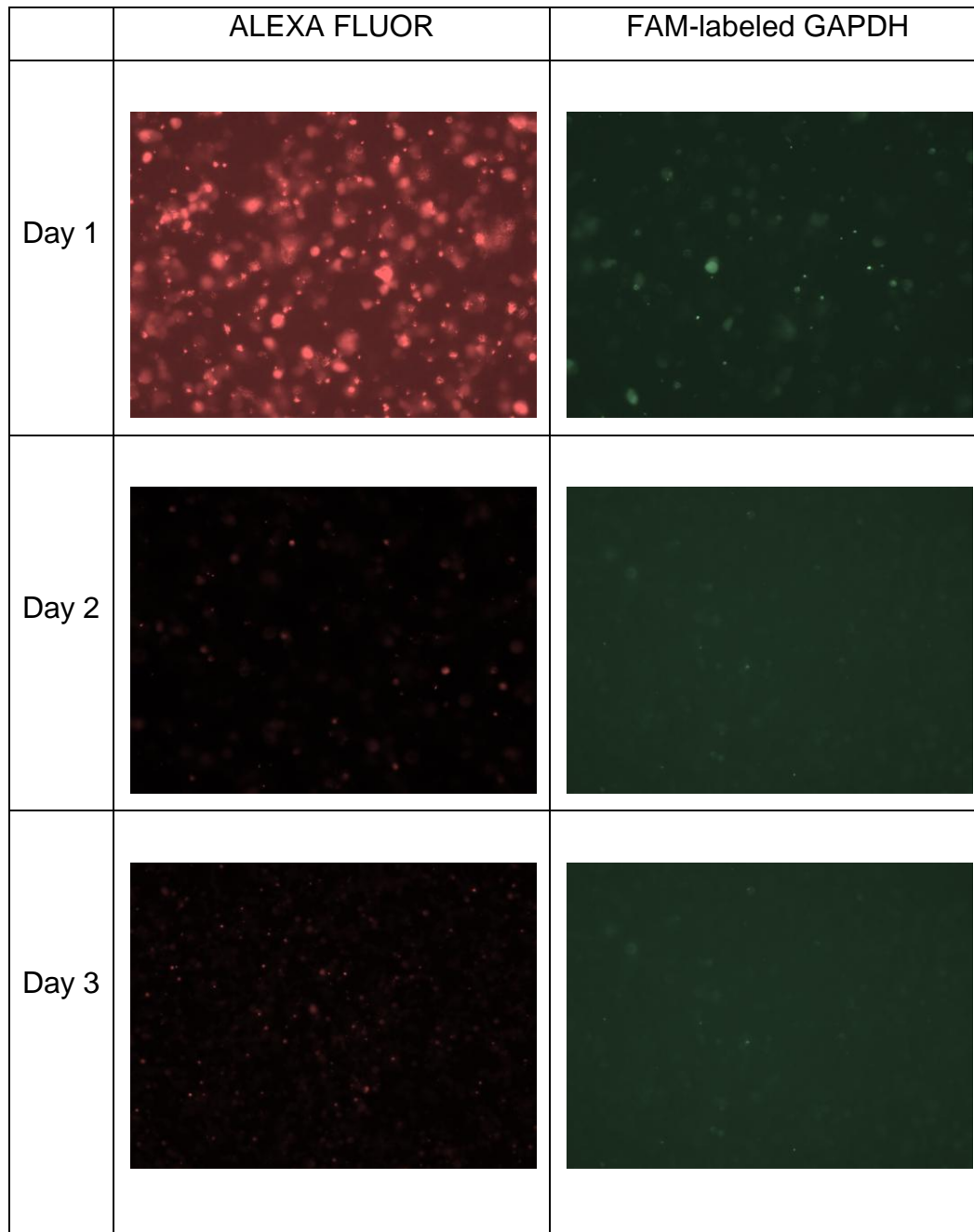
Figure 35 illustrates days 1-3 after Alexa fluor and FAM-labeled GAPDH transfection into HEK 293ETN cells. All images are shown in fluorescent view.

3.5.2.2 Quantification of GAPDH knockdown by FAM-labeled GAPDH positive control

As no dose response of HEK293ETN cells was seen after transfection, the cells transfected with the three lowest Alexa fluor and FAM-labeled GAPDH concentrations were selected for GAPDH knockdown quantification. GAPDH knockdown can be analyzed on a Western blot of positive siRNA control transfected HEK293ETN cells probed for GAPDH. GAPDH bands could be quantified using Western blot analysis software to obtain quantitative values for GAPDH knockdown by FAM-labeled GAPDH. Quantified GAPDH bands needed to be normalized to β-actin to quantified GAPDH to determine the actual percentage of GAPDH knockdown. Actin is a ubiquitous gene expressed in high abundance in every eukaryotic cell. Actin is a well established protein for Western blot normalization (Li-Cor Biosciences)

The experimental procedure was following: 75, 100 and 125 nanomolar of Alexa Fluor, FAM-labeled GAPDH transfected HEK293ETN cells were lysed, loaded in triplicates onto an SDS-PAGE gel, ran on the gel, transferred to a PVDF membrane and probed for GAPDH. The Western blot of 75, 100 and 125 nanomolar of Alexa Fluor and FAM-labeled GAPDH transfected HEK293ETN cells was probed with an infrared dye conjugated secondary antibody against the GAPDH primary antibody species. Secondary antibody infrared signal was detected with an infrared imager.

Figure 36: Western blot of positive siRNA controls. Probe for GAPDH and β-actin
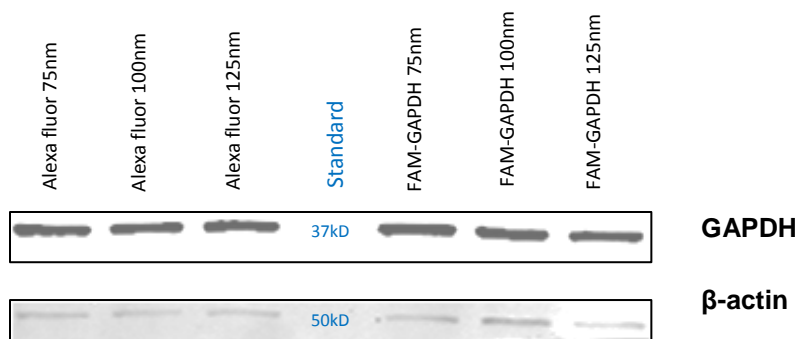
Figure 36 shows the Western blot of 75, 100, 125 nanomolar Alexa fluor and FAM-labeled GAPDH transfected HEK293ETN cells. GAPDH 36kD bands are detected in all cells after GAPDH probe. Actin is evenly expressed at 42kD. Abbreviations: FAM-GAPDH= FAM-labeled GAPDH, nm = nanomolar

GAPDH and Actin bands were individually quantified with Li-COR Western blot analysis software and subtracted from background. GAPDH band quantification values were normalized by respective Actin band quantification values e.g Alexa fluor 75nm GAPDH band quantification values versus Alexa fluor 75nm β-Actin band quantification values etc. Normalized GAPDH quantification values were then divided by control Alexa fluor quantification values to calculate GAPDH knockdown efficiency. Each Alexa fluor control, 75, 100 and 125 nanomolar Alexa fluor, is represented as 0% in figure 7 because Alexa fluor sequence is not specific for any human gene. Alexa fluor oligonucleotide sequence is not capable of achieving human protein knockdown.

Table 9: Western blot of positive siRNA controls quantification, normalization and knockdown efficiency values

Probe for GAPDH					
Transfected siRNA	**QV (- bg)**	**Norm**	**Ratio**	**Ratio (%)**	**KE (%)**
Alexa fluor 75nm	346.3	288.6	1	100%	0%
Alexa fluor 100nm	384.7	192.4	1	100%	0%
Alexa fluor 125nm	429.9	252.9	1	100%	0%
FAM-GAPDH 75nm	385	256.7	0.889402	89%	11%
FAM-GAPDH 100nm	365	280.8	1.459679	69%	31%
FAM-GAPDH 125nm	410.5	273.7	1.08219	92%	8%
Probe for β-actin					
Transfected siRNA	**QV (- bg)**				
Alexa fluor 75nm	1.2				
Alexa fluor 100nm	2				
Alexa fluor 125nm	1.7				
FAM-GAPDH 75nm	1.5				
FAM-GAPDH 100nm	1.3				
FAM-GAPDH 125nm	1.5				

Table 4 lists the quantification, normalization and knockdown efficiency values for the Western blot of positive siRNA controls (figure 11), probed for GAPDH and β-actin. Abbreviations: QV = quantification value, - bg = minus background, norm = normalized values, KE = GAPDH knockdown efficiency

Figure 37: calculated knockdown GAPDH efficiencies of positive control RNAi
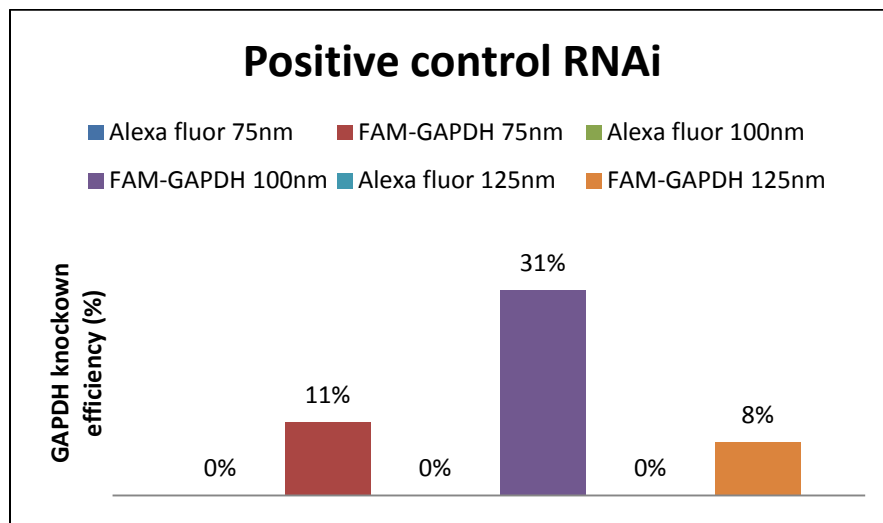
Figure 37 illustrates the calculated GAPDH knockdown efficiencies, in percent, of positive control RNAi with Alexa fluor and FAM-GAPDH concentrations of 75, 100 and 125 nanomolar. Alexa fluor controls have 0% GAPDH knockdown efficiency.

The anticipated siRNA high knockdown efficiency of ≥50% was not achieved in this positive control RNAi experiment. The highest GAPDH knockdown efficiency 31% was achieved by FAM-labeled GAPDH 125nm, followed by FAM-labeled GAPDH 75nm with 11% and lastly, FAM-labeled GAPDH 125nm with 8% efficiency.

These quantification results confirm no visualized dose response of HEK293ETN cells after Alexa Fluor and FAM-labeled GAPDH transfection with increasing concentrations of transfected siRNA.

3.6 SNTB1 RNAi with synthetic siRNAs SNTB1 and SNTB1 custom

Even though low GAPDH knockdown efficiency by FAM-labeled GAPDH ≤50% was concluded from positive control RNAi experiments, the function of used positive control siRNAs could be verified. The next aim was to advance to the main SNTB1 RNAi experiment utilizing SNTB1 specific synthetic siRNAs to down regulate SNTB1 over expression in HEK293ETN cells.

Two SNTB1 specific siRNAs, SNTB1 and SNTB1 custom, were used for realizing SNTB1 RNAi. Table 5 lists the differences of SNTB1 and SNTB1 custom siRNA.

Table 10: The difference between SNTB1 and SNTB1 custom siRNA

SNTB1	SNTB1 custom
• Designed against mouse SNTB1 • Targets the 1148 region of SNTB1 gene	• Has a custom design based on the sequence targeted by a lentiviral <u>sh</u>ort <u>h</u>airpin <u>RNA</u> shRNA (previously vetted by Norimasa Tamehiro, Freeman Laboratory, MGH. Unpublished data) • The lentiviral shRNA targets the 944 region of SNTB1 gene • Sequence of SNTB1 custom is TTTCTTCACGTAAGGTGTGGC

Table 10 lists the differences between SNTB1 and SNTB1 custom siRNA used for SNTB1 RNAi experiments.

Including multiple siRNA against the same target is in agreement with literature, which states that multiple targets within a gene can achieve different knockdown efficiencies (Behlke; 2006. Ambion, Inc). Additionally using two SNTB1 specific siRNAs in cell culture experiments allows one to compare knockdown efficiencies of both siRNAs, to determine the best SNTB1 siRNA for in-vivo mouse RNAi.

3.6.1 Lipofectamine 2000 mediated transfection of SNTB1 and SNTB1 custom

SNTB1 or SNTB1 custom have to be transfected into the same well of HEK293ETN cells with SNTB1 expression construct pSKO253 to achieve SNTB1 knockdown. In the first set of lipid-mediated synthetic siRNA transfection experiments, Lipofectamine 2000 reagent was used.

In order to ascertain optimal SNTB1 and SNTB1 custom concentration two different concentrations, 30 and 60 pmole of each siRNA, were included in SNTB1 RNAi

experiment. 60pmole SNTB1 and SNTB1 custom correlates with the recommended concentrations for Silencer siRNA transfection whereas 30pmole was chosen randomly.

Controls for SNTB1 and SNTB1 custom transfected HEK293ETN cells were cells transfected with either solely pcDNA 3.1 ("empty vector"), pSKO 253; or both pSKO 253 and negative siRNA. Negative siRNA targets a non-human protein resulting in no knockdown of human protein.

In correlation to positive control RNAi, a Western blot of transfected HEK 293ETN cell lysates had to be prepared to quantify knockdown efficiency. In the first Western blot, cell lysates of all Lipofectamine 2000 transfected wells were included. These were HEK293ETN cells transfected with

1) pcDNA3.1
2) pSKO253
3) pSKO253 + negative control siRNA #1
4) pSKO253 + SNTB1 custom 60 and 30 pmole
5) pSKO253 + SNTB1 custom 60 and 30 pmole

HEK293ETN cells were lysed, their proteins separated on a SDS-PAGE gel and transferred to a PVDF membrane. The Western blot was probed for c-myc and β-actin. A c-myc Immunobot probe helped to determine the size of myc-tagged SNTB1 while the β-actin probe served as loading control.

All transfected cells had the right size of recombinant protein after c-myc probe. In pcDNA 3.1 transfected cells only one 49kD c-myc should be present. PSKO253 should in agreement to prior over expression experiment (figure 38), have two protein bands: one for myc-tagged SNTB1 and one for c-myc. Other SNTB1 expression constructs plus synthetic siRNA transfected HEK293ETN cells, pSKO253 + negative control siRNA #1, pSKO253 + SNTB1 custom 60 and 30 pmole, pSKO253 + SNTB1 custom 60 and 30 pmole, should like pSKO253 have one myc-tagged SNTB1 59kD band and one c-myc band.

Although in the pSKO253+SNTB1 or pSKO253+SNTB1 custom transfected cells a reduction in thickness of the myc-tagged SNTB1 band in comparison to pSKO253 and pSKO253+ negative siRNA #1 references should occur.

Interestingly the pSKO253+ negative control siRNA #1 myc-tagged SNTB1 band was thinner than pSKO253+ SNTB1 60/ 30 pmole and pSKO253+ SNTB1 custom 30 pmole. An opposite result was expected, that the myc-tagged SNTB1 band of pSKO253+ negative control siRNA #1 has a higher bandwidth than myc-tagged SNTB1 band of pSKO253+ SNTB1 60/ 30 pmole and pSKO253+ SNTB1 custom 30 pmole on c-myc probed blot.

The possible explanations for this unusual result will be discussed in the discussion part of this Master thesis.

Figure 38: Western blot of Lipofectamine 2000 transfection SNTB1 and SNTB1 custom
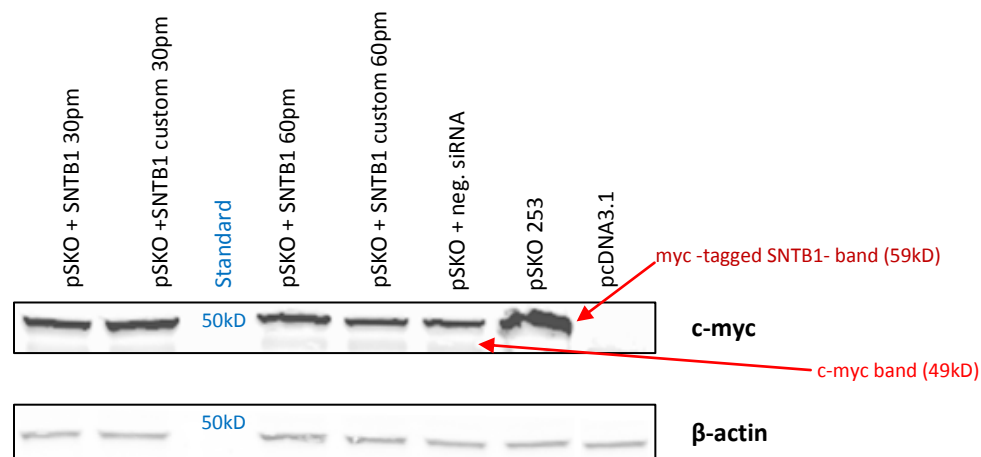
Fig. 38 illustrates the Western blot of Lipofectamine 2000 transfection of SNTB1 and SNTB1 custom, probed for c-myc and β-actin. The plasmid and synthetic siRNAs transfected into HEK293ETN are listed above respective bands. SKO253 was abbreviated to pSKO at times. Actin loading control confirms even protein loading.

3.6.1.1 Quantification Western blot of Lipofectamine 2000 transfection SNTB1 and SNTB1 custom

C-myc and β-actin bands on Western blot of Lipofectamine 2000 transfection SNTB1 and SNTB1 custom (figure 13), were quantified with Li-COR Western blot analysis

software and subtracted from respective background. C-myc band quantification values were normalized by corresponding β-actin band quantification values e.g pSKO253+ SNTB1 custom 60pm myc tagged SNTB1 band was normalized by its pSKO253+ SNTB1 custom 60pm β-actin band. Normalized myc-tagged SNTB1 quantification values of pSKO253 + SNTB1 custom 60/ 30 pmole and pSKO253 + SNTB1 custom 60/ 30 pmole were divided by pSKO253+ negative siRNA#1 control. The siRNA in pSKO253+ negative siRNA#1 control does not target any human gene. Therefore no SNTB1 knockdown can be achieved in HEK293ETN cells transfected with pSKO253+ negative siRNA#1. As a reference pSKO253+ negative siRNA#1 has 0% SNTB1 knockdown efficiency (figure 14).

Table 11: Western blot of Lipofectamine 2000 transfection SNTB1 and SNTB1 custom, quantification, normalization and knockdown efficiency

Probe for c-myc					
Transfected siRNA	**QV (- bg)**	**Norm**	**Ratio**	**Ratio (%)**	**KE (%)**
pcDNA3.1 (control)	42.4	20.19	1	100%	0%
pSKO253 (control)	182.9	101.61	1	100%	0%
pSKO+ neg. siRNA (control)	200.2	100.10	1	100%	0%
pSKO+SNTB1 custom 60pmole	91.3	41.50	0.414585	41%	59%
pSKO+ SNTB1 60pmole	101.8	50.90	0.508492	51%	49%
pSKO+ SNTB1 custom 30pmole	116.7	55.57	0.555159	56%	44%
SKO+SNTB1 30 pmole	85.5	47.50	0.474525	47%	53%

Probe for β-actin	
Transfected siRNA	**QV (- bg)**
pcDNA3.1	2.1
pSKO253	1.8
pSKO+ neg. siRNA	2
pSKO+SNTB1 custom 60pmole	2.2
pSKO+ SNTB1 60pmole	2
pSKO+ SNTB1 custom 30pmole	2.1
pSKO+SNTB1 30 pmole	1.8

Table 11 lists the quantification, normalization and knockdown efficiency values for the Western blot of Lipofectamine 2000 transfection SNTB1 and SNTB1 custom (figure 13), probed for c-myc and β-actin. Abbreviations: QV = quantification value, -bg = minus background, norm = normalized values, KE = GAPDH knockdown efficiency

Figure 39: Western blot of Lipofectamine 2000 transfection SNTB1 and SNTB1 custom, SNTB1 knockdown efficiency
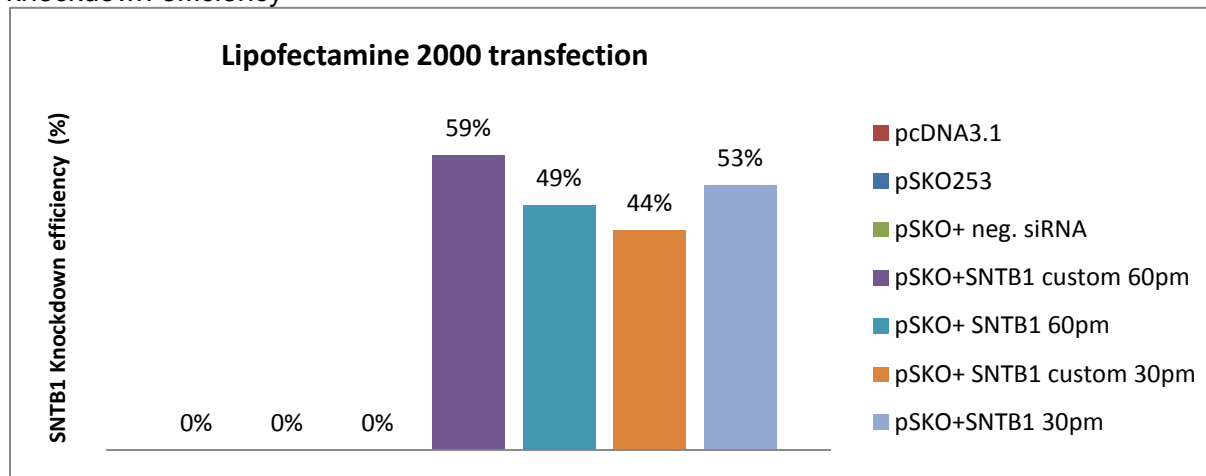
Fig. 39 visualizes the Western blot of Lipofectamine 2000 transfection SNTB1 and SNTB1 custom, SNTB1 knockdown efficiency.

Two SNTB1 siRNAs, SNTB1 custom 60 pmole and SNTB1 30 pmole, realized ≥50% SNTB1 knockdown in HEK293ETN cells. These siRNAs fulfilled the criteria for high knockdown efficiency. The other siRNAs were low efficient achieving ≤50% SNTB1 knockdown efficiency. The knockdown efficiency values that were derived are a representation of only one well transfected with respective plasmid-siRNA lipoplexes. As knockdown efficiency can be influenced by numerous factors and can thus vary from well to well, confidence in data can be increased if cells of three wells transfected with the same plasmid-siRNA lipoplexes are represented on the same Western blot.

3.6.2 Lipofectamine RNAiMAX mediated transfection of SNTB1 and SNTB1 custom

In order to compare SNTB1 knockdown efficiency by different SNTB1 custom and SNTB1 concentrations, a second synthetic siRNA transfection experiment had to be done.

In the second SNTB1 RNAi, lipid based RNAi Lipofectamine RNAiMAX was used. Lipofectamine RNAiMAX is a special formulation for simultaneous plasmid and siRNA transfections. Lipofectamine 2000 was replaced with Lipofectamine RNAiMAX because

higher siRNA cellular intake and knockdown efficiencies were guaranteed by manufacturer.

Lipofectamine RNAiMAX transfection of SNTB1 plasmids and siRNAs were similar to the one of lipofectamine 2000 transfection. The same plasmid DNA, siRNA were transfected onto seeded HEK293ETN cells in a Poly-D-lysine coated 24 well plate and the same method Western blot were utilized to evaluate SNTB1 knockdown efficiency after probe for c-myc. The plasmid DNA and or siRNA transfected into cells were:

1) pcDNA3.1
2) pSKO253
3) pSKO253 + negative control siRNA #1
4) pSKO253 + SNTB1 custom 60 and 30 pmole
5) pSKO253 + SNTB1 custom 60 and 30 pmole,

All transfected HEK293ETN cells were lysed but only the content of wells transfected with pSKO253 + negative control siRNA #1, pSKO253 + SNTB1 custom 60 and 30 pmole, pSKO253 + SNTB1 custom 60 and 30 pmole were loaded in triplicates onto two SDS-PAGE gel. Each gel contained plasmid+ siRNA of the same concentration with its control pSKO253 + negative control siRNA #1. Loading each gel with the same SNTB1 custom and siRNA allowed direct comparison of the caused SNTB1 RNAi by respective concentration. Additionally including triplicates of transfected cells allowed one to increase significance and confidence in data. In contrast if there is just one example of plasmid-siRNA transfected cells one could assume a false positive result.

The two SDS-PAGE gels of SNTB1 custom and SNTB1 60/ 30 pmole were transferred onto a PVDF membrane. Immunoblots were probed for c-myc and β-actin.

Figure 40 and 41 shows that myc-tagged SNTB1 is expressed by all transfected HEK293ETN. Both 60 and 30 pmole SNTB1 custom and SNTB1 were not able to efficiently mediate SNTB1 knockdown. Quantification of c-myc bands were not necessary in these immunoblotting cases because visually one could already see same bandwidth of myc-tagged SNTB1 bands in SNTB1 custom 60/ 30pmole, SNTB1 60/ 30pmole and reference pSKO253+ negative control siRNA #1.

Figure 40: Western blot of Lipofectamine RNAiMAX SNTB1 custom and SNTB1 60pmole transfection

Figure 40 shows the Western blot of Lipofectamine RNAiMAX SNTB1 custom SNTB1 60pmole transfection. Myc-tagged SNTB1 59kD and β-actin 49kD bands are expressed at correct size. Individual samples were loaded in triplicates.

Figure 41: Western blot of Lipofectamine RNAiMAX SNTB1 custom and SNTB1 30pmole
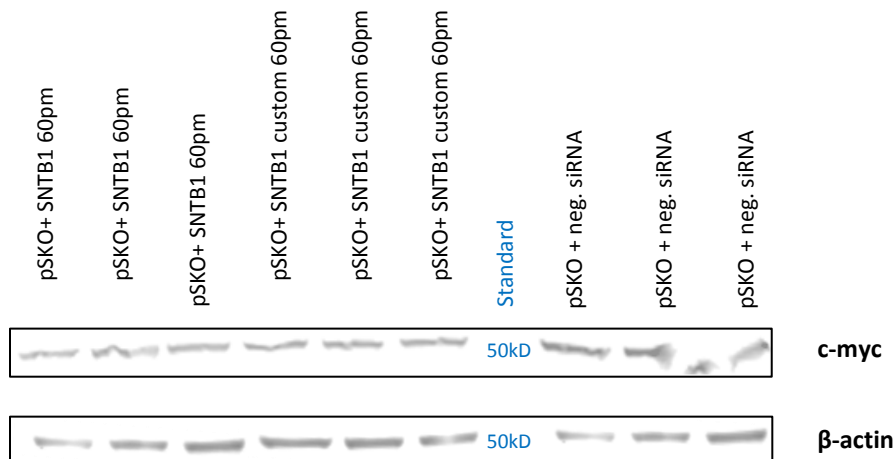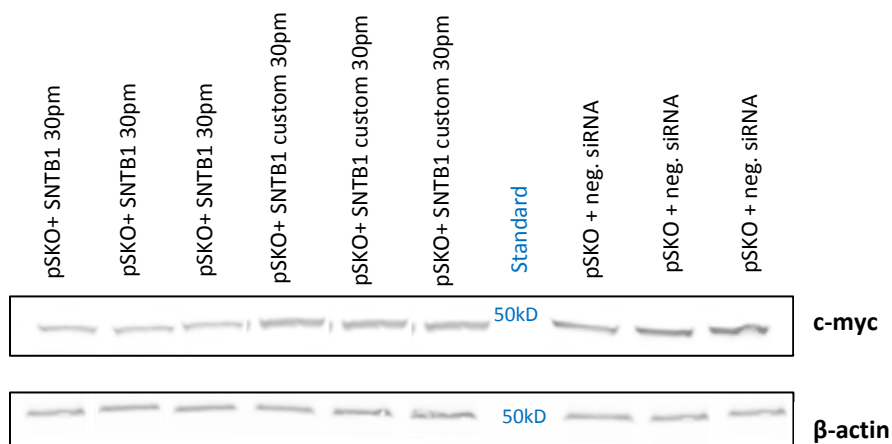

Figure 16 shows the Western blot of Lipofectamine RNAiMAX SNTB1 custom and SNTB1 30pmole transfection. Myc-tagged SNTB1 59kD and β-actin 49kD bands are expressed at correct size. Individual samples were loaded in triplicates

Taken together, with Lipofectamine RNAiMAX-mediated transfection SNTB1 custom and SNTB1 60/ 30 pmole were unable to achieve high ≥50%.SNTB1 knockdown efficiency.

4   Discussion

ABCA1-mediated cholesterol efflux function is of critical importance in macrophages which can accumulate cytotoxic cholesterol derived from ingestion of cellular debris. Cholesterol engorged macrophages are the cause for atherosclerosis (Cuchel and Radar; 2006).

Although a lot is known about ABCA1 cholesterol efflux function, little is known about how ABCA1 actually achieves cholesterol efflux.

4.1   Western blot analysis of Syn$^{\alpha1-/-\beta2-/-}$ macrophage phenotype

Three Syntrophin isoforms, SNTA1, SNTB1 and SNTB2, have been shown to stabilize ABCA1 expression (Okuhira et al; 2005). Using RNAi and immunoblotting approaches, the relation of ABCA1 and its downstream protein interaction partners Syntrophins could be analyzed in Syn$^{\alpha1-/-\beta2-/-}$ macrophages.

In immortalized Syn$^{\alpha1-/-\beta2-/-}$ macrophages only the last Syntrophin isoform SNTB1 is present. SNTB1 expression had to be validated in Syn$^{\alpha1-/-\beta2-/-}$ macrophages before starting RNAi experiments. Furthermore SNTB1 up regulation as a compensatory response to SNTA1 and SNTB2 deletion in Syn$^{\alpha1-/-\beta2-/-}$ macrophages results from an unpublished paper had to be confirmed.

Unfortunately SNTB1 expression analysis using immunoblotting was not possible due to a non-specific SNTB1 antibody. It is important to note that the used monoclonal SNTB1 antibody in this study was not the same as the one used successfully in unpublished data because former antibody aliquots were finished before start of this Master study.

Instead another monoclonal SNTB1 antibody, produced in another rabbit as the first SNTB1 antibody, had to be used. Both SNTB1 antibodies used in this study and unpublished paper were kind gifts from a University laboratory, provided in natural state without prior purification or validation steps.

The dilution of antibodies for immunoblotting is influential for target protein band detection on Western blot. Probably the first SNTB1 antibody used in unpublished data had a higher quality than the second one, allowing better binding to SNTB1 protein on Western blot at higher antibody dilutions. Antibody binding assays could help to

determine optimal antibody concentrations for efficient SNTB1 binding in order to repeat phenotype confirmation studies of Syn$^{\alpha 1-/-\beta 2-/-}$ macrophages.

Another argument could be that the used SNTB1 antibody could bind to SNTB1 on the Western blot but due to the low endogenous expression of the protein, the actual SNTB1 bands could not be detected since the threshold for infrared detection was not exceeded. When detected antibody infrared signals are below threshold they are considered as background by an infrared imager (Odyssey manual, Li-Cor Biosciences).

Chemiluminescence SNTB1 detection involving <u>H</u>orse <u>r</u>adish <u>p</u>eroxidase HRP conjugated secondary antibody could be used as an alternative to infrared signal detection, to circumvent non-detection of low protein expression on Western blot (information from Michael Fitzgerald). Reason for this is that with Chemiluminesence an amplification of secondary antibody signal occurs over time (information from Michael Fitzgerald).

With the help of an anti-Syntrophin antibody, against SNTA1 and SNTB2, the phenotype of Syn$^{\alpha 1-/-\beta 2-/-}$ macrophages could, although in part, be confirmed.

4.2   Western blot analysis of ABCA1 and ApoE expression in Syn$^{\alpha 1-/-\beta 2-/-}$ and ABCA1$^{-/-}$ macrophage

Degree of protein expression is reflective of the cellular demand for a protein at a certain time.

In the case of ABCA1, a varying degree of ABCA1 protein levels were seen on ABCA1 probed Western blots. Variation in ABCA1 protein levels in Syn$^{\alpha 1-/-\beta 2-/-}$ and ABCA$^{-/-}$ macrophages were also observed in unpublished paper. Syn$^{\alpha 1-/-\beta 2-/-}$ macrophages consistently had bands with thicker bandwidth than their C57BL/6J controls and ABCA1$^{-/-}$ cells. This result indicates that there is a higher ABCA1 demand in Syn$^{\alpha 1-/-\beta 2-/-}$ than in C57BL/6J macrophages. This raises the questions:

- If ABCA1 is up regulated due to the absence of SNTA1 and SNTB2 in Syn$^{\alpha 1-/-\beta 2-/-}$ macrophages?

- Is ABCA1 expression increased and stabilized by the help of SNTB1 in $Syn^{\alpha 1-/-\beta 2-/-}$ macrophages?

Further proteomics will be necessary to prove Syntrophin-ABCA1 relation in macrophages.

ApoE is a major component of <u>v</u>ery <u>l</u>ow <u>d</u>ensity <u>l</u>ipoproteins VLDLs. VLDLs remove excess cholesterol from the blood and transports it to the liver for processing (<u>g</u>enetic <u>h</u>ome <u>r</u>eference GHR). ApoE has been implicated to Alzheimer's disease (Kim, Basak and Holtzmann; 2009).

Interestingly ApoE was absent in $Syn^{\alpha 1-/-\beta 2-/-}$ macrophages.This result could mean that SNTA1 and SNTB2 isoforms are necessary for ApoE cholesterol acceptor function. If this is true $Syn^{\alpha 1-/-\beta 2-/-}$ macrophages have the potential to be used as a cell model to understand Alzheimer's disease, or other diseases involving ApoE.

$ABCA^{-/-}$ macrophages should not express ApoE, which was confirmed in figure 6. This result is logical because ApoE needs to accept effluxed cholesterol from ABCA1. If there is no ABCA1 transporter in the cell membrane no cholesterol efflux and thus no cholesterol uptake by ApoE can occur.

The expected outcome after ApoE probe of Immunoblot is presence of an ApoE band in C57BL/6J and $ABCA1^{+/+}$ wild type controls. Unexpectedly ApoE was not expressed in $ABCA^{+/+}$ macrophages. This is an odd result since ApoE works as a cholesterol efflux acceptor. ApoE should therefore be present in $ABCA^{+/+}$ macrophages. This unusual result made one question $ABCA^{+/+}$ cell integrity.

After review of cell culture protocols, equipments and inspection of cell incubator the possible harm to cell integrity was discovered. A yeast infection was detected in cultured $ABCA^{+/+}$ cells, which probably exposed the cells to abnormal or toxic conditions resulting in altered cell phenotype or genotype.

A Western blot experiment using intact $ABCA^{+/+}$ and $ABCA^{-/-}$ macrophages has to be performed to erase doubts of results.

4.3 Lipid-mediated transfection of synthetic siRNAs
Positive siRNA controls

Lipid-mediated transfection of positive siRNA controls, Alexa fluor and FAM-labeled GAPDH into HEK293ETN cells achieved low GAPDH knockdown efficiency (figure 12). The highest reached GAPDH knockdown efficiency 31% was with FAM-labeled GAPDH 100nmolar. 31% knockdown efficiency is clearly under the set threshold of ≥50% for interpreting a siRNA as highly knockdown efficient.

Low cellular intake of FAM-labeled GAPDH 75, 100 or 125nmolar prior to Immunoblot quantification already predicted low GAPDH knockdown efficiency. Even with higher amounts of FAM-labeled GAPDH, no higher GAPDH knockdown efficiency could be achieved. This result demonstrates that HEK293ETN cells did not experience a dose response relationship to increased FAM-labeled GAPDH concentrations.

In dividing cells, gene silencing lasts only 3 to 7 days, presumably because of siRNA dilution with cell division (Song et al; 2003).

GAPDH gene silencing lasted 3 days. A decrease in HEK293ETN cellular uptake of FAM-labeled GAPDH took place over 1-3 days . HEK293ETN are rapidly dividing cells which require splitting every two days. This means FAM-labeled GAPDH was rapidly diluted in cells, negatively affecting its GAPDH knockdown efficiency.

Transfection efficiency varies according to cell type and transfection agent (supplemental information Ambion, Inc). Alexa fluor and FAM-labeled GAPDH were products bought from different vendors (see materials and methods section) which optimized their respective product utilizing different lipid based reagent and cell type to achieve high protein knockdown efficiencies (see websites of Ambion, Inc and Invitrogen™).

For example, the supplier of Alexa fluor optimized siRNA cellular intake with Lipofectamine 2000 or Lipofectamine RNAiMAX in immortal Henrietta Lacks HeLA cells. Higher cellular intake and distribution of Alexa fluor in comparison to FAM-labeled GAPDH was visualized in transfected HEK293 cells. GAPDH RNAi results could be interpreted that low GAPDH silencing is a result of an unsuitable transfection reagent that could not aid in efficient siRNA delivery.

Transfection is dependent on cell type and transfection agent. Maybe in another cell type, as HEK293 cells, a higher GAPDH knockdown efficiency would have been achieved? Or maybe another type of FAM-labeled GAPDH delivery i.e. electroporation, into cells would induce higher GAPDH silencing?

To answer these questions more time for enhancing RNAi experiments are needed.

In regards to evaluating GAPDH knockdown efficiency via Western blot, an alternative approach could have been possible.

In this Master study, all positive siRNA control transfected HEK293 cells from the same well were lysed for immunoblotting. These lysed cells do not necessarily represent all cells which included Alexa fluor and FAM-labeled GAPDH into their cytoplasm.

To exclude HEK293 cells from Western blot that did not intake fluorescently labeled Alexa fluor and FAM-labeled GAPDH, fluorescence activated cell sorting FACS can be applied (information from Mason Freeman). Thus only HEK293ETN cells who clearly endocytosed Alexa fluor and FAM-labeled GAPDH can be included in Immunoblot to evaluate GAPDH knockdown. This alternative approach allows the Immunoblot of transfected cells to be a representation of actual GAPDH silencing.

To increase confidence in GAPDH RNAi data, mRNA of Alexa fluor and FAM-GAPDH transfected HEK293 cells can be isolated, amplified and quantitated through reverse transcription–polymerase chain reaction RT-PCR (information from Michael Fitzgerald). RT-PCR is sensitive enough to enable quantitation of RNA from a single cell (Subbu Dharmaraj, Life Technologies™)

Lipid-mediated transfection of SNTB1 and SNTB1 custom siRNA

Low SNTB1 knockdown efficiency was concluded for most SNTB1 and SNTB1 custom concentrations.

The only exceptions to this low SNTB1 knockdown efficiency trend were Lipofectamine 2000 transfected pSKO253+ SNTB1 custom 60pmole and pSKO253+ SNTB1 30pmole. PSKO253+ SNTB1 custom 60pmole induced 59% SNTB1 knockdown whereas pSKO+

SNTB1 30pmole realized 53% SNTB1 knockdown. Both values are just slightly above the siRNA high knockdown efficiency threshold of ≥50%.

As already mentioned in the paragraph for positive siRNA controls, all siRNA transfected cells of a well were lysed and added to Western blot analysis.

To achieve SNTB1 interference in HEK293ETN, SNTB1 expression construct pSKO253 and SNTB1 custom or SNTB1 were encapsulated in lipoplexes and transfected into the same well of HEK293ETN cells. There is the possibility that some cells only ingested pSKO253 plasmid DNA or SNTB1 siRNA or both.

If pSKO253 is included into HEK293ETN cells, plasmid DNA can replicate triggering over expression of SNTB1, seen as myc-tagged SNTB1 on Western blot. When SNTB1 custom or SNTB1 siRNA are taken up by a cell the opposite occurs, SNTB1 expression is down regulated.

Over expressed SNTB1 signal will negatively influence SNTB1 knockdown values leading to lower calculated knockdown efficiencies than actually achieved by siRNAs in HEK293ETN cells.

Unfortunately SNTB1 custom and SNTB1 are not labeled with a fluorescent dye to enable selection of RNAi positive HEK293ETN cells.

Despite ~50% SNTB1 knockdown efficiency of SNTB1 custom and SNTB1 per Lipofectamine 2000-mediated transfection, a even lower SNTB1 knockdown efficiency was realized in HEK293ETN cells transfected with Lipofectamine RNAiMAX reagent.

Lipofectamine RNAiMAX mediated SNTB1 RNAi results are confusing considering Lipofectamine RNAiMAX is believed to be the most favorable reagent for siRNA transfection (Zhao et al; 2008).

SNTB1 knockdown efficiency by SNTB1 custom and SNTB1 60/ 30 pmole could not attain high knockdown efficiency as seen on the c-myc probed immunoblots of transfected HEK293ETN cells. For that reason c-myc bands did not have to be quantified to determine SNTB1 knockdown efficiency by SNTB1 custom and SNTB1 30 or 60pmole.

Anyway low SNTB1 knockdown efficiency by SNTB1 custom and SNTB1 60 and 30pmolar would have been concluded from Western blot and its subsequent quantification.

In summary the acquired RNAi results of this Master study are a reflection of multiple influential factors and potential technical pitfalls. Some influential factors on efficient siRNA delivery to cells are:

- **Cell type:** HEK293 cells are known to be an easy-to-transfect cell line enabling high amounts of recombinant protein production after plasmid transfection (Trevor and Smart; 2004). But are HEK293 really the right cell model for optimizing lipid-mediated siRNA transfections for use in macrophages? Different cell types have different cell membrane permeability.

  Macrophages are differentiated cells which are difficult to transfect with synthetic siRNA. Synthetic siRNA inhibition of SNTB1 expression reduced cholesterol efflux from bone marrow-derived mouse macrophages by 30% (Okuhira et al; 2005) whereas lentiviral mediated SNTB1 RNAi in primary $Syn^{\alpha1-/-\beta2-/-}$ macrophages resulted in ≥30% SNTB1 knockdown (unpublished paper).

- **Cell density before lipid-mediated transfection:** For the dose response evaluation of Alexa fluor and FAM-labeled GAPDH 75-200nmole (figures 8 and 9) 100000 HEK293 cells were seeded per well.

  In the second positive siRNA transfection with the goal to evaluate GAPDH knockdown efficiency over the course of 3 days, 150000 HEK293ETN cells were seeded per well (figure 10). Higher cellular siRNA intake was realized with 150000 HEK293 cells.

  More experiments are desired to test optimal cell density for lipid-mediated positive siRNA control transfection.

- **Susceptibility of siRNA to ribonucleases:** siRNA are extremely sensitive to ribonucleases. Ribonucleases can be found everywhere e.g. skin, hair, perspiration etc (Working with RNA basics. Technical notes, Ambion® products and technologies). Although effective measures were taken to prevent Ribonuclease degradative action on siRNA, each handling step i.e. visualization

of transfected cells, lysis and preparation for SDS-PAGE; could have possibly introduced Ribonucleases to RNAi experiments influencing protein knockdown success.

- **Way of transfection:** For lipid-mediated transfection cells were transfected in the conventional way. At first HEK293ETN cells were seeded into wells of a 24 well plate, before addition of plasmid-siRNA lipoplexes.

  An alternate way is reverse transfection enabling better cell-DNA contact upon transfection.

- **Serum in media:** Sera in media have been shown to have an inhibitory action on transfection mediated by lipoplexes to different cell types (Simoes et al; 1999. Nchinda, Ueberla and Zschoernig; 2001).

  The cell culture media used in this Master study contained 10% fetal bovine serum FBS. Plasmid-siRNA lipoplexes were transfected into HEK293 cells cultured in serum-free media OptiMEM and an hour post-transfection serum containing media was added.

- **Phosphate buffered saline PBS wash before visualization of Alexa fluor and FAM-labeled GAPDH:** siRNA transfected HEK293 cells were washed with PBS before visualization under a microscope to improve visibility of Alexa fluor and FAM-labeled GAPDH cellular intake. The PBS wash was done ~24 hours after positive siRNA control transfection, any siRNA stuck to cell membrane about to undergo endocytosis are unfortunately probably washed away.

- **Endosomal escape:** Endosomal escape is the rate limiting step of DNA delivery to cells (Nguyen et al, 2012). The right time point for endosomal escape of plasmid DNA and siRNA are pivotal for DNA delivery to nucleus or cytoplasm; otherwise the nucleic acids are degraded by lysosomal nucleases.

5   Conclusion

Ongoing work in the Freeman/ Fitzgerald laboratory has focused on studying the function of the ABCA1-Syntrophin complex. Thus an immortalized $Syn^{\alpha 1-/-\beta 2-/-}$ macrophage cell line which still expresses SNTB1 endogenously was created. According to unpublished Freeman/ Fitzgerald laboratory data, deletion of the SNTA1 and SNTB2 isoforms results in only a partial reduction in the ability of ABCA1 to interact with ApoA-I and reduced cell surface levels of ABCA1.

However, interpretation of this data is limited by a compensatory response or up regulation of the third and last Syntrophin isoform, SNTB1, present in $Syn^{\alpha 1-/-\beta 2-/-}$ macrophages.

Thus, although we have shown that knocking out the SNTA1 and SNTB2 isoforms has a minor impact on macrophage efflux function it will be necessary to also suppress the expression of SNTB1 in the context of the $Syn^{\alpha 1-/-\beta 2-/-}$ macrophages.

The aim of this Master thesis was to test if suppression of SNTB1 in the context of $Syn^{\alpha 1-/-\beta 2-/-}$ macrophages has a more dramatic impact on macrophage efflux function mediated by ABCA1.

To test this hypothesis three specific aims were proposed

1. Verify and quantify SNTB1 up regulation in $Syn^{\alpha 1-/-\beta 2-/-}$ macrophages.
2. Use synthetic siRNAs to suppress SNTB1 in $Syn^{\alpha 1-/-\beta 2-/-}$ macrophages.
3. Test the impact of SNTB1 suppression both in cell culture efflux assays and in a mouse animal model.

SNTB1 up regulation could not be verified due to a non-specific SNTB1 antibody. Hence a new SNTB1 antibody has to be used. Hopefully the new SNTB1 antibody could help demonstrate SNTB1 up regulation in $Syn^{\alpha 1-/-\beta 2-/-}$ macrophages.

The optimization experiments for lipid-mediated transfection of synthetic siRNAs into HEK293 cell models required a lot of time. The function of Alexa fluor, FAM-labeled GAPDH, SNTB1 custom and SNTB1 siRNA could be proven

Due to limited time, this Master study lasted 6 months, SNTB1 RNAi in $Syn^{\alpha1-/-\beta2-/-}$ macrophages was not realizable.

Furthermore SNTB1 knockdown efficiency would have probably been significantly lower in $Syn^{\alpha1-/-\beta2-/-}$ macrophages in comparison to easy-to-transfect HEK293 cells. In other words SNTB1 knockdown efficiency in $Syn^{\alpha1-/-\beta2-/-}$ macrophages would have been low efficient.

Limited time was also the reason influencing the test for the impact of SNTB1 suppression both in cell culture efflux assays and in a mouse animal model.
The impact of SNTB1 suppression on cell culture efflux assays and in a mouse animal model is part of current work in the Freeman/ Fitzgerald laboratory.

Taken together the results of this Master thesis helped to discover a cell model for ApoE related diseases and understand the complexities of experimental RNAi.

Further research on ABCA1-SNTB1 interaction is necessary to prove SNTB1's influence on ABCA1-mediated chlolesterol efflux.

If research is successful in establishing the stabilizing role of Syntrophins on ABCA1 expression, Syntrophins have the potential to be used as drug targets to manipulate cholesterol trafficking pathways to alleviate life-threatening diseases like Atherosclerosis and Alzheimer's disease.

6 References

1. ABCA1 information http://www.uniprot.org/uniprot/O9547
2. Advances in experimental medicine and biology 991.
3. Ahn A. H., Freener C. A., Gussoni E., Yoshida M., Ozawa E., and Kunkel L. M. The three human Syntrophin genes are expressed in diverse tissues, have distinct chromosomal locations, and each bind to Dystrophin and its relatives. JBC 271: 2724–2730
4. Ahn AH, Kunkel LM.(1995) Syntrophin binds to an alternatively spliced exon of dystrophin. J Cell Biol 3:363-71.
5. Aiello, R. J., D. Brees, P. A. Bourassa, L. Royer, S. Lindsey, T. Coskran, M. Haghpassand, and O. L. Francone. 2002. Increased atherosclerosis in hyperlipidemic mice with inactivation of ABCA1 in macrophages. Arterioscler Thromb Vasc Biol 22:630-7.
6. Alberts B, Johnson A., Lewis J, Raff M., Roberts K. and Walter P. (2007). Molecular Biology of the cell. 5th edition. New York, USA. Garland Science Taylor and Francis group
7. Albrecht, D. E., D. L. Sherman, P. J. Brophy, and S. C. Froehner. 2008. The ABCA1 cholesterol transporter associates with one of two distinct dystrophin-based scaffolds in Schwann cells. Glia 56:611-8.
8. Yang LY, Liu CS, Lin W. (2000). Identification of novel human genes evolutionarily conserved in Caenorhabditis elegans by comparative proteomics. Genome Res.10: 703-13.
9. Behlke M. (2006). Progress Towards in Vivo Use of siRNAs. Molecular therapy 13: 644-670.
10. Berg J. M., Tymoczko J. L., and Stryer L. (2002). Biochemistry.5th edition. New York, USA. W.H. Freeman and Company. Accessed online on 1/9/2013. Link: http://www.ncbi.nlm.nih.gov/books/NBK21154/
11. Bernstein E., Caudy A. A., Hammond S. M. and Hannon G. J. (2001). Role for a bidentate ribonuclease in the initiation step of RNA interference. Nature 409: 363-366.
12. Blasi, E., B. J. Mathieson, L. Varesio, J. L. Cleveland, P. A. Borchert, and U. R. Rapp.(1985). Selective immortalization of murine macrophages from fresh bone marrow by a raf/myc recombinant murine retrovirus. Nature 318:667-70.
13. Brunham, L. R., R. R. Singaraja, M. Duong, J. M. Timmins, C. Fievet, N. Bissada, M. H. Kang, A. Samra, J. C. Fruchart, B. McManus, B. Staels, J. S. Parks, and M. R. Hayden. (2009). Tissue specific roles of ABCA1 influence susceptibility to atherosclerosis. Arterioscler Thromb Vasc Biol 29:548-54.
14. Buechler, C., A. Boettcher, S. M. Bared, M. C. Probst, and G. Schmitz. (2002). The carboxyterminus of the ATP-binding cassette transporter A1 interacts with a beta2-syntrophin/utrophin complex. Biochem Biophys Res Commun 293:759-65.
15. Carthew RW, Sontheimer EJ (2009) Origins and Mechanisms of miRNAs and siRNAs. Cell. 136: 642-55.
16. Cassie Turano. Link for figure 4: http://www.studyblue.com/notes/note/n/pathophysiology-/deck/4659789 [accessed on 12/29/2013]
17. Cholesterol and other lipids in your blood; online lecture held by Tracy Fulton, University of California, USA. Link: http://www.youtube.com/watch?v=_oLXa4SfsVs.
18. Chroni, A., T. Liu, M. L. Fitzgerald, M. W. Freeman, and V. I. Zannis. (2004). Cross-linking and lipid efflux properties of apoA-I mutants suggest direct association between apoA-I helices and ABCA1. Biochemistry 43:2126-39.
19. Cooper G. M. (2000). The Cell: A Molecular Approach. 2nd edition. Sunderland, USA. Sinauer Associates. Accessed online on 1/9/2013. Link: http://www.ncbi.nlm.nih.gov/books/NBK9839/.

20. Dean M. (2002). The human ATP-binding cassette (ABC) transporter superfamily. Bethesda, USA. National Center for Biotechnology Information [NCBI]. Accessed online on 1/9/2013. Link: http://www.ncbi.nlm.nih.gov/books/NBK3/?term=abca1

21. Delude C. (2009). Tangier disease: one island's treasure. Protamag, Massachusetts general hospital [MGH].

22. Dominiska D. and Dykxhoorn D. M. (2010). Breaking down the barriers: siRNA delivery and endosome escape. JCS 123: 1183-1189.

23. Doyle M, Badertscher L, Jaskiewicz L, Güttinger S, Jurado S, Hugenschmidt T, Kutay U, Filipowicz W. The double-stranded RNA binding domain of human Dicer functions as a nuclear localization signal. RNA19:1238-52

24. Dykxhoorn D. M., Novina C. D. and Sharp P. A. (2003). Killing the messenger:short RNAs that silence gene expression. Nature Rev 4: 457-467.

25. Eckardstein A.V., Langer C., Engel T., Schaukal I., Cignarella A, Reinhardt J., Lorkowski S., Li Z., Zhou X., Cullen P., and Assmann G. (2001). ATP binding cassette transporter ABCA1 modulates the secretion of apolipoprotein E from human monocyte-derived macrophages. FASEB J. 15, 1555–1561.

26. Elbashir S. M., Harborth J., Lendeckel W., Yalcin A., Weber K. and Tuschl T. (2001a). Duplexes of 21 nucleotide RNAs mediate RNA interference in cultured mammalian cells. Nature 411: 494-498.

27. Elbashir S. M., Lendeckel W. and Tuschl T. (2001b). RNA interference is mediated by 21- and 22-nucleotide RNAs. Genes Dev 15: 188-200.

28. Ferrer J., Jez J. M., Bowman M. E., Dixon R. A. and Noel J. P. (1999). Structure of chalcone synthase and the molecular basis of plant polyketide biosynthesis. Nat Struct Biol 8:775-84.

29. Fire A., Xu S., Montgomery M.K., Kostas S. A., Driver S.E. and Mello C. C. (1998). Potent and specific genetic interference by double-stranded RNA in Caenorhabditis elegans. Nature. 1998 391:806-11.

30. Fitzgerald M. L., Moore K. J. and Freeman M. W. (2002). Nuclear hormone receptors and cholesterol trafficking: the orphans find a new home. J Mol Med 80:271–281.

31. Fitzgerald M. L., Morris A. L, Chroni A., A. J. Mendez, Zannis V. I. and Freeman M. W (2004). ABCA1 and amphipathic apolipoproteins form high-affinity molecular complexes required for cholesterol efflux. JLR 45:287–294.

32. Fitzgerald ML, Mujawar Z, Tamehiro N. (2010) ABC transporters, atherosclerosis and inflammation. Atherosclerosis. 211:361-70.

33. Fitzgerald, M. L., A. J. Mendez, K. J. Moore, L. P. Andersson, H. A. Panjeton, and M. W. Freeman. (2001). ATP-binding cassette transporter A1 contains an NH2-terminal signal anchor sequence that translocates the protein's first hydrophilic 387 domain to the exoplasmic space. J Biol Chem 276:15137-45.

34. Fitzgerald, M. L., A. L. Morris, A. Chroni, A. J. Mendez, V. I. Zannis, and M. W. Freeman. 2004. ABCA1 and amphipathic apolipoproteins form high-affinity molecular complexes required for cholesterol efflux. J Lipid Res 45:287-94.

35. Fitzgerald, M. L., A. L. Morris, J. S. Rhee, L. P. Andersson, A. J. Mendez, and M. W. Freeman. 2002. Naturally occurring mutations in the largest extracellular loops of ABCA1 can disrupt its direct interaction with apolipoprotein A-I. J Biol Chem 277:33178-87.

36. Fitzgerald, M. L., K. Okuhira, G. F. Short, J. J. Manning, S. A. Bell, and M. W. Freeman. 2004. ATP-binding cassette transporter A1 contains a novel C-terminal VFVNFA motif that is required for its cholesterol efflux and ApoA-I binding activities. J Biol Chem 279:48477-85.

37. Fitzgerald, M. L., Z. Mujawar, and N. Tamehiro. 2010. ABC transporters, atherosclerosis and inflammation. Atherosclerosis 211:361-70.

38. Francone, O. L., L. Royer, G. Boucher, M. Haghpassand, A. Freeman, D. Brees, and R. J. Aiello. 2005. Increased cholesterol deposition, expression of scavenger receptors, and

response to chemotactic factors in Abca1-deficient macrophages. Arterioscler Thromb Vasc Biol 25:1198-205.

39. Freeman MW. (2006). Statins, cholesterol, and the prevention of coronary heart disease. FASEB J 20:200-1

40. Fukunaga R, Han BW, Hung JH, Xu J, Weng Z, Zamore PD. (2012). Dicer partner proteins tune the length of mature miRNAs in flies and mammals. Cell. 151:533-46

41. Geissmann, F., M. G. Manz, S. Jung, M. H. Sieweke, M. Merad, and K. Ley. 2010. Development of monocytes, macrophages, and dendritic cells. Science 327:656-61.

42. Genetics home reference [GHR] 2012. http://ghr.nlm.nih.gov/condition/familial-hdl-deficiency

43. Gitlin L., Karelsky S. and Andino R. (2002). Short interfering RNA confers intracellular antiviral immunity in human cells. Nature 418: 430-435.

44. Gonzalez M. and Li F. (2004). DNA replication, RNAi and epigenetic inheritance. Epigenetics 7:14-19

45. Gregory R. I., Chendrimada T. P., Cooch N. and Shiekhattar R. (2005). Human RISC couples microRNA biogenesis and posttranscriptional gene silencing. Cell 123: 631–640.

46. Gu S., Jin L., Zhang Y., Huang Y., Zhang F., Valdmanis P. N. and Kay M. A. (2012). The loop position of shRNAs and pre-miRNAs is critical for the accuracy of Dicer processing in vivo. Cell 151, 900–911.

47. Hossmann K. A. and Heiss W. (2009). Neuropathology and pathophysiology of stroke. Brainin M., Heiss W. Textbook of Stroke Medicine p. 1-8. Cambridge, UK. Cambridge Univ. Press.

48. http://avery.rutgers.edu/WSSP/StudentScholars/project/introduction/worms.html [accessed on 10/23/2013]

49. http://ed.ted.com/lessons/rnai-slicing-dicing-and-serving-your-cells-alex-dainis [accessed on 11/21/2013]

50. http://edoc.hu-berlin.de/dissertationen/lu-yinghong-2006-04-24/HTML/chapter2.html [accessed on 10/9/2013]

51. http://ghr.nlm.nih.gov/gene/APOE [assessed on 11/19/2013]

52. http://hek293.com/ [accessed on 25/2/2014]

53. http://invitrogen.cnpg.com/Video/flatFiles/646/index.aspx [accessed on 12/3/2013]

54. http://invitrogen.cnpg.com/Video/flatFiles/646/index.aspx [assessed on 1/10/2014]

55. http://mankinlab.cpb.uic.edu/lectures/PMPG507%20-%20RNA%20AS%20DRUG%20AND%20AS%20DRUG%20TARGET/RNA%20as%20drug.pdf [accessed on 10/9/2013]

56. http://phenome.jax.org/db/q?rtn=strains/details&strainid=7 [accessed on 9/24/13]

57. http://research.jax.org/grs/type/inbred/index.html [accessed on 9/24/13]

58. http://www.abdserotec.com/toll-like-receptor-minireview-tlr.html [assessed on 12/19/2013]

59. http://www.allthingsstemcell.com/2009/02/hematopoietic-stem-cells/comment-page-1/ [accessed on 1/29/2014]

60. http://www.antibodydirectory.com/moreinfos.php?Item=152024 [accessed on 1/6/2014]

61. http://www.bio.davidson.edu/genomics/method/Westernblot.html [accessed on 9/22/13]

62. http://www.discoverymedicine.com/N-Manjunath/2010/05/07/advances-in-synthetic-sirna-delivery/ [accessed on 10/8/2013]

63. http://www.labome.com/method/Nucleic-Acid-Delivery-Lentiviral-and-Retroviral-Vectors.html [assessed on 2/2/2014]

64. http://www.lifetechnologies.com/us/en/home/life-science/rnai/rna-interference-overview.html [accessed on 10/8/2013]

65. http://www.lifetechnologies.com/us/en/home/life-science/rnai/rna-interference-overview.html [assessed on 11/19/2013]

66. http://www.lifetechnologies.com/us/en/home/references/ambion-tech-support/nuclease-enzymes/general-articles/the-basics-rnase-control.html/#1 [accessed on 10/9/2013]
67. http://www.lifetechnologies.com/us/en/home/references/ambion-tech-support/rnai-sirna/tech-notes/optimizing-sirna-transfection-for-rnai.html [assessed on 2/19/2014]
68. http://www.lifetechnologies.com/us/en/home/references/gibco-cell-culture-basics/introduction-to-cell-culture.html
69. http://www.nature.com/nrg/multimedia/rnai/animation/index.html [accessed on 11/21/2013]
70. http://www.nature.com/nrg/multimedia/rnai/index.html [accessed on 9/23/13]
71. http://www.ncbi.nlm.nih.gov/books/NBK2018/ [accessed on 10/9/2013]
72. http://www.nobelprize.org/nobel_prizes/medicine/laureates/2006/ [accessed on 12/3/2013]
73. http://www.pbs.org/wgbh/nova/body/rnai-explained.html [accessed on 10/9/2013]
74. http://www.ruf.rice.edu/~bioslabs/studies/sds-page/gellab2b.html [accessed on 9/22/13]
75. http://www.sigmaaldrich.com/catalog/product/sigma/85120602?lang=en&region=US [accessed on 9/24/13]
76. http://www.sigmaaldrich.com/labware/labware-products.html?TablePage=22692573 [accessed on 9/24/2013]
77. http://www.springer.com/biomed/book/978-1-4614-4743-6 [accessed on 9/23/13]
78. http://www.uniprot.org/uniprot/Q8WYQ5 [assessed on 1/10/2014]
79. http://www.youtube.com/watch?v=5ZE7o_bRekk [accessed on 11/21/2013]
80. http://www.youtube.com/watch?v=A2OS1kv5kgU&list=PL1MoHcJwNQWaXecHNqkfD8nRy3sfTIe1V [accessed on 1/5/2014]
81. http://www.youtube.com/watch?v=d8x83SjMotQ [accessed on 11/21/2013]
82. http://www.youtube.com/watch?v=S9hsMSnyeLI [accessed on 1/3/2014]
83. J. Manikandan1, and S.D. Kumar2*
84. Janowski B. A.., Grogan M. J., Jones S.A., Wisely G. B., Kliewer S. A., Corey E. J., and Mangelsdorf D. J. (1999). Structural requirements of ligands for the oxysterol liver X Receptors LXRα and LXRβ. PNAS 96: 266–271.
85. Khera, A. V., M. Cuchel, M. de la Llera-Moya, A. Rodrigues, M. F. Burke, K. Jafri, B. C. French, J. A. Phillips, M. L. Mucksavage, R. L. Wilensky, E. R. Mohler, G. H. Rothblat, and D. J. Rader. 2011. Cholesterol efflux capacity, high-density lipoprotein function, and atherosclerosis. N Engl J Med 364:127-35.
86. Kim WS, Ordija CM, Freeman MW. (2003) Activation of signaling pathways by putative scavenger receptor class A (SR-A) ligands requires CD14 but not SR-A. Biochem Biophys Res Commun. 310:542-9.
87. Kontush A, Chapman MJ. (2006) Antiatherogenic small, dense HDL--guardian angel of the arterial wall? Nat Clin Pract Cardiovasc 3:144-53.
88. Koseki, M., K. Hirano, D. Masuda, C. Ikegami, M. Tanaka, A. Ota, J. C. Sandoval, Y. Nakagawa-Toyama, S. B. Sato, T. Kobayashi, Y. Shimada, Y. Ohno-Iwashita, F. Matsuura, I. Shimomura and S. Yamashita. (2007). Increased lipid rafts and accelerated lipopolysaccharide-induced tumor necrosis factor-alpha secretion in Abca1-deficient macrophages. J Lipid Res 48:299-306
89. Lai CH, Chou CY, Ch Aigner A. (2007). Applications of RNA interference: current state and prospects for siRNA-based strategies in vivo. Appl Microbiol Biotechnol 76:9–21.
90. Lau PW, Guiley KZ, De N, Potter CS, Carragher B, MacRae IJ. (2012). The molecular architecture of human Dicer. Nat Struct Mol Biol. 19:436-40.
91. Lee R. C., Feinbaum R. L. and Ambros V. (1993). The C. elegans heterochronic gene lin-4 encodes Small RNAs with antisense complementarity to lin-14. Cell, Vol. 75, 843-854.
92. Lim YC, Garcia-Cardena G, Allport JR, Zervoglos M, Connolly AJ, Gimbrone MA Jr, Luscinskas FW (2003) Heterogeneity of endothelial cells from different organ sites in T-cell subset recruitment. Am J Pathol. 162:1591-601.

93. Link of figure 9: http://nursing-resource.com/tangier-disease/ Accessed online on 1/9/2013.

94. Lund-Katz S, Phillips MC (2010) High density lipoprotein structure-function and role in reverse cholesterol transport. Subcell Biochem. 51:183-227

95. MacRae I. J., Zhou K., Li F., Repic A., Brooks A. N., Zacheus W. C., Adams P. D. and Jennifer A. Doudna. (2006). Structural basis for double-Stranded RNA processing by Dicer. Science 311: 195-198.

96. Maqsood MI, Matin MM, Bahrami am, Ghasroldasht MM. (2013) Immortality of cell lines: challenges and advantages of establishment. Cell Biol Int 37: 1038-1045

97. Martinez J., Patkaniowska A., Urlaub H., Luehrmann R., and Tuschl T. (2002). Single-stranded antisense siRNAs guide target RNA cleavage in RNAi. Cell 110, 563–574.

98. Matranga C.,Tomari Y., Shin C., Bartel D. P. and Zamore P.D. (2005). Passenger strand cleavage facilitates assembly of siRNA into Ago2-containing RNAi enzyme complexes. Cell 123: 607–620

99. Meister G. and Tuschl T. (2004). Mechanisms of gene silencing by double-stranded RNA. Nature 431: 343-349

100. Meister G., Landthaler M., Peters L., Chen P.Y., Urlaub H., Luehrmann R. and Tuschl T. (2005). Identification of novel Argonaute-associated proteins. Current Biology 15: 2149–2155.

101. Michael Brainin IMC University of Applied Sciences Krems, lecture on Stroke..

102. Motamedi M. R., Verdel A, Colmenares S. U., Gerber S. A., Gygi S. P.,1,2 and Moazed D. (2004)Two RNAi complexes, RITS and RDRC, physically interact and localize to noncoding centromeric RNAs. Cell 119: 789–802.

103. Murphy K. (2012) Janeway's Immunobiology. 8th edition. New York,USA. Garland Science, Taylor & Francis Group, LLC.

104. Nykaenen A., Haley B. and Zamore P. D. (2001). ATP requirements and small interfering RNA structure in the RNA interference pathway. Cell107, 309–321.

105. Pak J., Maniar J. M., Mello C. C., and Fire A. (2012). Protection from feed-forward amplification in an amplified RNAi mechanism. Cell 151, 885–899.

106. Peiser L, Gordon S. (2001). The function of scavenger receptors expressed by macrophages and their role in the regulation of inflammation. Microbes Infect. 2001 2:149-59.

107. Peter Lechner, IMC University of Applied Sciences Krems, metabolic syndrome lecture

108. Piehler A. P., Özcürümez M. and Kaminski W. (2012). A-subclass ATP-binding cassette proteins in brain lipid homeostasis and neurodegeneration. Front Psychiatry 3:1-17.

109. Rand T. A., Petersen S., Du S., and Wang X. (2005). Argonaute2 Cleaves the Anti-guide strand of siRNA during RISC activation. Cell 123: 621–629.

110. Santamarina-Fojo S., Remaley A. T., Neufeld E. B., and Brewer H. B. J. (2001). Regulation and intracellular trafficking of the ABCA1 transporter. J Lipid Res 42: 1339–1345.

111. Schwarz D. S., Hutvagner G.,Du T., Xu Z., Aronin N. and Zamore P. D. (2003). Asymmetry in the assembly of the RNAi enzyme complex. Cell 115, 199–208.

112. Sidahmed A. M.E and Wilkie B. Endogenous antiviral mechanisms of RNA Interference: a comparative biology perspective (2010). RNAi: from Biology to clinical applications. Min and Ichim W. T..RNA Interference, Methods in Molecular Biology, vol. 623, Springer Science + Business Media, LLC 2010.

113. Song E., Lee S., Dykxhoorn D. M., Novina C., Zhang D., Crawford K., Cerny J., Sharp P.A., Lieberman 2,3 J., Manjunath N., and Shankar1 P. (2003). Sustained small interfering RNA-mediated Human Immunodeficiency Virus type 1 inhibition in primary Macrophages. JVI 77: p. 7174–7181.

114. Song J., Smith S. K., Hannon G. J., L. Joshua-Tor (2004). Crystal structure of Argonaute and its implications for RISC slicer activity. Science 305: 1434-1437.

115.   Tamehiro N., Zhou S., Okuhira K., Benita Y., Brown C. E., Zhuang D. Z., Latz E., Hornemann T., Eckardstein A. V., Xavier R. J., Freeman M. W. and Fitzgerald M. L. (2008). SPTLC1 binds ABCA1 to negatively regulate trafficking andCholesterol efflux activity of the transporter. Biochemistry 47(23): 6138–6147.

116.   Tinsley J. M., Blake D. J., Zuellig R. A,. Davies K. E. (1994). Increasing complexity of the dystrophin-associated protein complex. Proc Natl Acad Sci 18:8307-13.

117.   Venkateswaran A., Laffitte B. A., Joseph S. B., Mak P. A., Wilpitz D. C., Edwards P. A. and Tontonoz P. Control of cellular cholesterol efflux by the nuclear oxysterol receptor LXRα. PNAS 97: 12097–12102.

118.   Volpe T. A. ,Kidner C., Hall I. M., Teng G., Grewal S. I. S, and Martienssen R. A. (2002). Regulation of heterochromatic silencing and Histone H3 Lysine-9 methylation by RNAi. Science 297: 1833-1837.

119.   Wawrzyniak AM , Kashyap R. and Pascale Zimmermann (2013). Phosphoinositides and PDZ domain scaffolds. Capelluto D. G. S. Lipid-mediated protein signaling. Dordrecht, Netherlands. Springer Science+Business Media .

120.   Welker NC, Pavelec DM, Nix DA, Duchaine TF, Kennedy S, Bass BL. (2010). Dicer's helicase domain is required for accumulation of some, but not all, C. elegans endogenous siRNAs. RNA16:893-903.

121.   Yu J, DeRuiter S. L. and Turner D. L. (2002). RNA interference by expression of short-interfering RNAs and hairpin RNAs in mammalian cells. PNAS 99: 6047–6052.

122.   Zamore P. D., Tuschl T., Sharp P. A. and Bartel D. P. (2000). RNAi: Double-Stranded RNA directs the ATP-dependent cleavage of mRNA at 21 to 23 nucleotide Intervals. Cell 101, 25–33.

123.   Devasthanam AS, Tomasi TB. Dicer in immune cell development and function. Immunol Invest. 2014;43(2):182-95.

124.   Maillard PV, Ciaudo C, Marchais A, Li Y, Jay F, Ding SW, Voinnet O. (2013) Antiviral RNA interference in mammalian cells. Science. 2013 Oct 11; 342(6155):235-8

125.   Rao DD, Vorhies JS, Senzer N, Nemunaitis J.. siRNA vs. shRNA: similarities and differences. Adv Drug Deliv Rev. 2009 Jul 25;61(9):746-59.

126.   Hutvagner G, Simard MJ. Argonaute proteins: key players in RNA silencing. Nat Rev Mol Cell Biol. 2008 Jan; 9(1):22-32.

127.   Pfeffer S, Meister G, Landthaler M and Tuschl T (2005). RNA silencing. B.I.F. FUTURA 20: 83-91

128.   Ouellet DL and Provost P (2010). Current Knowledge of MicroRNAs and Noncoding RNAs in Virus-Infected Cells. RNAi: from Biology to clinical applications. Min and Ichim W. T..RNA Interference, Methods in Molecular Biology, vol. 623, Springer Science + Business Media, LLC 2010.

129.   Gavrilov K, Saltzman WM Therapeutic siRNA: principles, challenges, and strategies. Yale J Biol Med. 2012 Jun;85(2):187-200.

130.   Castel SE, Martienssen RA. RNA interference in the nucleus: roles for small RNAs in transcription, epigenetics and beyond. Nat Rev Genet. 2013 Feb;14(2):100-12.

131.   Schirle NT, MacRae IJ. The crystal structure of human Argonaute2. Science. 2012 May 25; 336(6084):1037-40.

132.   Kulkarni M, Ozgur S, Stoecklin G. On track with P-bodies. Biochem Soc Trans. 2010 Feb;:242-51.

133.   Parker R.and Sheth U. (2009) P Bodies and the control of mRNA translation and degradation. Molecular Cell 25: 635-645.

134.   Beckham CJ, Parker R (2008) P bodies, stress granules, and viral life cycles. Cell Host Microbe 3(4):206-12.

135. Yu JY, DeRuiter SL, Turner DL. (2002) RNA interference by expression of short-interfering RNAs and hairpin RNAs in mammalian cells. Proc Natl Acad Sci U S A. 99(9):6047-52.
136. Li Y, Lu J, Han Y, Fan X, Ding SW. (2013) RNA interference functions as an antiviral immunity mechanism in mammals. Science Oct 11; 342(6155):231-4.
137. Speer T, Rohrer L, Blyszczuk P, Shroff R, Kuschnerus K, Kränkel N, Kania G, Zewinger S, Akhmedov A, Shi Y, Martin T, Perisa D, Winnik S, Müller MF, Sester U, Wernicke G, Jung A, Gutteck U, Eriksson U, Geisel J, Deanfield J, von Eckardstein A, Lüscher TF, Fliser D, Bahlmann FH, Landmesser U. Abnormal high-density lipoprotein induces endothelial dysfunction via activation of Toll-like receptor-2. Immunity. 2013 Apr 18;38(4):754-68.
138. Leona D. Samson BEH.109: Laboratory Fundamentals in BiologicalEngineering. Module 3. Massachusetts Institute of Technology [MIT].
139. RNA interference guide, Ambion, Inc; 2006.
140. Diane Carrera. Dec RNAi. pdf. Topic RNA interference MacMillan Group Meeting, January 21, 2009
141. Working with RNA: the basics. Ambion, Inc 2012.
142. Aigner A. (2007) Applications of RNA interference: current state and prospects for siRNA-based strategies in vivo.Appl Microbiol Biotechnol.76:9-21
143. Stewart SA, Dykxhoorn DM, Palliser D, Mizuno H, Yu EY, An DS, Sabatini DM, Chen IS, Hahn WC, Sharp PA, Weinberg RA, Novina CD. Lentivirus-delivered stable gene silencing by RNAi in primary cells. RNA. 2003 Apr;9(4):493-501
144. Petri S. and Meister G. Sirna Design Principles And Off-Target Effects (2010). Jürgen Moll and Riccardo Colombo (eds.), Target Identification and Validation in Drug Discovery: Methods and Protocols, Methods in Molecular Biology, Springer Science+Business Media New York 2013
145. Simões S, Slepushkin V, Pretzer E, Dazin P, Gaspar R, Pedroso de Lima MC, Düzgüneş N. Transfection of human macrophages by lipoplexes via the combined use of transferrin and pH-sensitive peptides. J Leukoc Biol. 1999 Feb;65(2):270-9.
146. Thomas P. and Smart T G (2005) HEK293 cell line: A vehicle for the expression of recombinant protein Journal of Pharmacological and Toxicological Methods 51 187–200.
147. Fedorov Y, Anderson EM, Birmingham A, Reynolds A, Karpilow J, Robinson K, Leake D, Marshall WS, Khvorova A. Off-target effects by siRNA can induce toxic phenotype. RNA. 2006 Jul;12(7):1188-96. Epub 2006 May 8.
148. Cuchel M, Rader DJ Macrophage reverse cholesterol transport: key to the regression of atherosclerosis? Circulation. 2006 May 30;113(21):2548-55
149. Kim J, Basak JM, Holtzman DM. The role of apolipoprotein E in Alzheimer's disease.
150. Neuron. 2009 Aug 13;63(3):287-303
151.